Influence of chemical and mechanical stress on Precision-cut Lung Slices

Von der Fakultät für Mathematik, Informatik und Naturwissenschaften der RWTH Aachen University zur Erlangung des akademischen Grades einer Doktorin der Naturwissenschaften genehmigte Dissertation

vorgelegt von

Diplom-Humanbiologin

Constanze Dassow

aus Bad Oldesloe

Berichter: Universitätsprofessor Dr. Stefan Uhlig
Universitätsprofessor Dr. Werner Baumgartner

Tag der mündlichen Prüfung: 18. März 2010

Diese Dissertation ist auf den Internetseiten der Hochschulbibliothek online verfügbar.

You didn't think it was gonna be that easy, did you?
You know, for a second there, yeah, I kinda did.

Kill Bill: Vol. 1

Publications contributing to this study

Henjakovic M., Martin C., Hoymann HG., Sewald K., Ressmeyer AR., Dassow C., Pohlmann G., Krug N., Uhlig S., Braun A. Ex vivo lung function measurements in precision-cut lung slices (PCLS) from chemical allergen-sensitized mice represent a suitable alternative to in vivo studies. Toxicol Sci 106:444-53, 2008

Dassow C., Wiechert L., Martin C., Schumann S., Müller-Newen G., Pack O., Guttmann J., Wall WA., Uhlig S. Biaxial distension of precision-cut lung slices. J Appl Physiol 108:713-21, 2010

Abstracts

Dassow C., Wiechert L., Martin C., Schumann S., Müller-Newen G., Guttmann J., Wall WA., Uhlig S (2009): Biomechanics of Precision-Cut Lung Slices during Biaxial Distension. Am J Respir Crit Care Med, Apr 2009, 179: A1243

Dassow C., Martin C., Barrenschee M., Uhlig S. (2008): Induction of Amphiregulin in Precision-Cut Lung Slices. Am J Respir Crit Care Med, Apr 2008, 177: A195

Dassow C., Martin S., Schumann S., Guttmann J., Uhlig S. (2007): Stretching precision-cut lung slices as a new model to investigate overexpansion of the lung. Perspektiven der pneumologischen Pharmakotherapie, Symposium der Paul-Martini-Stiftung

Table of Contents

Abbreviations

°C	degree Celsius
μg	microgram
μm	micrometres
μM	micromolar
ADAM	A Disintegrin And Metalloproteinase
AHR	Airwayhyperresponsiveness
ALI	Acute Lung Injury
AP-1	Activator Protein 1
ARDS	Adult Respiratory Distress Syndrome
Areg	Amphiregulin
AT I/II	Alveolar Type I/II
ATF2	Activating Transcription Factor 2
ATP	Adenosine Triphosphate
BAL	Bronchoalveolarlavage
Ca^{2+}	$Calcium^{2+}$
$CaCl_2$	Calcium chloride
COPD	Chronic Obstructive Pulmonary Disease
Cox-2	Cyclooxygenase-2
CSF-3	Colony Stimulating Factor-3
CXCL	Chemokine (C-X-C motif) ligand
CXCR	CXC Chemokine Receptor
DAG	Diacylglycerol
DMSO	Dimethyl sulfoxide
DNA	Desoxyribonucleic acid
DNCB	Dinitrochlorobenzene
dNTP	deoxynucleotide triphosphate
DRB	5,6-Dichloro-1-β-D-ribofuranosylbenzimidazole
DTT	Dithiothreitol
EC_{50}	Half Maximal Effective Concentration
ED_{50}	Half Maximal Effective Dose
e.g.	exempli gratia
EGF	Epidermal growth factor
Elk-1	Ets Like Gene1
ERK	Extracellular Signal-regulated Kinase
Et-1	Endothelin-1
EU	European Union
FAK	Focal Adhesion Kinase
Fcε-receptor	Fragment crystallizable epsilon-receptor

FE(M)	Finite Element (Model)
FEV1	Forced Expiratory Volume 1
GM-CSF	Granulocyte Macrophage Colony-Stimulating Factor
h	hours
His	Histamine
Hz	Hertz
i. e.	id est
IgE	immunoglobulin E
IL	Interleukin
IP_3	Inositol trisphosphate
IPL	Isolated Perfused Lung
JAK	Janus Kinase
JNK	c-Jun N-terminal Kinase
KCl	Kaliumchloride
kg	kilogram
Lif	Leukemia Inhibitory Factor
LMW	Low Molecular Weight
LPR	Late Phase Response
LPS	Lipopolysaccharide
Ltd 4	Leukotriene D4
MAPK	Mitogen-activated Protein Kinase
mbar	millibar
Mch	Methacholine
MEM	Minimum Essential Medium
mg	milli gram
$MgSO_4$	Magnesium sulfate
MIP-1A	Macrophage Inflammatory Protein 1A
MIP-2	Macrophage Inflammatory Protein 2
ml	millilitre
MLCK	Myosin Light Chain Kinase
mm	milli metres
mmHg	millimetre of Mercury
MMP	Matrix Metalloproteinase
MTT	(3-(4,5-Dimethylthiazol-2-yl)-2,5-diphenyltetrazolium bromide
Na/K-ATPase	Sodium/Kaium-ATPase
Na^+	$Sodium^+$
NaCl	Sodiumchloride
NaH_2PO_4	Monosdiumphosphate
$NaHCO_3$	Sodium hydrogene carbonate
NFκB	nuclear factor kappa-light-chain-enhancer of activated B cells

nm	nano metres
nM	nano molar
NO	Nitric Oxide
n. s.	non significant
p38	protein 38
PAF	Platelet-activating Factor
PaO_2:FiO_2	Partial pressure of arterial O_2:Fraction of inspired O_2
PCLS	Precision-cut Lung Slices
PDE_4	Phosphodiesterase 4
PDMS	Polydimethylsiloxane
PEEP	Positive End-Expiratory Pressure
PenH	Enhanced Pause
PIP_2	Phosphatidylinositol-4,5-bisphosphate
PKC	Protein kinase C
PLCγ	Phospholipase C γ
PVC	Pressure Controlled Ventilation
RAR	Rapidly Adapting Receptor
RNA	ribonucleic acid
ROCK	Rho-associated, Coiled-coil Containing Protein Kinase
RTq-PCR	Real-time Reverse-transcription PCR
SAPK	Stress-Activated Protein Kinase
SD	Standard Deviation
SEM	Standard Error of the Mean
Ser	Serotonin
SH2	Src Homology 2
Src	Sarcoma
SRE	Stretch Response Element
STAT	Signal Transducers and Activators of Transcription
Th1/2	T helper 1/2
TLR	Toll-like Receptor
TMA	Trimellitic anhydrate
TNFα	Tumor Necrosis Factor alpha
TP-receptor	Thromboxane Receptor
TRPA	Transient Receptor Potential Cation Channel, Subfamily A
TRPV	Transient Receptor Potential Vanilloid
VILI	Ventilator Induced Lung Injury

1. Introduction

1.1. Toxicity in the lungs

The degree to which a substance is able to damage an exposed organism is defined by the term toxicity. This toxicity can further be specified by the way the organism is affected by the toxicant. It can either affect the whole organism, as well as substructures like cells (cytotoxicity) or specific organs. Referring to the lungs toxicity towards the organ can be classified in two ways: the route of exposure and the source of the toxicant. As the lungs constitute the blood/air interface, the possible routes of exposure are via the cardiovascular system and by inhalation. Among the possible sources, the two most important groups are chemical substances and physical stimuli.

1.1.1. Chemical substances

1.1.1.1. Xenobiotics

Xenobiotics are chemicals found in organisms, which are normally not present or endogeneously produced. The body removes xenobiotics by xenobiotic metabolism consisting of chemical modification and secretion (Fig. 1.1). Although the liver is considered to be the most important organ in drug metabolism, other organs like the lungs can contribute significantly to the biotransformation of a compound in the body. Biotransformation is the process by which cells modify xenobiotics to facilitate the elimination of lipophilic substances to avoid accumulation in cell lipids. This biotransformation is maintained by mostly unspecific enzymes which can be found in the membranes of the endoplasmatic reticulum and mitochondria or unaffiliated in the cytoplasm. In a first step the xenobiotic is oxygenised, reduced or hydrolysed by phase I enzymes resulting in the appearance of more polar and reactive functional groups in the molecule (179). The hemoproteins encoded by the CYP genes (cytochrome P450-depending monooxygenases) are considered to be the most actively involved phase I enzymes and their expression pattern in the lung is well characterised (35). In general, biotransformation reactions are beneficial, although sometimes these enzymes transform otherwise harmless substances into more reactive intermediates, a process known as bioactivation. A classic example is the bioactivation of benzo(a)

pyrene into reactive forms capable of generating DNA adducts eventually leading to cancer formation in the lung (35).

The process is followed by a conjugation with endogenous molecules such as glucuronic acid, glutathione, sulphate and amino acids (Phase II reactions). Linking the xenobiotic to compounds produced by the organism allows renal or biliary secretion (179).

Situated at the air/blood interface the lung is a prominent target organ for chemically induced damage resulting from exposure to xenobiotics after inhalation or accumulation in the lung following systemic administration. Biotransformation depends on the amount and activity of transporting and metabolising enzymes present. Bronchial epithelial cells, alveolar epithelial cells, alveolar macrophages and Clara cells seem to be the most important cells for xenobiotic metabolism and toxicity. They possess a variety of metabolising enzymes and especially Clara cells show a high amount of cytochrome P450 mediated metabolism (35; 115).

Some examples of harmful chemicals to which the lung is accidentally or occupationally exposed by inhalation are polycyclic aromatic hydrocarbons, aromatic amines, halogenated compounds, aliphatic compounds, aldehydes and ketones (35).

Lung toxicity was mainly studied in relation to mutagenic and carcinogenic compounds from tobacco smoke (89). In addition, a specific lung toxicant due to particular
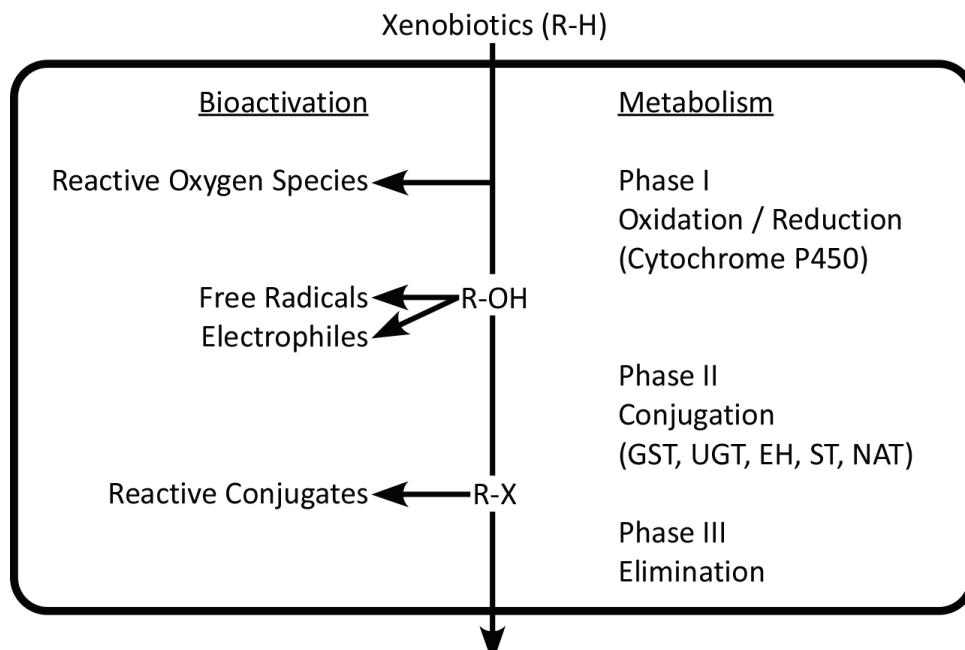
Figure 1.1: Simplified scheme of metabolism and bioactivation of xenobiotics. From reference (35). GST = glutathion S-transferase, UGT = UDP-glucuronyltransferase, EH = epoxide hydrolase, ST = sulphotransferase, NAT = N-acetyltransferase.

accumulation is the widely used herbicide paraquat. Other specific lung toxicants that have been studied are 4-ipomeanol, bleomycin, naphthalene and dichloroethylene (89).

1.1.1.2. Allergens and mediators

Atopic individuals respond to common, environmental antigens with an inappropriate IgE-production leading to hypersensitivity. IgE binds to the high affinity Fcε-receptor on mast cells (which can be found in the tissue at entry sites), circulating basophils and activated eosinophils (177).

Cross-linking of the bound IgE activates mast cells characterised by a degranulation which occurs within seconds (22). Histamine as one of the preformed mediators enhances vascular permeability and contracts smooth muscles (104). Mast cell derived enzymes like chymase, tryptase and serine esterases activate matrix-metalloproteases which alter matrix proteins and TNFα activates endothelial cells. Besides preformed mediators mast cells newly synthesise and secrete a variety of mediators (177): Chemokines (MIP-1a), PAF and cytokines (IL-4, IL-13, IL-3, IL-5, GM-CSF and TNFα) maintain the acute and chronic inflammatory response by attraction of other inflammatory cells like T-lymphocytes, basophils and eosinophils (177). Arachidonic acid is produced from membrane phospholipids and metabolised to prostaglandins, thromboxanes and leukotrienes (176). These lipid mediators cause bronchoconstriction, vasoconstriction, enhanced vascular permeability and stimulate mucus secretion intensifying the inflammatory response.

Mast cell mediators and Th2-cytokines, namely IL-5, Eotaxin-1 and -2, accumulate and activate eosinophils and basophils which secrete a wide range of toxic proteins and enzymes in addition to cytokines, chemokines and lipid mediators (177).

The inflammatory response to an allergen occurs in two phases: the early allergic response and the late phase response. The early allergic response develops as a consequence of released and synthesised toxic mediators from mast cells resulting in enhanced vascular permeability and bronchoconstriction (177).

Induced synthesis of leukotrienes, chemokines and cytokines in activated mast cells trigger the late phase response by mobilising leukocytes like eosinophils and Th2-lymphocytes to the focus of inflammation. The late phase response is characterised by a second contraction of the smooth muscle, ongoing edema and promotes the formation of airway hyperresponsiveness. The hyperresponsiveness to unspecific stimuli is often due to chronic inflammation of the airways even in the absence of the allergen (177).

The most severe symptom of allergic asthma, which can become life-threatening, is constriction of the airways with airflow limitations. Reversibility of these airway obstructions is often only possible by treatment with ß-agonists or steroids as long term medication.
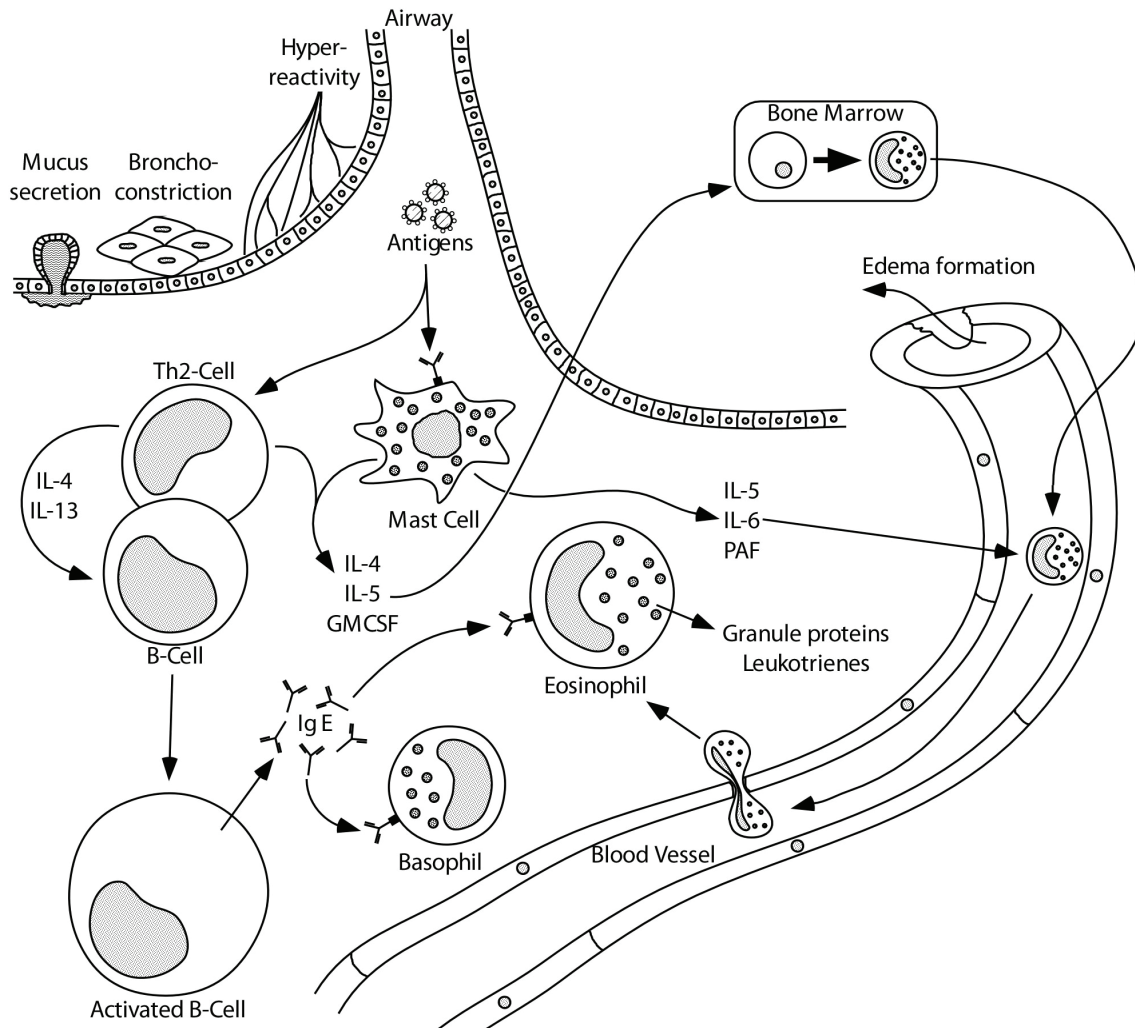
Figure 1.2: Simplified scheme of allergen exposure and airway inflammation. Degranulating mast cells and activated Th2-cells recruit leukocytes from the blood via transmigration. Released histamine and leukotriene leads to bronchoconstriction, mucus secretion and hyperreactivity of the airway. Activated B cells produce and release IgE. Secreted granule proteins of eosinophils injure the airway.

1.1.1.3. Clinical relevance: Asthma bronchiale

Asthma bronchiale is one of the most common types of occupational lung diseases in developed countries. In Germany 10 % of the children and 5 % of the adult population develop asthma bronchiale (218). A wide range of industrial chemicals can induce such respiratory allergic reactions and lead to the manifestation of occupational asthma. Industrial organic chemicals like toluene isocyanate, reactive dyes and acid anhydrides, such as trimellitic anhydride (TMA) are already known or are suspected to cause respiratory allergy and occupational asthma (17; 257; 313). Whereas the specific mechanisms of the respiratory sensitisation by such chemicals are still not fully elucidated hypersensitivity seems to be associated with the development of a Th2-profile (11; 61; 62). Skin sensitisers, such as 2, 4-dinitrochlorobenzene, normally

induce a Th1 cytokine phenotype (59; 105; 277). Nevertheless some skin sensitisers, e.g. dinitrofluorobenzene and trinitrochlorobenzene, are able to induce an IgE-independent hyperreactivity (32; 82-84).

1.1.2. Physical toxic stimuli

1.1.2.1. Mechanical forces in the lung

The lung is subjected to varying mechanical forces throughout development and life. Lung cells in their complex three-dimensional structure are exposed to different physical forces. Strain (change in length in relation to the initial length), stress (force per unit area), hydrostatic pressure and shear stress (force per unit surface area in the direction of flow exerted at the fluid/surface interface) are of capital importance in the lung. While cells of the alveolar walls and the epithelium are primarily subjected to stress and strain, shear forces appear mostly in the vascular endothelium (301).

Sensing physical stimuli is therefore a crucial mechanism to assure adequate lung functions. Airway sensors constantly transmit mechanical changes through vagal and other afferent pathways to the central nervous system to evoke reflex responses. Such specialised mechanoreceptors called rapidly adapting receptors (RARs) occur throughout the respiratory tract from the nose to the bronchi (99; 308). Besides these specialised structures there are mechanosensors localised on the cytoplasmic membrane that are able to respond to mechanical forces applied to cells or generated internally. Mechanosensors comprise stretch-activated ion channels, the extracellular matrix-integrin-cytoskeleton network, growth factor receptors and cell-cell adhesion molecules (99).

However, quantification of the extent to which different cell types undergo mechanical deformation is complicated. The kind of forces which are relevant in alveolar regions during breathing is still under discussion. Besides the notion that alveoli may extend during breathing, it has also been suggested that the inspired air flows in newly recruited airways, into ducti alveolares (34) or into recruited alveoli (73; 112; 254).

Physical forces during mechanical ventilation gain importance in association with pathophysiologic processes in injured lungs. Components that are associated with the so called ventilation-induced lung injury (VILI) are high tidal volumes and pressures (volutrauma, barotrauma), release of mediators leading to activation of inflammatory pathways (biotrauma) and repeated opening and closure of alveolar units (atelectotrauma) (201; 270).

Heterogeneity of the injured lung reduces the lung volume and predisposes the lung to mechanical forces which are physiologically abnormal. This is especially important when local distending forces differ to oppose heterogeneity and to restore lung expansion.

In general, the mechanical forces applied during ventilation can injure the lung in two ways: by physical disruption or activation of cytotoxic or proinflammatory responses.

1.1.2.2. Barrier disruption

The alveolar-capillary barrier is formed by the microvascular endothelium and the alveolar epithelium. To allow adequate gas exchange the alveolar-capillary membrane has to be extremely thin, resulting in an alveolar septum of 5 to 8 µm. Two different cell types form the alveolar epithelium: Flat alveolar type I cells which line 90% of the alveolus area and cuboidal type II cells functioning mainly as surfactant producing and secreting cells besides their function in ion transport. Alveolar type I cells may undergo extensive necrosis during lung injury. To a certain extend alveolar type II cells are capable of differentiation into type I cells to regenerate the epithelium. Consequences arising out of the loss of epithelial integrity are numerous. Normally the epithelial barrier is much less permeable than the endothelium which prevents leakage of fluid into the alveolus (295). Epithelial injury can therefore contribute to alveolar flooding (287). Injury to alveolar type II cells impairs the normal function to remove the fluid and furthermore reduces surfanctant production (91; 143).

The phenotype of alveolar type I cells being fragile in response to stretch in combination with the recruitment of inflammatory and reparative cells can lead to insufficent epithelial repair. The formation of hyaline membranes in alveolar walls and healing under profibrotic conditions can be the consequence (201; 287). Mechanical ventilation exposes the endothelium and the alveolar epithelial cells to relatively high wall stress. This induces also tensile strain and shear forces in the lung. Stress failure of capillaries occurs at high transmural pressures and high lung volumes probably due to increased longitudinal forces (79). Mechanical strain reduces the active sodium transport-dependent clearance of edema fluid from the airspaces. By filling alveoli and airways and additional inactivating surfactant the lung volume is reduced. Hence heterogeneity of the lung is promoted and results in greater overdistension of the remaining lung units accompanied with greater shear stress (79). Disruption of the alveolar-capillary barrier and increased permeability is an important mechanism responsible for the formation of alveolar edema. Release of inflammatory mediators into the circulation as a result of the loss of compartmentalisation is suspected to play a role in multisystem organ failure (79; 201).

1.1.2.3. Inflammation

A potential mechanism of ventilator-induced lung injury is the increased inflammation in response to mechanical stimuli. Overventilation activates canonical inflammation pathways in alveolar epithelial and endothelial cells by activation of transcription factors, such as NFκB. Cytokines (e.g. IL-1ß, TNFa, IL-6), chemokines (e.g. IL-8) and adhesion molecules are produced to recruit inflammatory cells into the airspace and bloodstream. Besides macrophages especially neutrophils seem to play an important role in the pathogenesis of acute lung injury (79; 201; 270).

1.1.2.4. Clinical relevance: ALI and ARDS

Acute Lung Injury (ALI) and Acute Respiratory Distress Syndrome (ARDS) are life-threatening disorders accompanied with a high mortality (2). They are characterised by a diffuse inflammation of the lung parenchyma triggered by an initial release of inflammatory mediators from endothelial and epithelial cells. Undefined alveolar damage leads to hypoxia and frequently to multiple organ failure.

In 1994 a new definition was recommended by the American-European Consensus Conference Committee. Since then ARDS is characterised by an acute onset, bilateral infiltrates on chest radiography and a pulmonary-artery wedge pressure of ≤ 18 mmHg or the absence of clinical evidence of left atrial hypertension. ARDS is considered to be present if PaO_2:$FiO_2 \leq 200$ mmHg, if the PaO_2:FiO_2 is ≤ 300 mmHg ALI is indicated, a milder form of ARDS considered as a precursor (287).

ARDS is a severe lung disease caused by a variety of clinical disorders that cause direct or indirect lung injury. Direct lung injury may be caused by pneumonia or the aspiration of the gastric contents, while indirect lung injury is caused in the setting of a systemic process such as sepsis or severe trauma.

In spite of the advances in supportive care and research a high morbidity accompanied by a high mortality remains. Only one phase III trial study publicated in 2000 by the ARDSnet ever showed a significant reduction of mortality, i. e. from 39.8 % to 31 % by reducing the tidal volume from the conventional 12 ml/kg to 6 ml/kg (2).

Although indispensable, mechanical ventilation of patients with respiratory failure has still adverse effects (79; 201). Lungs of ARDS patients are typically injured inhomogeneously which leads to overexpansion of intact lung areas. This overexpansion is assumed to cause ventilator-induced lung injury – both mechanically and by activation of the innate immune system (Biotrauma hypothesis) (68; 95).

1.1.2.5. Biotrauma hypothesis

The leading cause of death in patients with ARDS is the sepsis syndrome and multiple organ dysfunction syndrome rather than respiratory failure (170). Mechanical ventilation seems to be one factor responsible for this negative association (239). A number of animal and clinical studies have shown that mechanical ventilation per se can worsen pre-existing lung injury and produce VILI (69; 156; 201; 203; 263). The mechanism how mechanical ventilation exerts its detrimental effect is still unclear. Overdistension of the lung and shear forces generated during repetetive opening and collapse of atelectic regions exacerbate, or even initiates, lung injury and inflammation (67). Usually stretch is not pathologic for the lung and actually an important factor for lung growth and development, and for surfactant production (301). The altered pattern or magnitude of the lung stretch during mechanical ventilation could lead to alterations in gene expression and cell metabolism and to an upregulation of an inflammatory response (67; 263). Clinical studies and animal experiments support the hypothesis evidencing the release of proinflammatory mediators by hyperventilation correlating with multiple organ failure (116; 215; 252; 270; 283). Loss of compartmentalisation of the pulmonary response could trigger the release of inflammatory mediators in the systemic circulation followed by a compensatory anti-inflammatory response. The incapability of the organism for immune modulation or the persisting pulmonary injury may eventually lead to death (67).

Until today the mechanosensor in stretched lung tissue has not been conclusively identified. However, the transient receptor potential vanilloid-4 (TRPV4) channel may act as mechanosensitive cation channel (96). Dos Santos et al. suggested some mechanisms of mechanotransduction involving ion-channels, plasma membrane integrity and direct conformational changes in membrane associated molecules (Fig. 1.3).
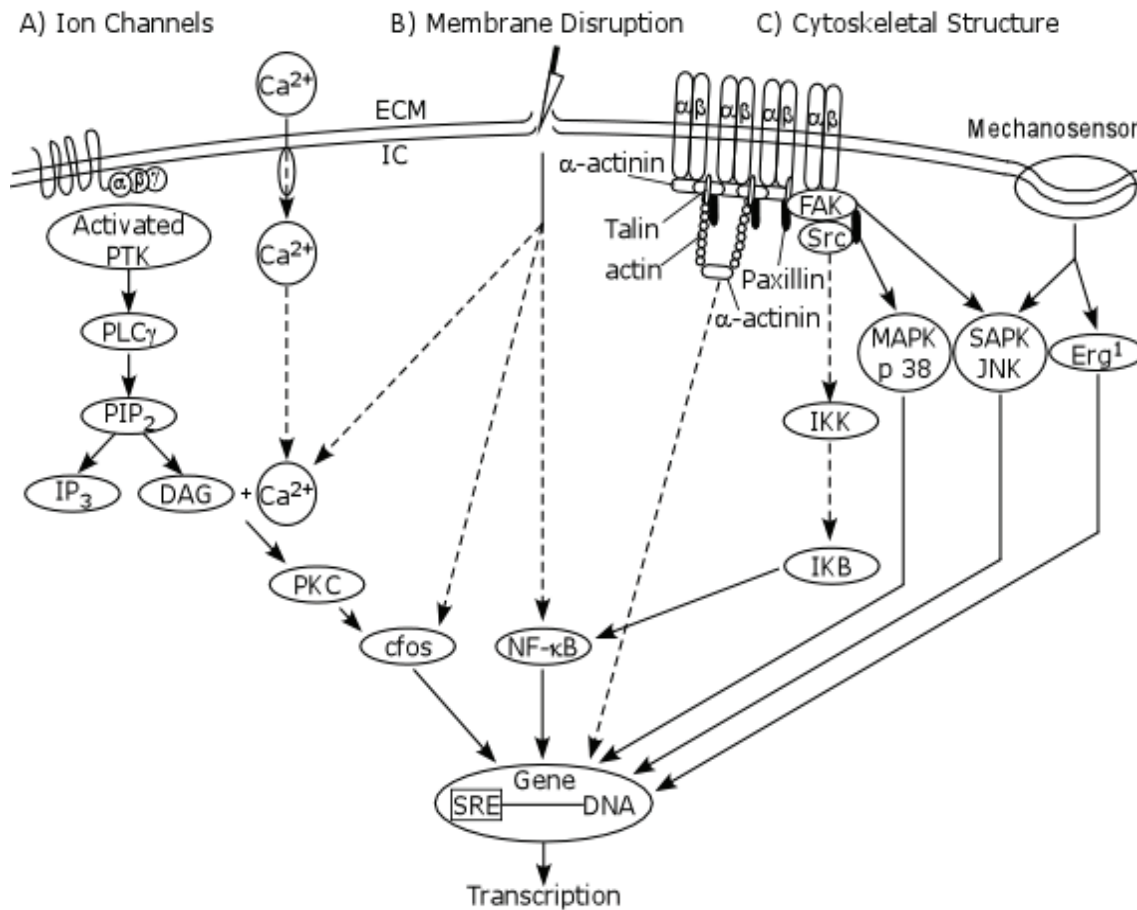
Figure 1.3: Putative mechanisms of mechanotransduction in VILI. Adopted from Reference (67). Activation of "stretch response elements" (SRE) via (A) mechanosensitive cation channels, calcium mobilisation and activation of the protein kinase C (PKC), (B) membrane disruption and calcium mobilisation, cfos and NFkB activation, (C) cytoskeletal structure with integrin mediated activation of mitogen-activated kinases and transcription factors. PLCγ = Phospholipase C γ; PIP_2 = Phosphatidylinositol-4,5-bisphosphate; IP_3 = Inositol trisphosphate; DAG = Diacetylglycerol; MAPK = Mitogen-activated protein kinase; SAPK = Stress-activated protein kinase; NFκB = nuclear factor kappa-light-chain enhancer of activated B cells.

Crucial signal transduction pathways that have been identified include the activation of NFkB, mitogen-activated protein kinases, Elk-1, ATF2, AP-1 and phosphoinositide-3-kinase (107; 132; 144; 146; 271; 272). This indicates that mechanical ventilation activates largely the same inflammatory mediators as microorganisms. To find appropriate therapeutical targets without altering the immune status of the patient it is important to identify proteins and genes selectively upregulated by overventilation (Fig. 1.4). Gene arrays adressed to this question tagged such genes and identified proteins such as amphiregulin (65).
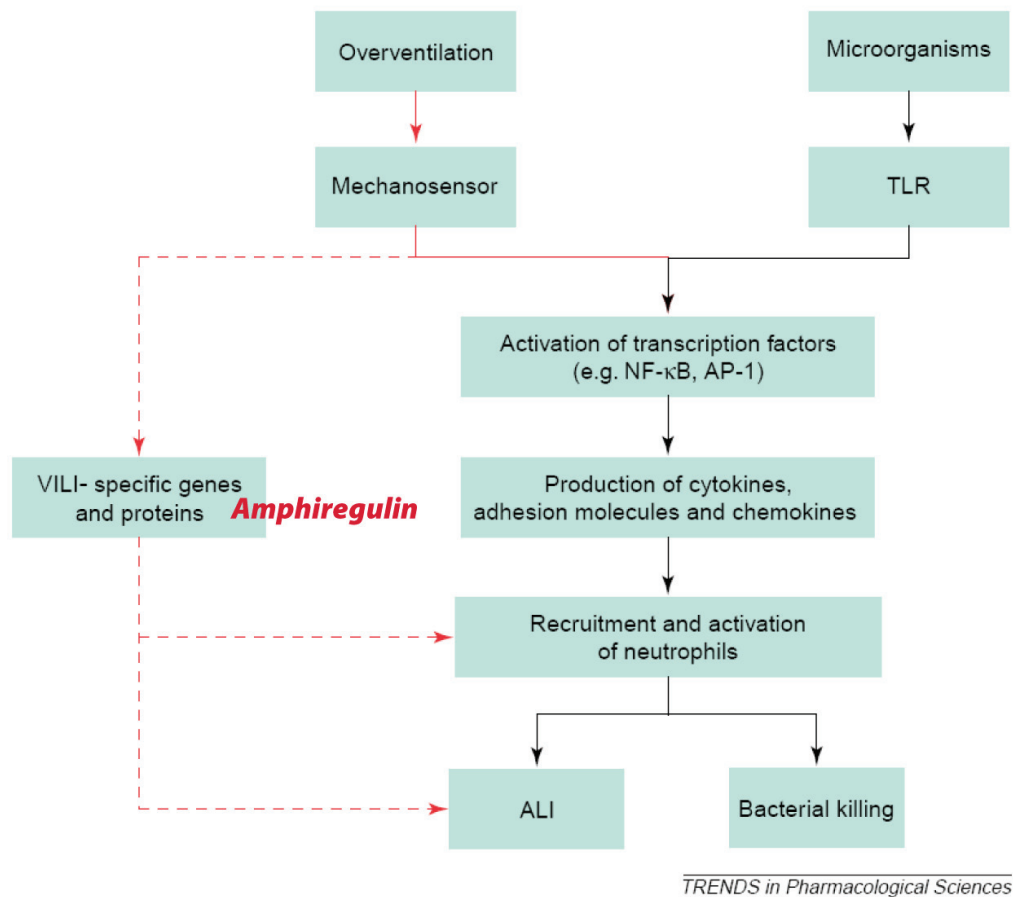
Figure 1.4: Initiation of ALI by both microorganisms and overventilation of lung tissue. VILI-specific genes, such as amphiregulin, and proteins may act as specific marker genes/proteins. VILI = ventilator-induced lung injury; TLR = Toll-like receptor; ALI = Acute lung injury. From Reference (270).

1.1.2.6. Amphiregulin

Amphiregulin, a polypeptide growth factor which belongs to the epidermal growth factor family, is a ligand of the receptor tyrosine kinase Erb B1 (49). It promotes the growth of keratinocytes and fibroblasts, which may play a role in mast cell mediated lung fibrosis (286). Most amphiregulin studies address its participation in cancer, especially in breast and lung cancer (122; 159; 297). Apart from mechanical stress amphiregulin is also upregulated by oxidative stress (hyperoxia) (258; 284).

Amphiregulin is a membrane-anchored protein which is cleaved by matrix-metalloproteinases like ADAM 17 (a disintegrin and metalloproteinase), a process referred to as "shedding" (228). In its soluble form amphiregulin can bind to Erb B1, which autophosphorylates key tyrosine residues. These tyrosine phosphorylated sites allow proteins to bind through their Src homology 2 (SH2) domains and leads to the

activation of downstream signalling cascades including the RAS/extracellular signal regulated kinase (ERK) pathway, the phosphatidylinositide 3-kinase (PI$_3$) pathway and the Janus kinase/Signal transducer and activator of transcription (JAK/ STAT) pathway. Activation of MAP kinases, PI$_3$ and transcription factors has been demonstrated in cell culture experiments (55; 193; 266). In addition cell culture experiments demonstrated that mechanical stretch activates Erb B1 via amphiregulin shedding (193) and revealed amphiregulin release as a mediator of TNFα-induced IL8-secretion (45).

1.2. Precision-cut lung slices (PCLS)

Organ slices have been used as an *in vitro* model for toxicological and biochemical studies for a long time. They represent an organ "mini-model" that closely resembles the organ from which it is prepared, with all cell types present in their original tissue-matrix configuration. The production of organ slices has been benefited enviromentally by the introduction of precision-cut tissue slices. Earlier techniques using manual equipment suffered from a lack of reproducibility within the slices and a relatively limited viability (194). In 1980 Krumdieck et al. overcame this problem by introducing an automated, mechanical tissue slicer (131). It allowed the production of relatively thin (200-500 µm) and identical slices providing an appropriate supply with gas and nutrient exchange by diffusion. Originally established for the production of liver slices the technique was adapted to other tissues such as kidney, heart and lung.

The precision-cut lung slice technique was introduced by Stefaniak et al. in 1992 (248). Compared to the relatively compact liver tissue the lung parenchyma is much softer due to its function as a dynamic organ. Although lung slices have been used as an *in vitro* system before the precision-cut slice technique together with filling the lung with low melting point agarose prior to the slicing process, improved the quality of lung slices.

The long-term maintenance of lung slices cultured in defined media was described shortly after by Siminsky et al. (237).

1.2.1. PCLS from different species

PCLS can be prepared from different mammals. The first lung slices were prepared from rat lungs followed later by human lungs (77; 248). Human lung tissue can be obtained from lung donors or from cancer patients undergoing surgery. Since then the technique has been expanded to different species such as mice (208), hamsters (221), guinea pigs (218), rabbits (238), cattle (88), horses (279) and monkeys (120; 217).

1.2.2. PCLS as an *in vitro* model

Using PCLS as a model has many advantages. First, up to 50 slices can be prepared from one lung. This does not only save animals but also helps to reduce experimental error by internal controls and statistical pairing (217). In contrast to cell cultures the anatomical structure of the lung is preserved. That means that not only one or two cell types of the lung are studied but the complete variety of lung cells embedded in their normal extracellular matrix environment. This is especially of interest in the context of cell stretch. The role of the extracellular matrix (e.g. integrins) as a stretch sensor has been under discussion for some time now (46; 99; 119; 123; 185; 209; 264). The intact microanatomy also allows for auxotonic smooth muscle contraction which may be closer to the *in vivo* situation than other *in vitro* methods, such as isotonic or isometric contractions (217). Another advantage of the model is that it provides the opportunity to study physiological responses in the same model in different species. This could be particularly useful in regard to species differences between animals and humans (51; 217; 265).

1.2.2.1. The use of PCLS in metabolism and toxicology

Lung slices are a useful tool for studying lung metabolism and toxicology because of the speed and simplicity of slice preparation. Several slices from one lung may be studied simultaneously avoiding experimental variations and decreasing animal numbers. Toxicities of paraquat, 3-methylindole and 1-nitronaphthalene to rat PCLS were the first to be investigated by Price et al. in 1995 using potassium content and protein synthesis as viability parameters (207). Shortly after, the use of human PCLS was demonstrated by exposing them to the pulmonary toxicants acrolein and nitrofurantoin (77). Until today especially rat PCLS have been extensively used to study pulmonary toxicants and to some extend they have been compared with cell culture experiments (169; 207). In addition, the pulmonary metabolism and the resulting effect to enzyme activity has been studied in PCLS for xenobiotics such as 7-ethoxycoumarin, diesel exhausts or jet fuel (106; 140; 205). Table 1.1 summarises the use of PCLS in metabolism and toxicology. Another application is the use of PCLS to study pathological mechanisms after exposure to viruses, cytokines or metabolites (70; 88; 111; 125).

Table 1.1: Metabolism and toxicological studies in PCLS.

Substance	Species	Process investigated (Reference)
[Ring-U-14C] Agaritine	Rat, mouse	Metabolism (208)
1-methylphenanthrene	Rat	GST activity, CYP1 induction/apoprotein-/ mRNA-levels, epoxide hydrolase activity (210; 212; 213)
1-nitronaphthalene	Rat	Viability by protein synthesis, potassium content (207)
3-methylindole	Rat	Viability by protein synthesis, potassium content (207)
4-(methylnitrosamino)-1-(3-pyridyl)-1-butanol	Hamster	Metabolism (221)
4-(methylnitrosamino)-1-(3-pyridyl)-1-butanone	Hamster	Metabolism (221)
7-Ethoxycoumarin	Rat, mouse, human	Metabolism, metabolic clearance, metabolic viability (57; 58; 205; 208; 273)
7-Hydroxycoumarin	Human, rat	Metabolism, metabolic clearance (57; 58)
Acrolein	Human, rat	Viability by protein synthesis (77; 169)
Aroclor 1254	Rat	mRNA expression of CYP forms, CYP1A induction (136; 206)
Arsenite	Rat	Immediate early gene expression (296)
Beclomethasone dipropionate	Human	Metabolism (181)
Benzo(a)pyrene	Rat	Induction of CYP forms, mRNA and apoprotein levels, DNA adducts, epoxide hydrolase activity (102; 103; 136; 206; 210-213)
Benzo(b)fluoranthene	Rat	CYP1 induction, mRNA and apoprotein levels, epoxide hydrolase activity, GST activity (210; 212; 213)
Budenoside	Human	Metabolism (181)
Ciclesonide	Human	Metabolism (181)
Cigarette smoke	Guinea pig	Endothelial dysfunction (305)
Cotinine	Rat	CYP1A form induction (206)
Coumarin	Rat	Metabolism (205)
Dibenzo(a,h)anthracene	Rat	CYP1 induction, mRNA and apoprotein levels, epoxide hydrolase activity, GST activity (210; 212; 213)
Dibenzo(a,l)pyrene	Rat	CYP1 induction, mRNA and apoprotein levels, epoxide hydrolase activity, GST activity (210; 212; 213)
Diesel exhaust	Rat	Toxicity by DNA alterations, inflammatory response (140)
DNCB	Mouse	Ex-vivo lung functions (110)
Erucin	Rat	Modulation of pulmonary carcinogen-metabolising enzyme system (101)
Fluoranthene	Rat	CYP1 induction, mRNA and apoprotein levels, epoxide hydrolase activity, GST activity (210; 212; 213)
Fluticasone propionate	Human	Metabolism (181)
Jet Propulsion Fuel-8	Rat	Toxicity by ATP content (106)
Lidocaine	Human, rat	Metabolism (57)
Methyltestosterone	Rat	Metabolic clearance (58)
Nicotine	Rat	CYP1A form induction (206)
Nitrofurantoin	Human	Viability by protein synthesis, NPSH (77)
Paraquat	Rat	Viability by protein synthesis, potassium content (207)
ß-naphthoflavone	Rat	mRNA expression of pulmonary CYP forms, CYP1A form induction (136; 206)
Sulphoraphane	Rat	Modulation of pulmonary carcinogen-metabolising enzyme system (101)
Testosterone	Human, rat	Metabolism, metabolic clearance (57; 58)
TMA	Mouse	Ex-vivo lung functions (110)
Warfarin	Rat	Metabolic clearance (58)

1.2.2.2. The use of PCLS in pharmacology

In 1995 Martin et al. introduced rat PCLS as a model for pharmacological studies of airways (153). Bronchoconstriction of single airways in response to mediators such as methacholine was measured and analysed using videomicroscopy. These studies were extended to different species (mice, human) and to various airway sizes addressing also peripheral airways (155; 304). The measurement of vasoconstriction was also established in PCLS (108). Besides responses to endogenous and exogenous stimuli, broncho- or vasoconstriction in PCLS has been compared to other *in vitro* models like the isolated perfused and ventilated mouse and rat lung (108; 152) or invasive pulmonary tests *in vivo* (110). PCLS have become an important *ex vivo* alternative to *in vivo* respiratory measurements of bronchoconstriction to allergens. For example, the immediate allergic response of the airways was assessed in lung slices of ovalbumin-sensitised animals or in passively sensitised lung slices of naïve animals (303; 304). In connection with asthma bronchoconstriction in PCLS has been used as a model to study clinical properties of β2-adrenoceptor-agonists (53; 182; 253) or PDE4-inhibitors (151).

1.2.2.3. The use of PCLS in signalling mechanisms

Lung slices have been successfully employed in the study of mediators and mechanisms involved in airway contraction (133; 134; 152; 155; 172; 200; 246; 251; 303; 304). Furthermore, calcium signalling in smooth muscle cells of the airways can be studied (12). Besides mechanistic investigations of bronchoconstriction PCLS have also become a valuable tool for studying pathomechanisms of vascular diseases like pulmonary hypertension (191; 245; 247). PCLS also provide a convenient method to study local immune reactions of biologically active agents (111).

1.3. Experimental models

1.3.1. Models of lung toxicity and metabolism

In vivo studies of lung metabolism and toxicology are complicated because of the relative small mass of lung tissue and an enormous blood flow. This makes it difficult to measure arteriovenous differences of most circulating metabolites. Systemic influences such as infiltration of phagocytic cells or formation of immune complexes

at the site of injury aggravate the complexicity of such *in vivo* studies (81). For drug development it is indispensable to use experimental animals to determine the major toxicities of a new compound, since only in an intact organism the complex interplay of metabolism and drug exposure can be examined.

Apart from the *in vivo* methods many *in vitro* systems have been developed. The isolated perfused mouse or rat lung maintains the lung as a whole organ. The lung is perfused with whole blood or substituted media via the pulmonary artery of artificially ventilated lungs. Uptake, metabolism and disposition can be examined as well as the interaction of exogenous and endogenous substances and their interactions (164; 302). Other *in vitro* studies include lung subcellular fractions, homogenates, homogenous populations of isolated or cultured cells, and mixed cell organ cultures.

Different cellular models from human pulmonary origin have been developed as experimental model to investigate the effect of xenobiotics on human lung (309). The best characterised and most widely used model probably is the adenocarcinoma A549 cell line, derived from pneumocytes type II, and the pulmonary adenocarcinoma NCI-H322, derived from bronchiolar Clara cells (6; 35). Although these cell lines express only a limited number of the phase I and phase II enzymes involved in detoxification or bioactivation, especially the A549 cells are considered to be a useful in vitro model. However, the use of lung tissue slices has always been viewed as an appropriate alternative to whole lung or cell culture models, even before the precision-cut lung slice technique (81). Especially the absence of cell-cell and cell-matrix connections in cell culture is an issue and may result in a loss of differentiated functions. Therefore *in vivo* metabolism may be mimicked by lung slices, where the number of animals required is decreased.

1.3.2. Models of allergy and asthma

1.3.2.1. *In vivo* asthma models

Studying asthma in human asthma patients is only possible to a certain extent. Bronchoalveolar lavage fluid and bronchial biopsies can be analysed in asthmatic patients after allergen challenge. Experiments of such kind have given some insight into cells and mediators playing a role in asthma (27; 184; 290). However, clinical settings can only reflect parts of asthma, bronchoconstriction for example can only be determined indirectly by measuring the FEV1 (forced expiratory volume in 1 second). Aside from being unpleasant such experiments are frequently some risk for the patient.

One class of *in vivo* models of asthma is represented by animals with naturally occurring recurrent airway obstruction (217). Cats for example spontaneously develop eosinophilic airway inflammation and airway hyperreactivity, the so called feline asthma. It is characterised by dyspnea, wheezing, cough and hyperplasia of submucosal glands, proliferation of goblet cells and smooth muscle hypertrophy (174). Exposure to inhaled aeroallergens showed allergen-specific IgE-production, airway hyperreactivity, eosinophilia and a Th2-cytokine profile in the BAL (187). Pathophysiological studies suggest important similarities between human and feline responses to inhaled allergens which need to be further examined (187; 216).

In principal, ponies can develop heaves, also characterised by recurrent airway obstruction, when they are housed in barns and fed with hay (64). It is featured by lower airway inflammation, bronchoconstriction and mucus accumulation (141). Clinical signs alternate with remission periods, which is comparable to some forms of industrial asthma in which hyperreactivity occurs only in acute airway obstruction (64). Basenji-Greyhound crossbred dogs show a nonspecific bronchial hyperreactivity to stimuli like metacholine or citric acid without allergen challenge. Being a main characteristic of human asthma this airway hyperresponsiveness makes them a useful tool to study specifically that part of asthma (113; 190).

Besides naturally occurent recurrent airway obstruction and AHR without provocation there are several models of airway obstruction and AHR after allergen sensitisation and challenge. Most models represent certain aspects of asthma. The range of animal models available is vast, with the most popular models being rodents, such as rats and mice, and guinea pigs. Compared with other models these are easy to handle and relatively cost effective (315). Rats have been used to study allergen-induced bronchoconstriction, eosinophilic inflammation, LPR, AHR and airway remodeling. Mice are in general an attractive model because of their well known immune system and the availibility of knock-out or transgenic strains. After sensitisation mice develop eosinophilia, AHR, increased IgE-levels, mucus hypersecretion and sometimes airway remodeling. Nevertheless the discrepancy in immunology and anatomy between mice and humans must be recognised (315). Airway anatomy and the response to inflammatory mediators of the guinea pig are similar to humans (220). It is characterised by a direct anaphylactic bronchoconstriction upon allergen challenge, LPR, AHR and an inflammatory response comparable with the human situation (220).

Some larger mammalian models using dogs, pigs, rabbits and sheep have been developed (315). Every one of them may address some aspects of human asthma more appropriate than the mouse model, but they also differ from humans in many ways and are extremely costly, with very few probes available (220; 315). The sheep model represents many pathophysiological properties of human allergic airway diseases. Sheep with a natural sensitivity to ascaris suum show an immediate EAR and a 6 to 8 hours delayed LPR after challenge with this antigen (4; 5; 244). AHR occurs mostly if

EAR and LPR were present before and especially the possible use of human relevant allergens like house dust mites makes this model promising (24; 137). Recently, even a model of airway remodelling in sheep has been developed (243).

1.3.2.2. *In vitro* asthma models

In vitro models concentrate on single physiological parameters of asthma. Most *in vitro* models involve small mammalian species to provide easy handling and cost efficiency. The closest *ex vivo* model to study allergic asthma may be the isolated perfused mouse, rat or guinea pig lung (108; 152; 234), where bronchoconstriction, vasoconstriction, edema and gas exchange can be investigated. Such systems allow better control, but do not save animals by using one lung per experiment.

Simplification of the whole lung can be achieved by tissue preparations cultured in organ baths (25; 124; 127; 202; 225; 231; 274). These preparations include parenchymal strips, isolated trachea or bronchi and vessels. They allow the examination of broncho- and vasoconstriction as well as smooth muscles. Since the tissue is separated from the surrounding tissue the comparison with the *in vivo* situation has remained difficult.

1.3.3. Models of physical stimuli

1.3.3.1. Clinical studies of mechanical ventilation

Acute respiratory distress syndrome was first described in 1967 (287). Since then a number of phase III, placebo-controlled clinical trials have been completed which had a significant impact on understanding the pathogenesis of ALI and ARDS, as well as providing evidence-based guidelines for better treatment of patients. Table 1.2 summarises some clinical studies and their outcome.

The possibility of ventilator-associated lung injury was first considered in the 1970 (288). Since then the most appropriate method of mechanical ventilation has been controversial. A variety of assumed lung protective strategies were investigated in clinical trials. The only intervention to date that has clearly shown a benefit in survival has been the 6 versus 12 kg/ml predicted body weight tidal volume trial which reduced mortality from 40 % to 31% (2). Follow-up studies with an increased PEEP to further improve the clinical outcome did not improve mortality (29). Several promising pharmacological therapies including surfactant, nitric oxide, glucocorticoids and lysofylline, have been studied in patients with acute lung injury and the acute

respiratory distress syndrome. However, none of these pharmacological treatments reduced mortality (38). Investigation of cytokines in clinical studies showed that ventilator settings influence pulmonary cytokine levels. Ranieri et al. found lower cytokine levels in BAL fluid of patients ventilated with low tidal volumes, which is consistent with the ARDSnet trial that found lower plasma IL-6 levels in the low tidal volume group (2; 215). In longitudinal studies higher cytokine levels were correlated with a worsened outcome (163).

Table 1.2: Different clinical trials of ARDS.

Description of trial	Number of patients	Year	Outcome	Reference
Extracorporeal membrane oxygenation	90	1979	No change in mortality	(312)
High-frequency jet ventilation	309	1983	No change in mortality	(33)
Prophylactic positive end-expiratory pressure (8cm of water)	92	1984	No benefit for patients at risk for ARDS	(197)
Glucocorticoids (during acute phase)	87	1987	No benefit	(21)
Extracorporeal removal of carbon dioxide	40	1994	No change in mortality	(173)
Surfactant	725	1996	No benefit	(8)
"Open-lung" approach (PEEP set by PVC)	53	1998	Decreased 28-day mortality but not in-hospital mortality	(7)
Low tidal volumes	120	1998	No benefit for patients at risk for ARDS	(250)
Low tidal volumes	116	1998	No change in mortality	(28)
Reduced tidal volumes	52	1999	No change in mortality	(30)
Low tidal volumes	861	2000	Mortality reduced from 40% to 31%	(2)
Lisofylline	235	2002	No benefit	(1)
Higher vs. lower level of PEEP	549	2004	No change in mortality	(29)
Glucocorticoid trial for persistent ARDS	180	2006	No change in mortality	(249)
Fluid and catheter treatment trial	1000	2006	No differences in clinical outcomes	(291; 294)
Low tidal volumes, recruitment maneuvers, high PEEP	983	2008	No change in mortality	(162)

1.3.3.2. *In vivo* models

In vivo models of ALI and mechanical ventilation have been studied in a variety of animals. Mice, rats, rabbits, dogs, sheep and pigs are most widely used. Most animal models of ALI are based on reproduction of human risk factors for ARDS, such as sepsis, lipid embolism, acid aspiration and ischemia reperfusion of pulmonary or distal vascular beds (158). Each of these risk factors has been tried to be reproduced in a variety of animals. The differences between each model and human lung injury as well

as the major advantages and disadvantages are outlined in Table 1.3. Models of ALI provide the opportunity to study mechanical ventilatory strategies in diseased lungs, known as two-hit models. Lots of studies dealt with the effect of PEEP, volume and pressure limits, and high frequency modes (16; 94; 280). Apart from the induction of ALI by risk factors, VILI can also be elicited solely by high tidal volume ventilation (298). Less complex ex-vivo models of VILI are represented by isolated lungs. This model is well established for rat (48; 219; 261; 262; 292) and mouse lungs (13; 43; 107; 283). Here, the experimental design focuses on ventilatory strategies alone (13; 43; 48), frequently in comparison with LPS (107; 219; 262; 292).

In almost all studies, cyclic overstretch increased alveolar levels of IL-8 or its rodent equivalent MIP-2. Depletion of Neutrophils in the lungs attenuated the IL-8 increase resulting in a model of less severe VILI (95). Wilson et al. related neutrophil recruitment in mice ventilated with high tidal volumes to increased levels of TNFα and MIP-2 in the BAL (298; 299). The critical role of neutrophil sequestration in mice was confirmed by Belperio et al. and connected to CXCR2 after a ventilation strategy of high peak pressure and stretch (19). IL-1β, IL-6 and to some extent TNFα were also induced in many studies (95). In general, cytokine levels seem to be higher with larger tidal volumes or absent PEEP or when animals are concomitantly subjected to other injurious strategies such as hyperoxia (13). Injured lungs seem to be far more susceptible to VILI than healthy lungs.

Table 1.3: Animal models of lung injury. From reference (158).

Model (Reference)	Similarities with ARDS	Differences with ARDS	Technical Issues
Oleic acid (233)	Acute and repair phases with similar histopathological and physiological features to human ARDS	Only a fraction of human ARDS is caused by fat embolism, does not model the physiopathology of septic ARDS	Good reproducibility Requires intravenous injection of oleic acid, which can be difficult in small animals
LPS (295)	Neutrophilic inflammatory response with increase in intrapulmonary cytokines	The changes in alveolar-capillary permeability are mild	Very reproducible
Acid aspiration (167)	Disruption of the alveolar/capillary barrier with neutrophilic infiltration	Humans aspirate gastric contents, not pure acid	Very reproducible Narrow difference between injurious and noninjurious doses
Hyperoxia (80)	Acute phase of epithelial injury and neutrophilic infiltration followed by type II cell proliferation and scarring	In normal human lungs, 100% oxygen has not induced lung injury; it is unclear whether hyperoxia is involved in the pathogenesis of ARDS	Good reproducibility Requires special equipment to administer and monitor the desired gas concentrations
Bleomycin (171)	Acute inflammatory injury followed by reversible fibrosis	No formation of hyaline membranes, physiopathological relevance unclear	Good reproducibility
Saline lavage (67; 135)	Depletion of surfactant Decreased lung compliance Impaired gas exchange	Without an additional stimulus, there is minimal impairment of permeability and little PMN recruitment	Animals must be anesthetized, intubated, and ventilated throughout the procedure and afterwards
Pulmonary ischemia/ reperfusion (229)	Increase in pulmonary vascular permeability PMN infiltration	The injury is usually hemorrhagic	Requires complex animal surgery
Nonpulmonary ischemia/ reperfusion (129)	Increased microvascular permeability and PMN sequestration in the lungs	The injury is mild, and the inflammatory component mostly limited to the interstitium	Requires complex surgery
Intravenous bacteria (56)	Interstitial edema, intravascular congestion, PMN sequestration	Minimal neutrophilic alveolitis; no hyaline membrane formation	Important biological variability
Intrapulmonary bacteria (78)	Increased permeability, interstitial edema, neutrophilic alveolitis	Positive cultures rare in early ARDS	Important biological variability
Peritonitis (157)	Increased permeability, variable degrees of neutrophilic alveolitis	Minimal hyaline membrane formation	Biological variability, lethal dose close to injury dose
Cecal ligation and puncture (281)	Increased permeability, variable neutrophilic alveolitis	Minimal hyaline membrane formation	Biological variability, surgery required

1.3.3.3. *In vitro* models

In vitro models of mechanostimulation can be divided in (i) stretching of lung tissue preparations, and (ii) stretching of lung cells.

1.3.3.4. Stretch of lung tissue preparations

Lung parenchymal strips have been widely used to investigate airway mechanics (52) and to measure dynamic properties of lung parenchyma (310). The strips can also be stretched. To this end, the tissue is attached to a clip on each side of the strip to stretch the strip vertically in an organ bath (255). Tanaka et al. used the technique to measure viscoelastic properties of rat lung strips dependent on maturation (255). Others found different magnitudes of stretch affecting elastance, tissue damping and tension (230). Using dog parenchymal strips Navajas et al. investigated the effect of nonlinear elasticity to the dynamic behaviour of the lung parenchyma (180). Investigations of such tissue preparations help describing parameters and boundary conditions to model tissue behaviour. Although the strips include a relatively intact microanatomy, the measured response is difficult to interpret with respect to the uniaxial application of stretch and because of the possible unequal fixation of the tissue. In addition it is complicated to set the applied stretches in relation to the whole organ. Thus the model is not useful to investigate biological parameters like cytokines.

1.3.3.5. Stretch to lung cells

Several approaches deal with the mechanostimulation of cells. They can be categorised in terms of the applied stretch or physical grade of the stretch applied. Application forms of stretch comprehend hydrostatic or direct platen contact, longitudinal in-plane uni- and biaxial stretch, bending and fluid shear stress (31). Cells are stretched using elastic biocompatible carrier membranes. By determining the membrane deformation the applied strain can be translated into tissue elongation (276). Amongst a variety of custom made mechanical devices, the Flexercell system is the best established (10; 15; 36). Cells are grown on flexible bottom culture plates which allow up to 30% elongation. A vacuum is used to apply a defined controlled static or dynamic deformation. A method that applies stretch directly to cells is the magnetic twisting stimulator (63). Ferromagnetic beads are coupled to the cells via the integrin receptor and twisted in a magnetic field. Twisting the integrin receptors directly affects the cytoskeleton, which is attached to the integrin receptor. However, this technique has been mostly applied to vascular endothelial cells addressing cell stiffness (42; 148).

Primary rat alveolar epithelial cells have been used extensively in cell stretch devices. Many studies have been done with isolated rat alveolar type II (AT II) cells stretched in mechanical devices like the Flexercell system. As soon as isolated AT II cells are cultured they loose their specific markers and start to differentiate. After 5 days in culture they have lost the AT II marker molecules and look more similar to AT I cells. Accordingly experiments with AT II cells have to be done in the first days culturing and take the loss of already modified cells. In AT II cells apoptosis and necrosis is increased after application of high amplitude mechanical stretch (97). The apoptosis is reduced by NO addition which is assumed to be released by alveolar macrophages (71). In addition, surfactant secretion is increased via the PGI_2-cAMP axis by cell surface stretching (224). This surface stretch seems to be dominated by the attached basal surface. In contrast to surface stretch induced by cyclical stretch, tonically held stretches lead to plasma membrane expansion via lipid insertion (75). Furthermore the inflammatory response in stretched cells was addressed by several studies. An increase of reactive oxygen species, namely superoxide, was observed and Hammerschmidt et al. found proinflammatory mediators to be induced (39; 98). In addition ERK 1 and 2 were induced in stretched cells presumably by activation of the EGF receptor and G proteins (55). To address barrier disruption and edema formation the Na/K-ATPase was investigated in AT II cells. The created transepithelial Na^+ gradient is important to keep fluid from the alveolar space. Na/K-ATPase activity was also increased by cyclic stretch (76). Otherwise cell integrity was mainly investigated in differentiated AT II cells, that may or may not represent AT I cells. Tschumperlin et al. examined the characteristics of stretch related to deformation-induced injury. Accordingly the degree of injury was greatest with cyclically stretch at high amplitudes (268). Paracellular permeability also seems to be increased by stretch in AT I cells (36). In agreement with the increased permeability Cavanaugh et al. found a disruption of tight junction structures and cell-cell attachment potentially due to an intracellular ATP reduction and actin perturbation (37). A variety of cell stretch experiments has also been done in immortalised cell lines especially in A549 cells. Adenocarcinoma A549 cells, derived from human type II pneumocytes, are well characterised and widely used as a model from human pulmonary origin. In stretched A549 cells particular regard has been paid to the investigation of inflammatory responses. The stretch-induced upregulation and production of IL-8 was investigated in many studies and seems to be associated with the upregulation of AP1 and NFkB (145; 282). Other proteins found to be involved are JNK, NIK, protein kinase C, Src protein tyrosine kinase, SAPK and p38 (66; 145; 214; 307). A synergistic effect of mechanical stretch and LPS on IL-8 induction has been reported by Ning et al. (186).

All of these models are applicable to a variety of questions concerning stress in the lungs. However, stretching of PCLS in a biaxial direction provides a link between *in vivo* models and cell culture models, which maintains the microanatomy with the

extracellular matrix on the one hand, and the cell culture-like handling on the other hand.

1.4. The bioreactor

The bioreactor was first described in 2008 by Schumann et al. as a pressure-driven strain-applicator which uses spherical deflection of a carrier membrane transmitting a well-defined tensile strain to a biological sample placed on top of it (232). The bioreactor consists of two similar vertically arranged cylindrical rigid chambers which are separated by a circular elastic membrane fixed in a membrane holder. Deflection of the carrier membrane is achieved by cyclic increase of pressure to the chamber below the membrane (Fig 1.5). Therefore, the membrane is distended with a biaxial tension which was used in a cell stretch model before (300). Combination of the bioreactor with PCLS seems to be a useful model to investigate lung stretch in relatively intact lung tissue in vitro, which will be discussed in detail in this work.
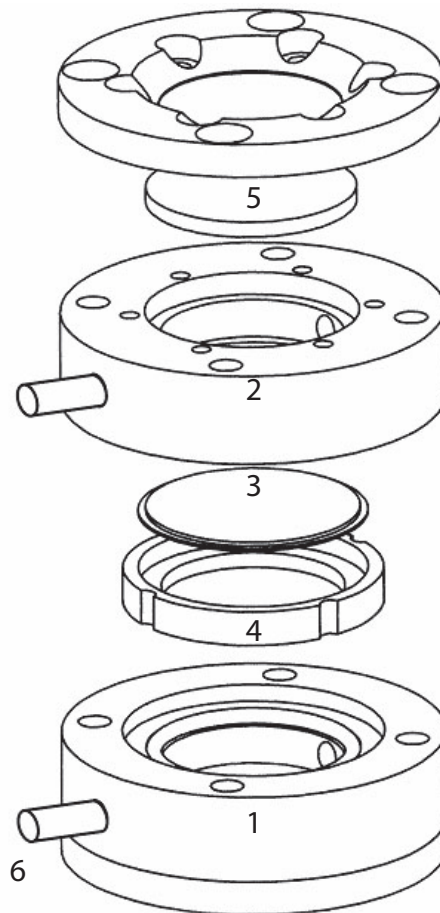
Figure 1.5: Schematic of the bioreactor which consists of the lower (1) and the upper chamber (2), separated by the membrane complex. A membrane (3) is fixed in the membrane holder (4). The upper chamber is equipped with a glass window to allow direct observation (5). Deflection of the membran is provided by volume input through an inlet in the lower chamber (6). From reference (232).

2. Aim of the study

Precision-cut lung slices represent an ideal link between *in vivo* models and cell culture. The model maintains a relatively intact microanatomy, the diversity of cell types of the lung and its extracellular matrix under cell culture conditions. The aim of this study was to use PCLS as a model to study different types of stress.

Bronchoconstriction caused by chemical allergens, such as TMA and DNCB, was investigated in PCLS and compared to invasive lung function measurements. The objective was to identify PCLS as an easy, reliable alternative method to measure lung function changes *ex vivo*.

To study mechanical stretch of lung tissue, a new model was developed to stretch PCLS in a bioreactor. It was our aim to investigate occurring forces on alveolar level and molecular stretch marker, such as amphiregulin.

PCLS from sheep, who are mammalians and therefore closer to humans than rodents, were established as a new model. To characterise them, it was our aim to identify the airway response to unspecific stimuli, such as methacholine. Furthermore, PCLS were prepared from adult and premature sheep to investigate age-dependent differences.

3. Material and Methods

3.1. Material

3.1.1. Instruments

Instrument	Manufacturer
Agilent Bioanalyser	Agilent Technologies, Santa Clara, USA
Beam splitter	Trim Scope, La Vision, BioTec, Bielefeld, Germany
Bench Laminair HB2448	Heraeus, Hannover, Germany
Bioreactor	Custom made by the group of Prof. Guttmann, Freiburg, Germany
Coring Tool	Black & Dekker battery operated screwdriver + self-made coring device
Digital camera (multi photon microscope)	Imager QE, La Vision BioTec, Bielefeld, Germany
ELISA reader	GENios, Tecan, Crailsheim, Germany
GeneChip® Rat Exon 1.0 ST Array	Affimetrix, Santa Clara, USA
Heraeus Fresco 17 Centrifuge	Heraeus, Hannover, Germany
Heraeus Multifuge 3SR+ Centrifuge	Heraeus, Hannover, Germany
Incubator	Heraeus, Hannover, Germany
Inverted microscope DMIRB and DMIL	Zeiss, Oberkochen, Germany
Krumdieck Tissue Slicer	Alabama research and development, Munford, USA
Leica MZ FLIII	Zeiss, Oberkochen, Germany
Light Cycler 480	Roche, Mannheim, Germany
Meta detector	LSM 510 Meta, Zeiss, Jena, Germany
Nano Drop 1000	Fisher Scientific, Wilmington, USA
Pressure transducer	Scientific Instruments, Aachen, Germany
Ti:Sa femtosecond laser	Coherent, Dieburg, Germany
Video camera JAI PROTEC	JAI20040, JAI Pulnix, Alzenau, Germany
Video camera Leica	Zeiss, Oberkochen, Germany
Video camera Visicam 1300 and 640	Visitron Systems, Munich, Germany
Waterbath WP10	P-D Indutriegesellschaft mbH, Dresden Germany

3.1.2. Software

Software	Manufacturer
GraphPad Prism 5 Software	GraphPad, San Diego, CA, USA
Imspector software	La Vision, BioTec, Bielefeld, Germany
JMP 7	SAS Campus Drive, Cary, USA
Light Cycler 480 software	Roche, Mannheim, Germany
Optimas 6.5	Optimas Corporation, Bothell, USA
R2	Team 2006, Vienna, Austria

3.1.3. Chemicals

Substance	Manufacturer
5-Hydroxytryptamin (Serotonin)	Sigma, Deisenhofen, Germany
5x first strand buffer	Invitrogen, Karlsruhe, Germany
Actinomycin D	Sigma, Deisenhofen, Germany
Apicidin	Sigma, Deisenhofen, Germany
$CaCl_2$	Sigma, Deisenhofen, Germany
Collagenase H	Roche, Mannheim, Germany
Cycloheximide	Sigma, Deisenhofen, Germany
Cytochalasine D	Sigma, Deisenhofen, Germany
Dexamethasone	Sigma, Deisenhofen, Germany
Dimethyl sulfoxide (DMSO)	Merck, Darmstadt, Germany
Dinitrochlorobenzene (DNCB)	Sigma, Deisenhofen, Germany
DNTPs	Peqlab, Erlangen, Germany
5,6-dichloro-1-beta-D-ribofuranosylbenzimidazole (DRB)	Sigma, Deisenhofen, Germany
Dithiothreitol (DTT)	Invitrogen, Karlsruhe, Germany
Endothelin-1	Bachem, Weil, Germany
Ethanol	Merck, Darmstadt, Germany
Formic acid	Merck, Darmstadt, Germany
Genistein	Sigma, Deisenhofen, Germany
Glucose	Sigma, Deisenhofen, Germany
Glutamine	PAA Laboratories, Pasching, Austria
HEPES	Sigma, Deisenhofen, Germany
Histamine	Sigma, Deisenhofen, Germany
Imipramine	Sigma, Deisenhofen, Germany
iso-propanol	Merck, Darmstadt, Germany
KCl	Sigma, Deisenhofen, Germany
Lanthanum (III) chloride	Sigma, Deisenhofen, Germany
LightCycler 480 SYBR Green I Master	Roche, Mannheim, Germany
Low melting point agarose	Gerbu, Gaiberg, Germany
Lipopolysaccharide (LPS)	Sigma, Deisenhofen, Germany
Leukotriene D_4 (LTD_4)	Biomol, Hamburg, Germany
Minimal essential medium (MEM) Aminoacids	PAA Laboratories, Pasching, Austria
Minimal essential medium (MEM) Vitamins	PAA Laboratories, Pasching, Austria
Metacholine	Sigma, Deisenhofen, Germany
Methanol	Merck, Darmstadt, Germany
$MgSO_4$	Sigma, Deisenhofen, Germany
ML-7	Biomol, Hamburg, Germany
(3-(4,5-Dimethylthiazol-2-yl)-2,5-diphenyltetrazolium bromide (MTT)	Sigma, Deisenhofen, Germany
NaCl	Sigma, Deisenhofen, Germany
NaH_2PO_4	Sigma, Deisenhofen, Germany
$NaHCO_3$	Sigma, Deisenhofen, Germany
Oligo dT primer $_{12-18}$	Invitrogen, Karlsruhe, Germany
PCR grade H_2O	Roche, Mannheim, Germany
Penicillin/Streptomycin	PAA Laboratories, Pasching, Austria
PP2	Calbiochem, Bad Soden, Germany
Primer	MWG, Ebersberg, Germany
Propidium iodide	Invitrogen, Karlsruhe, Germany
Rnase free water	Ambion, Darmstadt, Germany
Rnase Out	Invitrogen, Karlsruhe, Germany
Ruthenium Red	Sigma, Deisenhofen, Germany
Sodium pyruvate	PAA Laboratories, Pasching, Austria
Sphingosine-1-Phosphate	Biomol, Hamburg, Germany
SuperScript II Reverse Transkriptase	Invitrogen, Karlsruhe, Germany
Trimellitic anhydride (TMA)	Sigma, Deisenhofen, Germany
U46619	Cayman, Ann Arbor, Michigan, USA
Y27632	Tocris distributed by Biozol, Eching, Germany

3.1.4. Kits

Kit	Manufacturer
LIVE/DEAD viability/cytotoxicity kit	Invitrogen, Karlsruhe, Germany
NucleoSpin RNA II	Macherey-Nagel, Düren, Germany

3.1.5. Solutions

3.1.5.1. Slicing medium

$CaCl_2$	1.8 mM
$MgSO_4$	0.8 mM
NaH_2PO_4	1 mM
KCl	5.4 mM
NaCl	116.4 mM
Glucose	16.7 mM
$NaHCO_3$	26.1 mM
Hepes	25.17 mM

3.1.5.2. Incubation medium

$CaCl_2$	1.8 mM
$MgSO_4$	0.8 mM
NaH_2PO_4	1 mM
KCl	5.4 mM
NaCl	116.4 mM
Glucose	16.7 mM
$NaHCO_3$	26.1 mM
Hepes	25.17 mM
Sodium pyruvate	1 mM
50 x MEM Amino acids	20 ml/l
100 x MEM Vitamins	10 ml/l
Glutamine	2 mM

3.1.5.3. Double-concentrated incubation medium

Salts and additional substances were solved in half of the usual amount of Milli Q H_2O.

3.1.5.4. Agarose solution

Agarose was dissolved double-concentrated in Milli Q H_2O and mixed with the same amount of double-concentrated incubation medium at 37°C.

3.1.6. Animals

The animal experiments were approved by the local ethic committee (Landesamt für Natur, Umwelt und Verbraucherschutz, Nordrhein-Westfalen).

3.1.6.1. Rats

Female Wistar rats (approximately 300g) were obtained from Harlan Winkelmann (Borchen, Germany) and Janvier (Le Genest Saint Isle, France). Rats were maintained on laboratory food and tap water ad libitum in a regular 12h dark/light cycle at an ambient temperature of 22 °C. Acclimatization period was at least 7 days before use.

3.1.6.2. Mice

Mice were sensitised with TMA or DNCB by a standard sensitisation protocol and obtained by the group of A. Braun (ITEM, Hannover, Germany). The sensitisation protocol is illustrated in Figure 3.1.

3.1.6.3. Sheep

Lungs from sheep were obtained from our collaboration partner B. Kramer (Dept. of Pediatrics, Academisch ziekenhuis Maastricht, Maastricht, Netherlands).
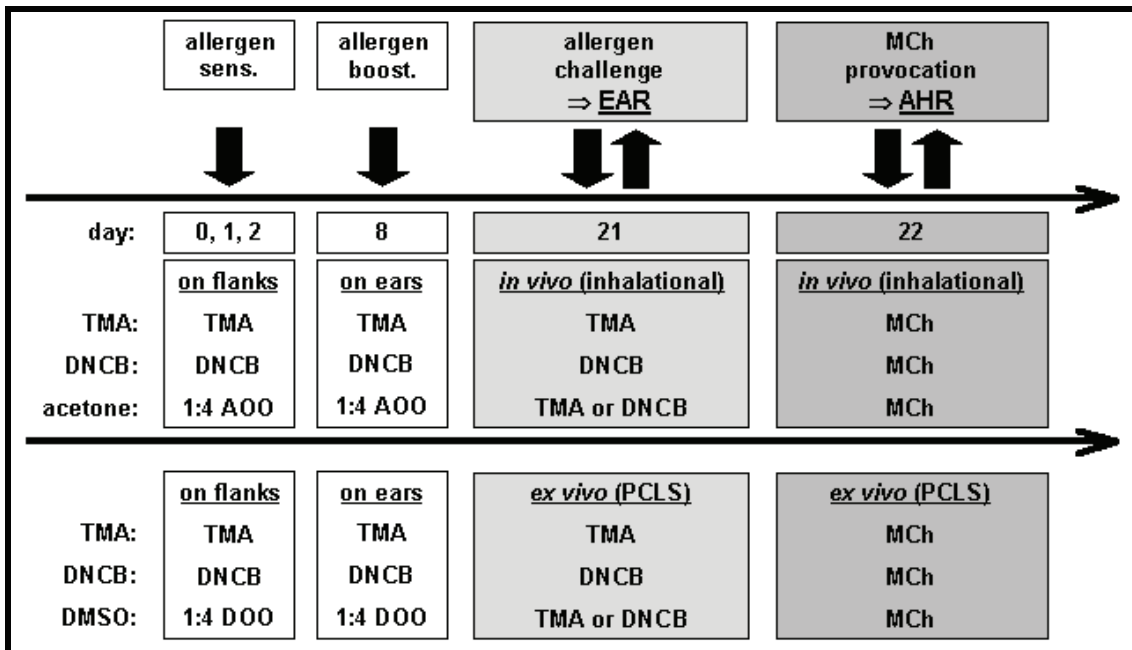
	allergen sens.	allergen boost.	allergen challenge ⇒ **EAR**	MCh provocation ⇒ **AHR**
day:	0, 1, 2	8	21	22
	on flanks	**on ears**	*in vivo* (inhalational)	*in vivo* (inhalational)
TMA:	TMA	TMA	TMA	MCh
DNCB:	DNCB	DNCB	DNCB	MCh
acetone:	1:4 AOO	1:4 AOO	TMA or DNCB	MCh
	on flanks	**on ears**	*ex vivo* (PCLS)	*ex vivo* (PCLS)
TMA:	TMA	TMA	TMA	MCh
DNCB:	DNCB	DNCB	DNCB	MCh
DMSO:	1:4 DOO	1:4 DOO	TMA or DNCB	MCh

Figure 3.1: Sensitisation protocol for actively sensitised mice with the chemicals TMA and DNCB. Animals were sensitised on days 0, 1 and 2 and boosted on day 8. Early allergic response (EAR) was performed on day 21 followed by airway hyperresponsiveness (AHR) on day 22. TMA = trimellitic anhydrate, DNCB = 2,4-dinitrochlorobenzene, AOO = acetone olive oil, DOO = DMSO olive oil, Mch = methacholine, EAR = early allergic response, AHR = airway hyperresponsiveness. From reference (110).

3.1.7. Anaesthesia

Pentobarbital solution (Narcoren) was purchased from Merial (Hallbergmoos, Germany).

3.2. Methods

3.2.1. Precision-cut lung slices

3.2.1.1. Preparation of rat lung slices

PCLS were prepared as previously described (153; 218) with the following modifications. After injection of 250 mg/kg pentobarbital the trachea was cannulated and the animals exsanguinated by cutting the vena cava inferior. Through the cannula, the lung was filled with a low melting-point agarose solution. After solidifying of the agarose on ice for 15 minutes the lobes were separated. Tissue cores were prepared with a rotating

sharpened metal tube. The cores were cut into 200 (physiological experiments) or 400 (stretching experiments) µm-thick slices with a Krumdieck tissue slicer. Subsequently, the PCLS were incubated at 37°C in a humid atmosphere in minimal essential media supplemented with penicillin (100 Units/ml) and streptomycin (0.1 mg/ml). The pH-value was adjusted to 7.2. To remove cell debris and the agarose, medium was changed every 30 minutes during the first 2 hours after slicing and every 60 minutes for the following 2 hours. Afterwards medium was changed every 24 hours.

3.2.1.2. Preparation of mouse lung slices

Mice were anesthetised with 200 mg/kg pentobarbital solution. PCLS were prepared as rat PCLS with the following modifications. After solidifying of the agarose-filled lung lobes on ice, the lobes were separated and embedded in 3 % agarose in cryotubes. The embedded lung lobes were solidified and cut into 220 µm thick slices with a Krumdieck tissue slicer.

3.2.1.3. Preparation of sheep lung slices

Sheep lung lobes were obtained from adult and newborn sheep after undergoing mechanical ventilation experiments. The lobes were filled with a 1.5 % low melting point agarose solution via the main bronchus. The lobe was cut into 1 cm thick plates, from which tissue cores around the airways were prepared. The cores were cut into 220 µm thick slices with a Krundieck tissue slicer.

3.2.2. Viability of PCLS

3.2.2.1. Measurement of MTT-reduction

The capability of PCLS to reduce MTT (3-[4,5-Dimethylthiazol-2-yl]-2,5-diphenyltetrazolium bromide) is dependent on mitochondrial activity and was used as a parameter of viability. PCLS were transferred into 24-well-plates (one PCLS per well) and incubated with 0.7 mg/ml MTT for 15 minutes. Subsequently, the supernatant was removed and the slices were lysed in 200 µl i-propanol/formic acid (95/5) for 20 minutes. 100 µl of the supernatant was transferred into 96-well microtiter plates. The reduced MTT was measured spectrophotometrically at 550 nm.

3.2.2.2. Live-Dead staining with propidium iodide

Confocal microscopy was used to assess the viability of stretched PCLS. Propidium iodide was used to stain nuclei of lysed cells (dead stain). PCLS were incubated with 4 µg/ml propidium iodide for 2 min. External dye was removed by washing the PCLS thrice. The fluorescent dye was excited at 543 nm with a helium-neon laser. Emission of propidium iodide was detected with a meta detector adjusted to a detection window of 552-627 nm (red staining).

To localise the nuclei autofluorescence of the PCLS (green) was recorded seperately (excitation at 488 nm with an argon laser / emission with a bandpath filter of 505-550 nm). Pictures are shown as an overlay.

3.2.2.3. Live-Dead staining with multi-photon microscopy

Viability of stretched PCLS was also determined by LIVE/DEAD viability/cytotoxicity assay visualised with multi-photon microscopy. PCLS were incubated with 5 µM Calcein AM (acetomethylester of calcein, live staining) and 10 µM ethidium homodimer (dead staining) for 30 minutes and then washed to remove external dye. The fluorescent dyes were excited at 800 nm with a Ti:Sa femtosecond laser, which laser beam was split up into 64 individual beams. The PCLS was simultaneously excited and scanned and the images were aquired using a digital camera. Emission of calcein AM was detected with an emission filter at 475-525 nm staining living tissue (cytoplasm, green) while ethidium homodimer, staining the nuclei and therefore marking dead cells (red), was detected at 600-650 nm. Emission of calcein AM and ethidium homodimer was recorded separately and is shown as an overlay.

3.2.2.4. Videomicroscopy of broncho-/ vasoconstriction

PCLS for videomicroscopy were selected by comparable airway or vessel size within the species (sheep respectively mice) and cultured in 24-well-plates (one slice per well). Every PCLS was covered with 1 ml medium and the PCLS was fixed with a nylon thread attached to a platinum wire. The 24-well-plate was positioned on the stage of an inverted microscope and recorded by a digital camera. Only completely relaxed airways were selected for the experiments. The area of the airway or the vessel was defined as 100 % and constriction was measured as percentage decrease to the initial area. A control image was taken before addition of the mediator and frames were recorded every 5 or 30 seconds for 5, 10 or 30 minutes (dependent on the study).

3.2.3. Gene array

Gene array experiments were accomplished by the group of B. Denecke (IZKF Biomat, RWTH Aachen, Germany).

3.2.3.1. RNA-Extraction

Frozen PCLS were powdered among liquid nitrogen cooling. Total RNA was isolated using the NucleoSpin RNA II Kit according to the manufacturers instructions. RNA quality was determined using the RNA 6000 Nano Assay (Agilent Bioanalyser) and quantity was assessed using the Nano Drop 1000.

3.2.3.2. Microarray

All further processing of the total RNA (300 ng RNA) was performed according to the GeneChip Whole Transcript (WT) Sense Target Labeling Assay Manual (Affymetrix). The fragmented labelled sample was hybridized to an Affymetrix GeneChip® Rat Exon 1.0 ST Array (~1 million probe sets covering 850000 exon clusters). The microarray analysis was performed using Bioconductor (86) packages under R2. Gene induction is given as fold increase of the log 2 values in the PCLS in comparison to the log 2 values of untreated lung tissue.

3.2.4. Real-Time PCR

3.2.4.1. RNA-Extraction

Frozen PCLS were powdered among liquid nitrogen cooling. Total RNA was isolated using the NucleoSpin RNA II Kit according to the manufacturers instructions.

3.2.4.2. Reverse Transcription (cDNA synthesis)

8µl of total RNA eluate were mixed with 2 µl 0.1 µg/ml Oligo(dT) $_{12-18}$ Primer and heated to 65°C for 10 Minutes. After cooling to 4°C, a mastermix consisting of 2µl 10 mM dNTP-Mix, 2µl 0.1 M DTT, 1µl 0.5 µg/ml RNaseOut, 1µl Superscript II Reverse Transcriptase

and 4 µl 5x first strand buffer [250 mM Tris-HCl (pH 8.3), 375 mM KCl, 15 mM MgCl$_2$] were added. The mixture was incubated at 37°C for 90 minutes to synthesize cDNA and subsequently heated to 95°C for 2 minutes to inactivate the enzymes. The finished product was then diluted with 30 µl Nuclease-free water to a final volume of 50 µl.

3.2.4.3. Quantitative Real Time Polymerase Chain Reaction (RTq-PCR)

To determine gene expression in PCLS cDNA was amplified by RTq-PCR using the LightCycler 480 system by Roche based on TaqMan PCR technology. 1 µl cDNA was mixed with 9 µl mastermix consisting of 5 µl LightCycler 480 SYBR Green I Master, 3 µl PCR grade H$_2$O and 0.5 µl forward and reverse primer, respectively.

Amplification was measured by addition of SybrGreen to the mastermix. SybrGreen intercalates into double-strand DNA and therefore reflects the amplification rate. Beta-2-microglobulin was used as housekeeping gene to normalize sample-to-sample differences of the target DNA-Sequence. Relative DNA concentrations of the samples were calculated by an internal standard curve. The LightCycler 480 Relative Quantification Software analyses amongst other things the sample's crossing point, the efficiency of the reaction and the number of cycles completed to define the final ratio as a function of PCR efficiency and determined crossing points. To control the specificity of the amplification, the melting temperature of every sample was determined. An individual, sharp peak indicates the desired product.

In the absence of absolute copy numbers and accordingly concentrations of the target DNA sequence gene expression is given as a fold increase.

3.2.4.4. Primer

Oligonucleotide sequences were purchased lyophilised from MWG and dissolved to a stock solution of 100 nM/ml. Primer were diluted to a working solution of 0.625 nM/ml.

Gene	Full name	Primer sequences (5`-3`)
Areg	amphiregulin	FP ACCTGCCATTGTCATCAG
		RP CGGCGGAGACAAAGACAA
B2M	beta-2-microglobulin	FP CCGTGATCTTTCTGGTGCTTGTCT
		RP ATCGGTCTCGGTGGGTGTGAAT
Ptgs2	prostaglandin-endoperoxide synthase 2 (Cox-2)	FP GGGTTGCTGGGGGAAGGAAT
		RP ACCAGCAGGGCGGGATACAG
Il6	interleukin 6	FP CCAGCCAGTTGCCTTCTTG
		RP AGTGCATCATCGCTGTTCATAC
Cxcl10	chemokine (C-X-C motif) ligand 10 (IP10)	FP GAACCCAAGTGCTGCTGT
		RP GTCTCAGCGTCTGTTCATGG
Cxcl2	chemokine (C-X-C motif) ligand 2 (MIP-2)	FP AATGCCTGACGACCCTACCA
		RP GTTAGCCTTGCCTTTGTTCAG

3.2.5. Pharmacological intervention studies

3.2.5.1. Inhibitor protocol

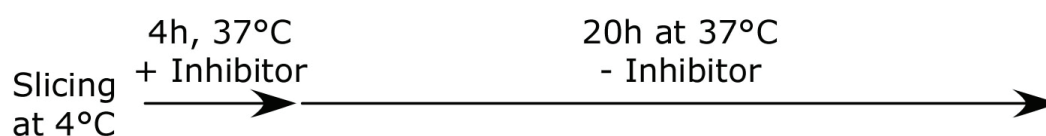Inhibitors were added to the slicing and incubation medium as indicated in Fig. 3.2.

Figure 3.2: Incubation protocol with presence (+) and absence (-) of inhibitors after the slicing process.

3.2.5.2. Inhibitors of transcription and translation

To inhibit amphiregulin RNA induction the transcription and translation were blocked with different inhibitors (Table 3.1). Those were present during the slicing process and the first 4h of incubation. Afterwards the inhibitor was removed from the incubation medium.

Table 3.1: Inhibitors of transcription and translation

Inhibitor	Function	Solved in	Concentration
Actinomycin D	Forms a stable complex with the DNA, inhibits movement of the RNA polymerase	Methanol	1 µg/ml
Cycloheximide	inhibits translation	Ethanol	20 µg/ml
5,6-Dichlorobenzimidazole riboside (DRB)	inhibitor of RNA synthesis	DMSO	50 µM
Apicidin	inhibitor of histone deacetylase	Ethanol	2 µg/ml

3.2.5.3. Inhibitors and mediators of signal transduction pathways

To investigate the signal transduction pathways by which amphiregulin expression is mediated, different inhibitors were used (Table 3.2). PCLS were sliced and incubated for the first 4h in presence of the inhibitors. With the last medium change inhibitors were removed.

Table 3.2: Inhibitors of signal transduction pathways

Inhibitor	Function	Solved in	Concentration
Imipramine	inhibitor of acid sphingomyelinase	Milli Q H2O	10 µM
Y27632	Selective Rho-Kinase inhibitor	Milli Q H2O	10 µM
PP2	Selective Src-Tyrosine-Kinase inhibitor	DMSO	10 µM
Sphingosine-1-phosphate	Cellular metabolite, derived from ceramide	Methanol	1,32 µM
Genistein	Specific inhibitor of tyrosine-specific protein kinases	DMSO	100 µM
Cytochalasin D	Fungal toxin, inhibits actin polymerization	Ethanol	1 µM
ML-7	Selective inhibitor of MLCK	Ethanol	30 µM
Ruthenium Red	Inhibits TRPV1, 4 and TRPA1, Ryanodine Receptor	Milli Q H2O	20 µM
Lanthanum Chloride	Blocks divalent cation channels (e.g. Ca^{2+})	Milli Q H2O	100 µM
Dexamethasone	Glucocorticoid anti-inflammatory agent	H2O	1 µM

3.2.5.4. Storage of PCLS at 4°C and 37°C

Groups of PCLS were stored at 4°C or 37°C as indicated in Figure 3.3. Samples were
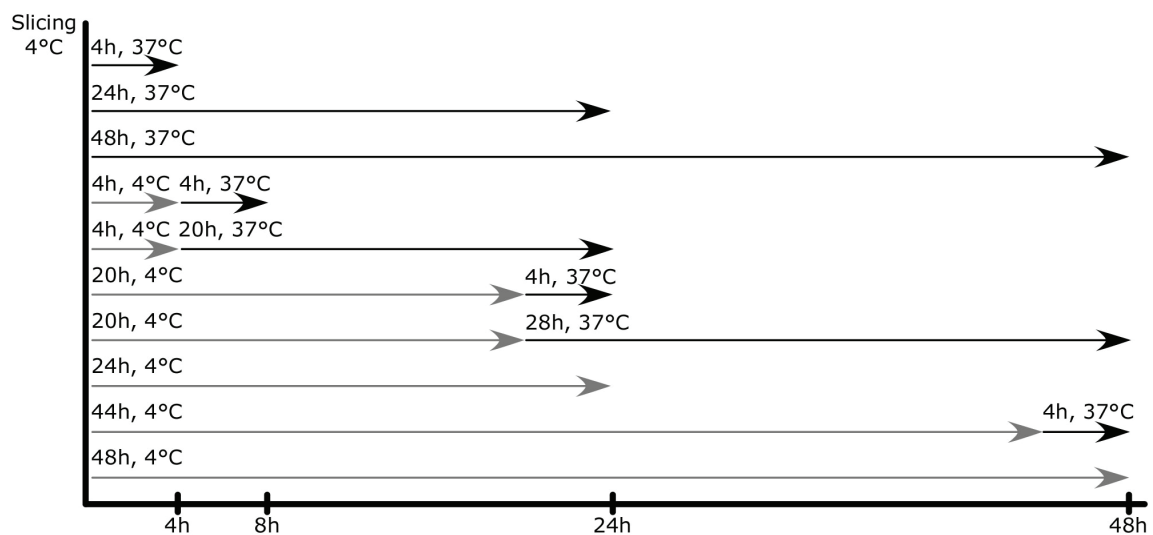

Figure 3.3: Incubation protocol of PCLS at different temperatures.

harvested 4h, 8h, 24h and 48h after the slicing process.

3.2.6. Pressure operated strain applying bioreactor

The bioreactor used for mechanostimulation consists of two sealed rigid chambers which are separated by a pliant carrier-membrane on which the test sample is fixed. After various futile attempts to fix the lung slices to the carrier membrane by gluing or letting them adhere to various membrane materials, we decided to fix the PCLS by clamping. The recently described bioreactor (232) was used with the following modifications. Two macrolon discs with an outer diameter of 30 mm and an aperture of 10 mm were placed between the upper and lower chamber of the bioreactor. By notches in an interval of 1.5 mm around the cut-out, leaving a space of approximately 150 μm between the discs, a PCLS was fixed on a flexible supporting membrane in the bioreactor. The membrane and the PCLS were both clamped between the macrolon discs. The PCLS were stretched by applying pressure to the lower chamber of the bioreactor.

3.2.6.1. Membranes

Membranes were produced by the Group of Prof. Guttmann in Freiburg as described in detail previously (9). Briefly: polydimethylsiloxane (PDMS) is an organic-based dual-component polymer composed of base resin and curing agent. By a spin-coating process inside a centrifuge, PDMS membranes were built by polymerisation of a two-component elastomer. During the spin-coating process, the material disperses, resulting in a plane film which is joined to a steel or macrolon ring. After the spin-coating process, the membranes were polymerised for 4h at 60°C resulting in an easy-to-handle membrane fixed in the carrier ring. The PDMS membranes had a thickness of approximately 30 μm with homogemous profiles as verified by optical coherence tomography. The elasticity of the membranes did not change during 24h of mechanostimulation.

3.2.6.2. Pressure application

PCLS were clamped into the bioreactor and pressure in the lower chamber of the bioreactor was measured with a custom built pressure transducer. Static pressure was applied using a syringe in order to determine the membrane excursions (needed for the strain calculations). The excursion of the lung slices was observed under a microscope and the excursion in Z-direction (height of the dome) was determined indirectly by means of a micrometer screw (see below). Cyclic pressure was applied using a constant pressure flow of 35 mbar to the lower chamber. A magnetic valve

was opened and closed in a 2 second rhythm to guarantee a periodic distension of the membrane.

3.2.6.3. Displacement readings

Displacement of the membrane and the PCLS by pressure application was measured via stereomicroscopy equipped with a micrometer screw. Difference in altitude of the membrane corresponds exactly with the difference in height of the microscope while focusing the same plane. Displacement in mm can be measured.
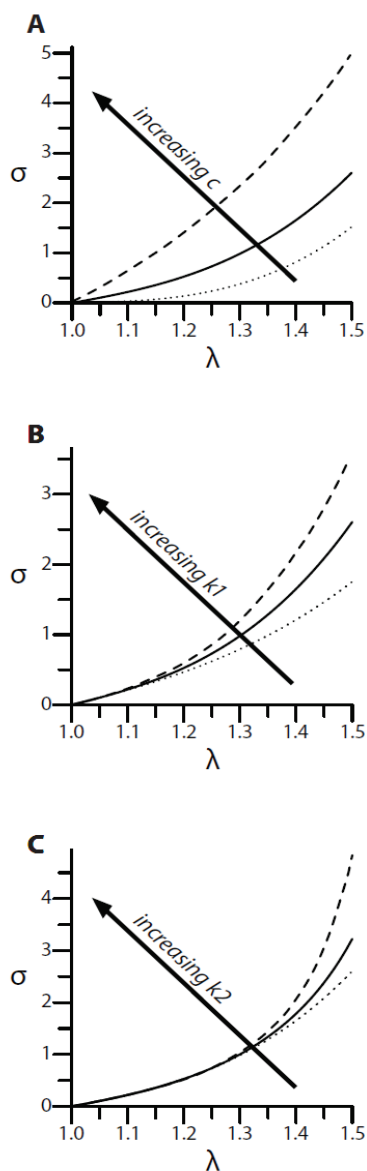

Figure 3.4: Influence of material parameters on the appearance of the stress-stretch curve. Exemplarily, a uniaxial tension test assuming perfect incompressibility of the tissue is investigated here. Plots show the relationship between the principal stretch λ and the Cauchy stress σ in load direction. In each subfigure, one constitutive parameter is varied arbitrarily, whereas the other two are kept constant. A: Variation of parameter c (dotted line: $c = 0.1$ kPa, solid line: $c = 1$ kPa, dashed line: $c = 3$ kPa). B: Variation of parameter k_1 (dotted line: $k_1 = 30$ kPa, solid line: $k_1 = 76.5$ kPa, dashed line: $k_1 = 130$ kPa). C: Variation of parameter k_2 (dotted line $k_2 = 13.5$ kPa, solid line $k_2 = 200$ kPa, dashed line $k_2 = 500$ kPa).

3.2.7. Mechanical model

Calculation of the strain was performed by Lena Wiechert (Group of Prof. Wall, München). The PDMS membrane and the tissue slice exhibit *qualitatively* comparable non-linear material characteristics – although individual *quantitative* tangential stiffnesses are very different – and can both be treated as isotropic, homogeneous continua. In the following, we assume an ideal clamping of the membrane-tissue construct in the bioreactor. Hence, membrane and tissue do not move relatively to each other for the pressure loadings considered here irrespective of their corresponding surface properties. Thus, slipping is supposed to be unlikely even if the surfaces were perfectly smooth. Experimental investigations in (9) also supported this assumption. Consequently, the resulting strain distribution is continuous across the membrane-tissue boundary. Since we are interested in the strains only – and not in the corresponding discontinuous stresses –, we modelled both components as one single homogeneous construct.

In order to simulate the deformation of the construct in the bioreactor, an appropriate non-linear material model had to be chosen. In this connection, we postulated a decoupled strain-energy density function Ψ in terms of the invariants I_1 and I_3 of the

right Cauchy-Green deformation tensor $\underline{\underline{C}} = \underline{\underline{F}}^T \cdot \underline{\underline{F}}$

(with $\underline{\underline{F}}$ denoting the local deformation gradient).

For the isochoric part, the following polyconvex function Ψ_{iso} (85; 293) was chosen

$$\Psi_{iso} = c(I_1 I_3^{-1/3} - 3) + \delta \frac{k_1}{2k_2} e^{k_2 \left(\frac{1}{3}I_1 - 1\right)^2 - 1},$$

with $\delta = 1$ if $I_1 > 3$ and $\delta = 0$ otherwise. The involved material parameters characterize the form of the resulting stress-strain curve of the tissue as illustrated in Fig. 3.4. The shear modulus-like parameter *c* refers to the initial slope of the curve, whereas $k_1 \geq 0$ and $k_2 > 0$ affect the local slope as well as the curvature of the nonlinear posterior part. The chosen volumetric function governing the transversal response of the membrane-tissue construct

$$\Psi_{vol} = \kappa \beta^{-2} (\beta \ln J - J^{-\beta} - 1)$$

follows (189) with $\beta = 9$ being an empirical coefficient, $J = \det(\underline{\underline{F}})$ and κ denoting a bulk modulus-like parameter.

The material parameters were determined such that the simulated dome displacement matched the experimentally derived one as well as possible (Fig. 4.26.), yielding *c* =

10 kPa, κ = 8.3 kPa, k_1 = 30 kPa and k_2 = 8.5 kPa. It should be emphasized that these parameters are needed for simulating the construct's behaviour only, so we do not intend to make any statement on the mechanical properties of the tissue slice alone here.

Nonlinear finite element (FE) simulations of the deformation in the bioreactor were performed with our in-house multi-purpose FE code BACI. By using the experimentally determined dome displacements as input to the model, further information on the local strain state of the tissue – which cannot be measured directly – should be provided. For this purpose, the membrane-tissue construct was discretized with 13300 linear hexahedral elements and fixed at the circumferential surface.

In order to specify the strain state of the membrane, the spatial stretch tensor

$$\underline{v} = \underline{\underline{F}} \cdot \underline{\underline{R}}^{-1}$$

(with $\underline{\underline{R}}^{-1}$ being the inverse of the local rotation tensor) was calculated in every finite element node. After the solution of the associated eigenvalue problem, the principal spatial stretches λ_α and corresponding directions

$\vec{n}_\alpha$ (with $\alpha \in [1,2,3]$) were determined.

3.2.8. Videomicroscopy of alveoli

Pictures of the Alveoli were taken at specific pressure points with a Visicam camera. Area and perimeter were evaluated by area and line measurement in the Optimas 6.5 software.

3.2.9. Treatment with collagenase

PCLS were incubated with 1 mg/ml collagenase H for 20 minutes at 37°C. After the incubation collagenase was removed by washing the PCLS with incubation medium.

3.2.10. Statistics

Data were analysed by either one factorial or multifactorial analysis in JMP 7. Heteroscedicity was correted by Box-Cox transformation prior to anylysis. Data were compared by the Tukey Hsd test (all versus all), Dunetts test (all versus control) or

Students t-test. Concentration-response curves, displacement curves and maximum contraction data were analysed in GraphPad Prism 5.

4. Results

4.1. Part I: Effect of mediators to Sheep PCLS

Sheep have been used as an asthma model, because they feature many pathophysiological characteristics of human asthma (3). However, sheep PCLS have yet not been established. In this study, production and responsiveness of sheep PCLS were studied. To investigate the responsiveness of mediators to sheep lung, adult sheep PCLS were compared to PCLS from premature baby sheep born by caesarian.

4.1.1. Viability of sheep PCLS

The viability of adult and premature sheep PCLS was evaluated by measurement of mitochondrial function via MTT test. In contrast to detergent-treated PCLS (data not shown) both adult and premature sheep PCLS showed MTT formation for at least 72h in culture, indicating viability of sheep PCLS for at least 3 days. Overall the MTT formation in premature sheep PCLS was higher compared to adult sheep PCLS. This difference was significant at 24h and 72h (Fig. 4.1).
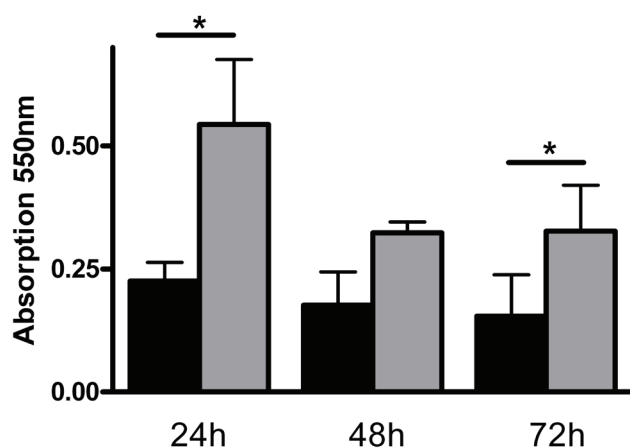

Figure 4.1: MTT formation in sheep PCLS. PCLS from adult (black columns) or premature sheep (dark grey columns) were cultured for 72h in incubation medium at 37°C and 5 % CO_2. Data are given as mean ± SD, n = 3 PCLS at minimum. Data was Box-Cox transformed and analysed by the Tukey HSD test.

4.1.2. Airway responses of sheep PCLS

The bronchoconstriction to mediators relevant in asthma was compared in adult and premature sheep PCLS. Cumulative concentration-response curves were performed for methacholine, serotonin and endothelin-1. Furthermore, the airway reactivity to histamine, leukotriene D_4 and U46619 was investigated. Both adult and premature sheep responded to methacholine, a stable acetylcholine derivative, with EC_{50} values of 70 and 187 nM, respectively (Fig. 4.2 A). The biogenic amines serotonin and histamine were also tested in sheep PCLS. Serotonin contracted the airways with an EC_{50} value of 122 nM in adult sheep and an EC_{50} value of 377 nM in premature sheep (Fig. 4.2 B). Surprinsingly, both adult and premature sheep did not respond to histamine (Fig. 4.2 C). No difference was observed in the concentration-response curves for endothelin-1, which constricted the airways with an EC_{50} value of 16 nM in adult and premature sheep PCLS (Fig. 4.2 D). As representatives for eicosanoids the stable TP-receptor antagonist U46619 and leukotriene D_4 were applied (Fig. 4.2 E, F). Leukotriene D_4 led to a bronchoconstriction in both adult and premature sheep airways. While the reaction of adult sheep was rather weak with a maximum contraction of 24.7 ± 20.4 % at concentrations of 100 nM, the premature sheep aiways contracted up to 77.6 ± 22.8 %. In contrast to premature sheep, which did not response to U46619, adult sheep airways contracted with a maximum of 33.5 ± 34.4 % at concentrations of 10 µM.
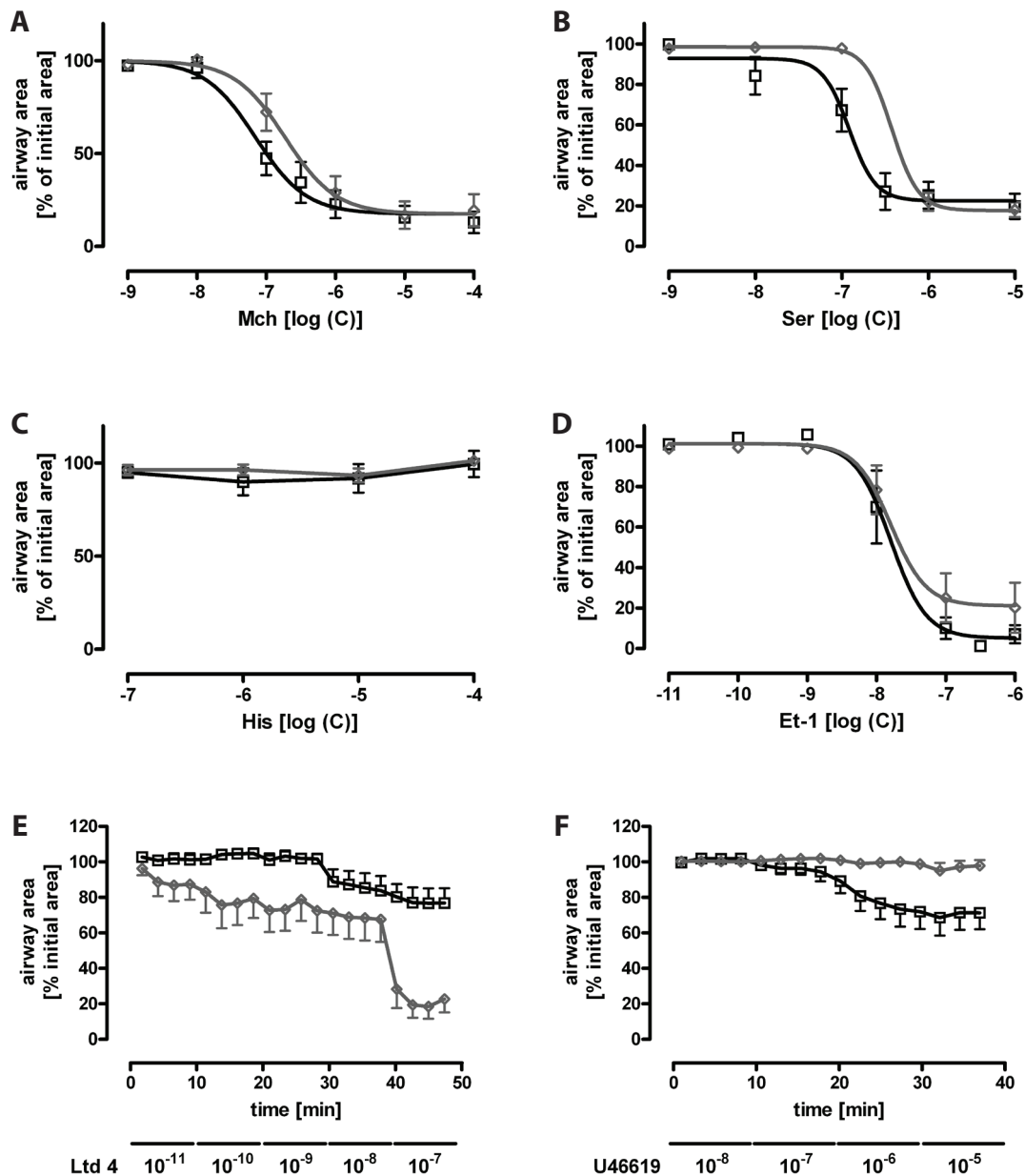
Figure 4.2: Bronchoconstriction in response to different mediators in PCLS from adult (black line) and premature (grey line) sheep. Concentration-response curves are shown for methacholine (A), serotonin (B), histamine (C), and endothelin-1 (D). Airway response over time is shown for leukotriene D$_4$ (E) and U46619 (F). Data are given as mean ± SEM, n = 8-14.

4.1.3. Mediator-induced vasoconstriction in sheep PCLS

Vessels in PCLS can be observed by videomicroscopy in the same manner as airways. While bronchial arteries are too small to be examined, the pulmonary vessels are observable. Pulmonary arteries and veins can be distinguished by their relative location to the airway and the amount of smooth muscle arount the vessel. Whereas the pulmonary artery is located very close to the airway and is characterised by a lot of smooth muscle, the vein is located farther with lower amounts of smooth muscle. Because of the relatively close location of the pulmonary arteries to the airways,

pulmonary arteries were investigated if they were present in PCLS. Vasoconstriction of pulmonary arteries was investigated and compared in adult and premature sheep PCLS. Leukotriene D_4, U46619 and endothelin-1 are also known to constrict vessels. Figure 4.3 shows the vasoconstriction of vessels to leukotriene D_4, U46619 and endothelin-1. No difference was observed between adult and baby sheep in response to endothelin-1, pulmonary arteries were constricted by an EC_{50} value of 19 nM. Adult sheep did not react to leukotriene D_4, however premature sheep at least reacted with a maximum contraction of 13.7 ± 18.7 % at concentrations of 100 nM. Both adult and premature sheep showed vasoconstriction to U46619 in a concentration dependent manner with maximum contractions of 29.8 ± 35.7 and 39.4 ± 30.9 % at concentrations of 10 µM, respectively. As expected, no vasoconstriction was observed in PCLS treated with methacholine, histamine or serotonin (data not shown).
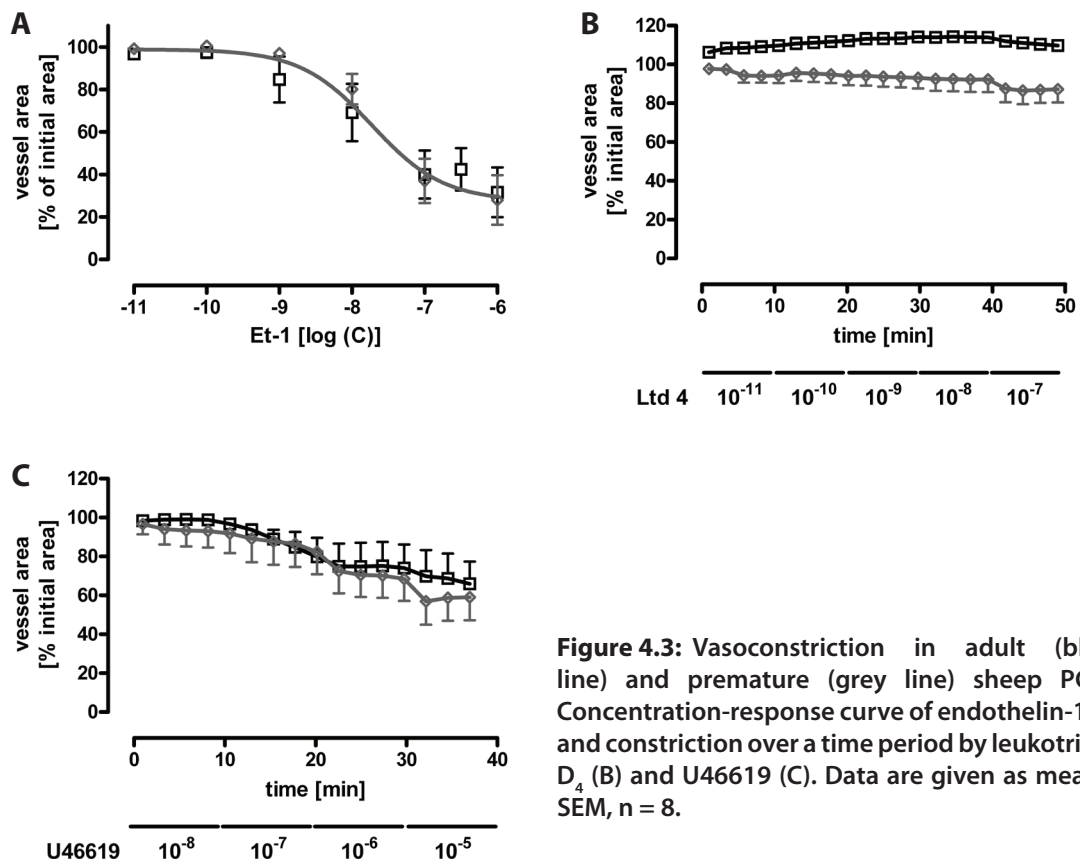

Figure 4.3: Vasoconstriction in adult (black line) and premature (grey line) sheep PCLS. Concentration-response curve of endothelin-1 (A) and constriction over a time period by leukotriene D_4 (B) and U46619 (C). Data are given as mean ± SEM, n = 8.

4.2. Part II: Effect of allergens to mouse PCLS

4.2.1. Effect of TMA and DNCB on lung function

The incidence of allergies is increasing and especially the lung and the skin play a critical role in allergen sensitisation. EU-projects like the Sens-it-iv project focus on the development of alternative *in vitro* models to animal testing, according to the 3R-concept created by Russell and Birch (replace, reduce and refine (226)). The study was designed to examine wether airway responses in PCLS are a suitable alternative to *in vivo* studies, especially with a view to the 3R concept. The aim was to characterise lung function after dermal exposure and pulmonary challenge of mice with the LMW chemicals TMA and DNCB, which are well characterised chemical allergens. TMA is a known respiratory allergen, while DNCB works as a contact allergen. Therefore two different aspects of asthma were investigated. Furthermore the aim was to examine wether PCLS are a predictible *in vitro* model for *in vivo* experiments.

Irritant effects of both allergens were excluded beforehand; incubation with 1.2 µg/ml TMA and 0.3 µg/ml DNCB did not effect the viability of PCLS (data not shown).

4.2.1.1. Induction of the EAR by TMA and DNCB

After dermal sensitisation with an allergen the EAR leads to a severe bronchoconstriction and inflammatory response after exposure to the corresponding allergen. To examine wether TMA and DNCB are able to induce EAR after active sensitisation, mice were provoked with TMA or DNCB, respectively. Invasive measurements to aquire lung function parameters are an established model. EAR of sensitised animals were studied after challenge with TMA or DNCB and compared to bronchoconstriction in PCLS of sensitised animals. No significant effect of TMA or DNCB on pulmonary resistance was observed (Fig. 4.4 A). Similarly airways of PCLS from sensitised and control animals did not contract after exposure to 1.2 µg/ml TMA and 1 µg/ml DNCB (Fig. 4.4 B).
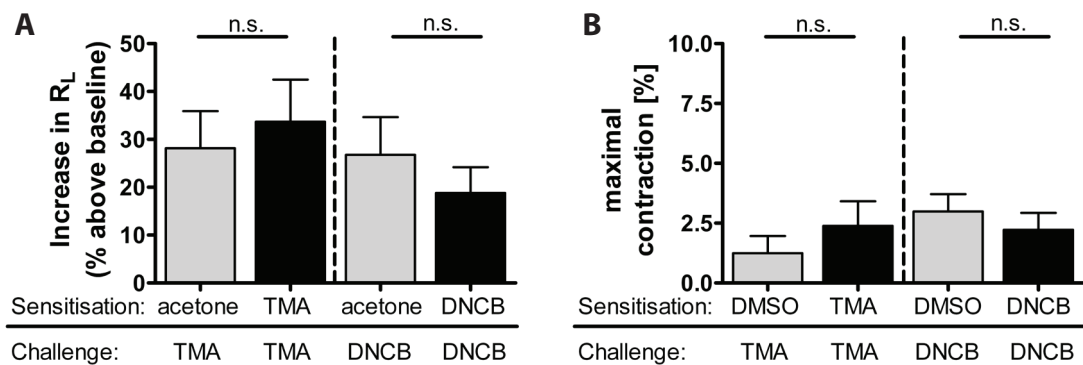
Figure 4.4: Comparison of the EAR *in vivo* and *ex vivo*. TMA- or DNCB-sensitised mice (A) or PCLS from sensitised mice (B) were challenged with TMA or DNCB. Sham sensitised animals with acetone or DMSO acted as a control. Bronchoconstriction in vivo is given as the percentage increase in pulmonary resistance and compared to the percentage in maximum airway contraction. *In vivo* experiments were accomplished by Maja Henjakovic (Hannover). Data are given as mean ± SEM, n = 6 to 12. Data were compared by the two-sided, unpaired t-test.

4.2.1.2. AHR in sensitised PCLS

24h after allergen challenge the unspecific AHR was measured *in vivo* (Fig. 4.5 A). Only TMA-sensitised mice showed a reduction of the ED_{50} in response to methacholine (0.21 µg vs. 0.06 µg). *Ex vivo* the response towards methacholine was investigated in the PCLS that were challenged with the allergen 16h before (Fig 4.5 B). While DNCB sensitisation had no effect, TMA significantly decreased the EC_{50} for methacholine-induced bronchoconstriction, indicating AHR. The corresponding EC_{50} values were 0.41 µM and 0.24 µM methacholine, respectively.
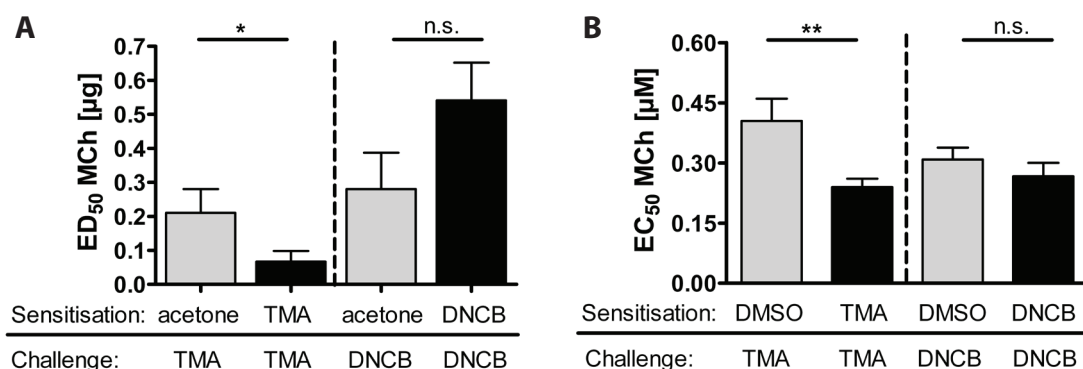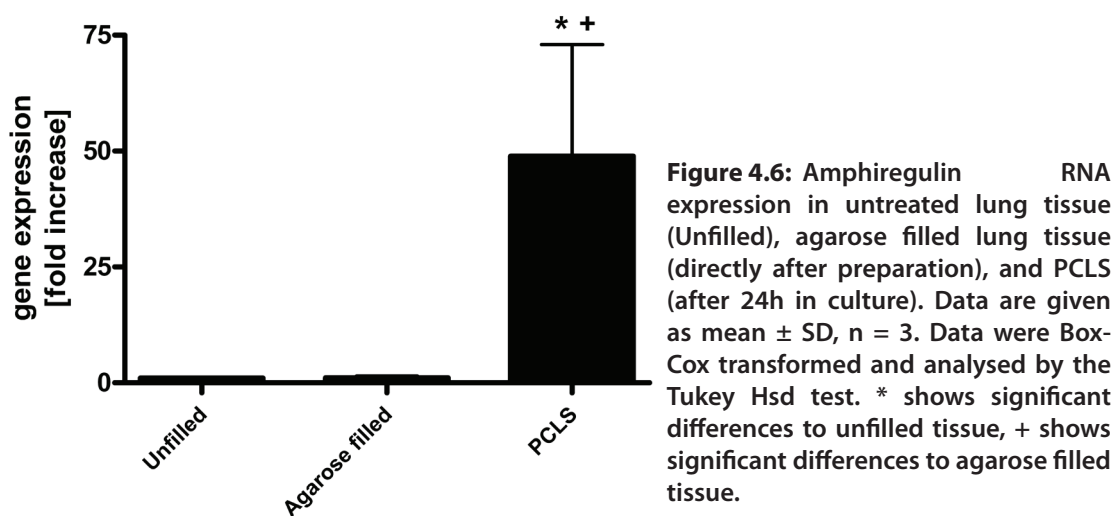

Figure 4.5: AHR *in vivo* (A) and *ex vivo* (B). ED_{50} and EC_{50} of methacholine were determined by application of different doses/concentrations. The *in vivo* experiments were performed by Maja Henjakovic (Hannover). Data are given in mean ± SEM, n = 5 or 6 (allergen sensitisation) or 12 (sham sensitisation). Data were compared by the two-sided, unpaired t-test.

4.3. Part III: Gene induction in PCLS

Amphiregulin has been identified as a gene that is upregulated specifically by mechanical stretch, while at the same time being unresponsive to inflammatory stimuli, such as LPS. Experiments in the isolated and perfused mouse lung model showed an induction of amphiregulin, specifically by overventilation and not influenced by LPS administration (65). The attempt to detect amphiregulin upregulation in stretched PCLS was complicated because of a strong upregulation of amphiregulin by the preparation procedure (Figure 4.6). The upregulation was significantly different in unfilled and agarose filled lung tissue.

Figure 4.6: Amphiregulin RNA expression in untreated lung tissue (Unfilled), agarose filled lung tissue (directly after preparation), and PCLS (after 24h in culture). Data are given as mean ± SD, n = 3. Data were Box-Cox transformed and analysed by the Tukey Hsd test. * shows significant differences to unfilled tissue, + shows significant differences to agarose filled tissue.

Amphiregulin RNA expression was followed over time after the slicing process. A maximum induction was found 4h after the slicing process, which decreased after 24h. Nevertheless a significant upregulation persisted until 48h in culture (Fig. 4.7).
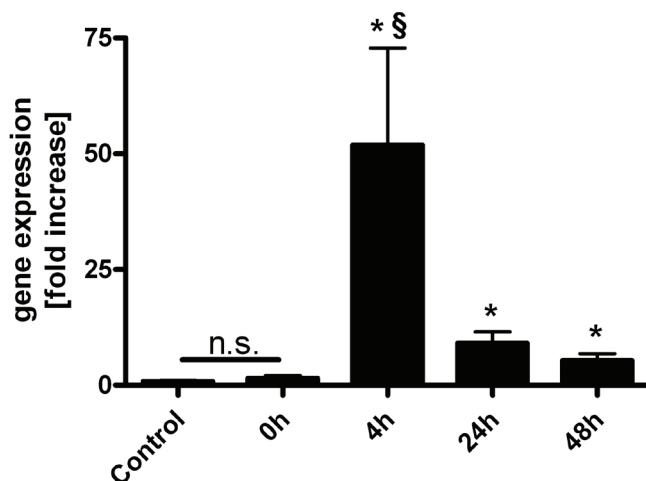
Figure 4.7: Amphiregulin RNA expression in untreated lung tissue (Control) in comparison with expression in PCLS directly (0h), 4h, 24h and 48h after the slicing process. Data are given as mean ± SD, n = 3. Data was Box-Cox transformed and analysed by the Tukey Hsd test. * shows significant differences to Control; § shows significant differences of the 4h group to all other groups. n.s. = non significant.

4.3.1. Gene induction 24h after the slicing process

To further examine gene expression in response to the slicing procedure, a gene array was performed comparing lung tissue to PCLS. 24h after the slicing process a variety of genes were upregulated, headed by immune response genes (Table 4.1). Besides classical inflammatory genes like Il-6 and Cxcl2 (MIP-2), also Lif, Csf3, Ccl7, Ccl2, Ptgs2 (Cox-2), Mmp3 and Cxcl10 were upregulated in PCLS. Interestingly, also Serpine1 was induced by the slicing process, which is known to play a role in tissue regeneration and wound healing. The amphiregulin gene was less upregulated in comparison to the genes mentioned above (Table 4.1).

Table 4.1: Gene induction by the slicing process as fold increase of the log 2 values compared to untreated lung tissue. Amphiregulin was not among the 10 top candidate genes, but still upregulated to a great extent.

Gene symbol	Protein	Fold increase (log 2)	Function
Il6	Interleukin-6	3.09	Immune response, response to mechanical stimulus, acute-phase response
Lif	Leukemia inhibitory factor	2.01	Immune response, cell surface receptor linked signal transduction, positive regulation of cell proliferation
Csf3	Colony stimulating factor 3 (granulocyte)	1.96	Immune response
Cxcl2	Chemokine ligand 2 (MIP-2)	1.92	Chemotaxis, inflammatory response, immune response
Ccl7	Chemokine (C-C motif) ligand 7	1.89	Transport, chemotaxis, inflammatory response
Mmp3	Matrix metallo- peptidase 3	1.88	Peptidoglycan metabolic process, proteolysis, collagen catabolic process
Ptgs2	Prostaglandin- endoperoxide synthase 2 (Cox-2)	1.84	Regulation of progression through cell cycle, prostaglandin biosynthetic process, cyclooxygenase pathway
Serpine1	Serine peptidase inhibitor	1.82	Response to reactive oxygen species, blood coagulation, wound healing, tissue regeneration
Ccl2	Chemokine ligand 2	1.77	Positive regulation of endothelial cell proliferation, chemotaxis, inflammatory response
Cxcl10	Chemokine ligand 10	1.75	Chemotaxis, inflammatory response, electron transport
Areg	Amphiregulin	1.33	Epidermal growth factor receptor signaling pathway

4.3.2. RNA expression

4.3.2.1. RTq-PCR

To validate the gene induction, RNA expression of selected genes was determined 24h after the slicing process by RTq-PCR (Fig. 4.8). IL-6 was upregulated to a great extend followed by MIP-2, Cox-2, IP-10 and amphiregulin. Larger than thousand fold increases may be explained by the relatively low levels of the corresponding RNA in untreated lung tissue.
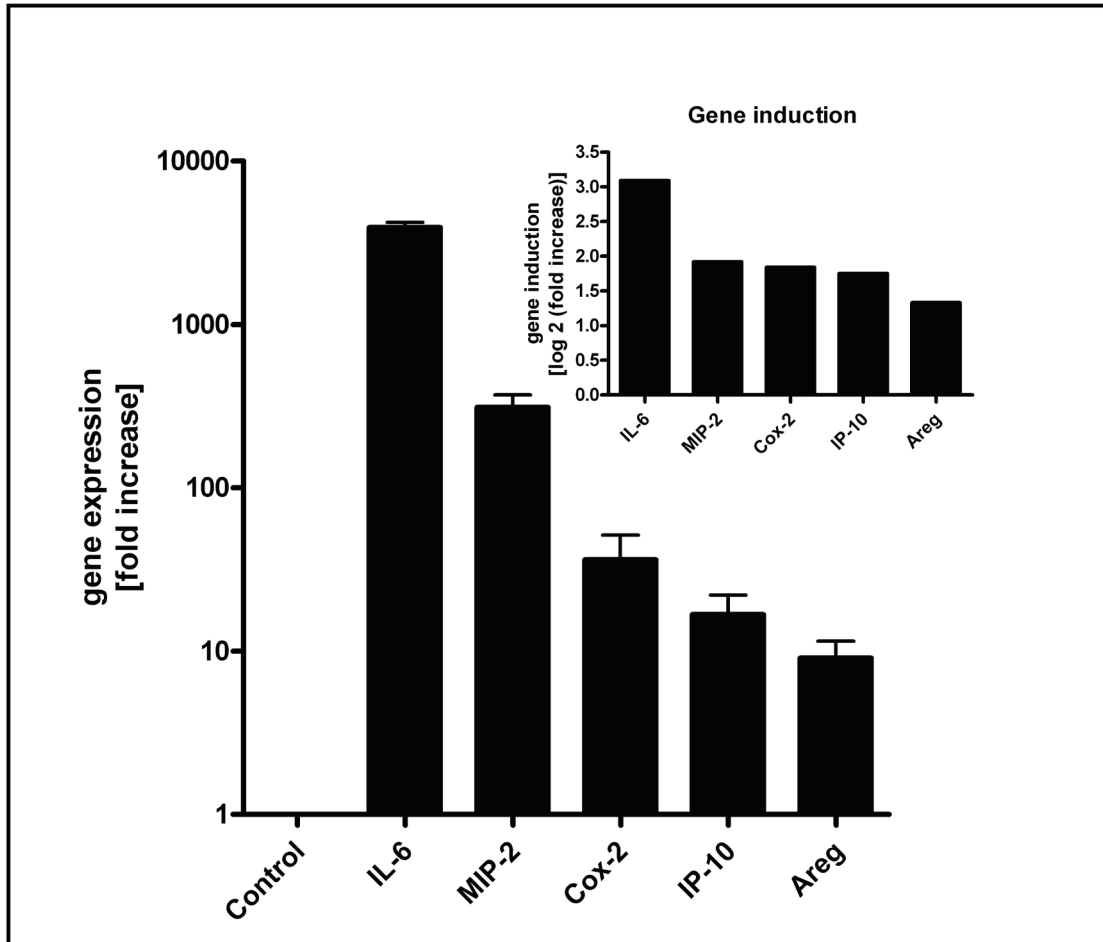
Figure 4.8: RNA induction 24h after the slicing process. Gene induction of IL-6, MIP-2, Cox-2, IP-10 and amphiregulin was determined in a gene array experiment (small insert) and verified by RTq-PCR. RNA data are given as mean ± SD, n = 3.

4.3.2.2. RNA expression of immune response genes

The induction of IL-6, MIP-2, Cox-2 and IP-10 was investigated by RTq-PCR (Fig. 4.9). RNA expression was determined 4h, 24h and 48h after the slicing process. Untreated lung tissue (neither agarose filled nor sliced; the left lower lung lobe was separated by a clamp before the agarose filling) served as control. RNA expression was also determined directly after the the slicing process (0h) before the PCLS were taken into culture at 37°C and 5 % CO_2.

Directly after the slicing process both IL-6 and MIP-2 were significantly induced. Maximum RNA expression was observed after 24h for IL-6 and MIP-2. After 48h the expression was reduced, but was still significantly upregulated in comparison with untreated lung tissue. Cox-2 upregulation also started directly after the slicing process
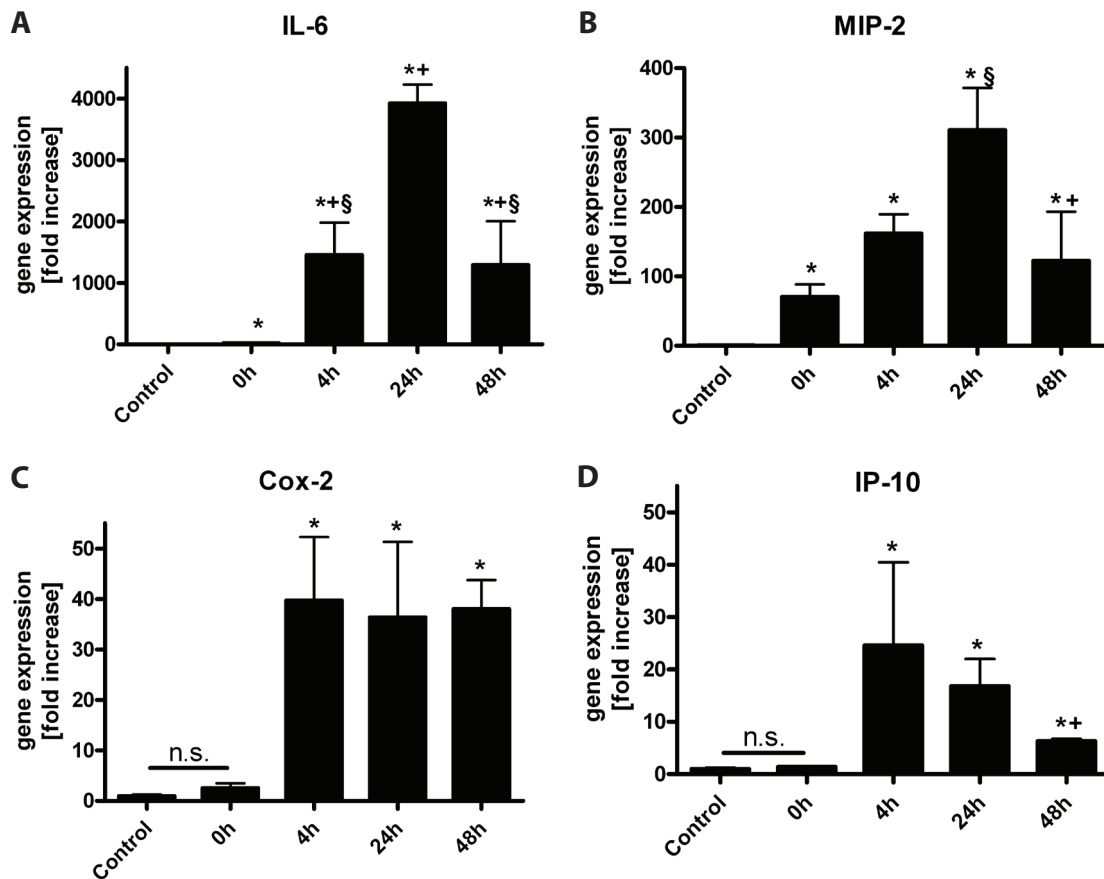
Figure 4.9: RNA expression after preparation of PCLS. Fold increase of IL-6 (A), MIP-2 (B), Cox-2 (C) and IP-10 (D) mRNA is shown 0h, 4h, 24h and 48h after the slicing process, compared to untreated lung tissue (Control). A: IL-6 mRNA induction after the slicing process; * shows significant differences to Control; + shows significant differences to the 0h group and § shows significant differences of the 4h group to the 24h and 48h group. B: MIP-2 mRNA induction after the slicing process; * shows significant differences to Control; $ shows a significant difference between the 0h group and the 24h group; + shows a significant difference between the 24h group and the 48h group. C: Cox-2 mRNA induction after the slicing process * shows significant differences to Control. D: IP-10 mRNA induction after the slicing process; * shows significant differences to Control; + shows a significant difference between the 24h group and the 48h group. n.s. = non significant. Data are given as mean ± SD (n = 3). Data was Box-Cox transformed and analysed by the Tukey Hsd test, p-values < 0.05 were considered significantly different.

and reached its maximum after 4h. This level of mRNA expression persisted until 48h after the slicing process.

IP-10 was upregulated to a maximal extent 4h after the slicing process. After 24h, the mRNA level was slightly, but not significantly, reduced. 48h after the slicing process there was a significant reduction in IP-10 levels compared to the 4h and 24h level. Nevertheless, also IP-10 was still significantly induced after 48h compared to the control. Like amphiregulin, IP-10 was not significantly induced directly after the slicing process.

4.3.2.3. RNA induction by LPS application

To investigate wether the RNA induction by the slicing process can be induced further, PCLS were treated with LPS 24h after the slicing process, because LPS is known to induce genes of the inflammatory response. Treatment of PCLS with LPS for 1h further induced IL-6, MIP-2, Cox-2 and IP-10 expression, indicating that the slicing process does not maximally increase the response of these genes (Fig. 4.10). In contrast to MIP-2, Cox-2 and IP-10 RNA expression the induction of IL-6 by LPS was not significant. As
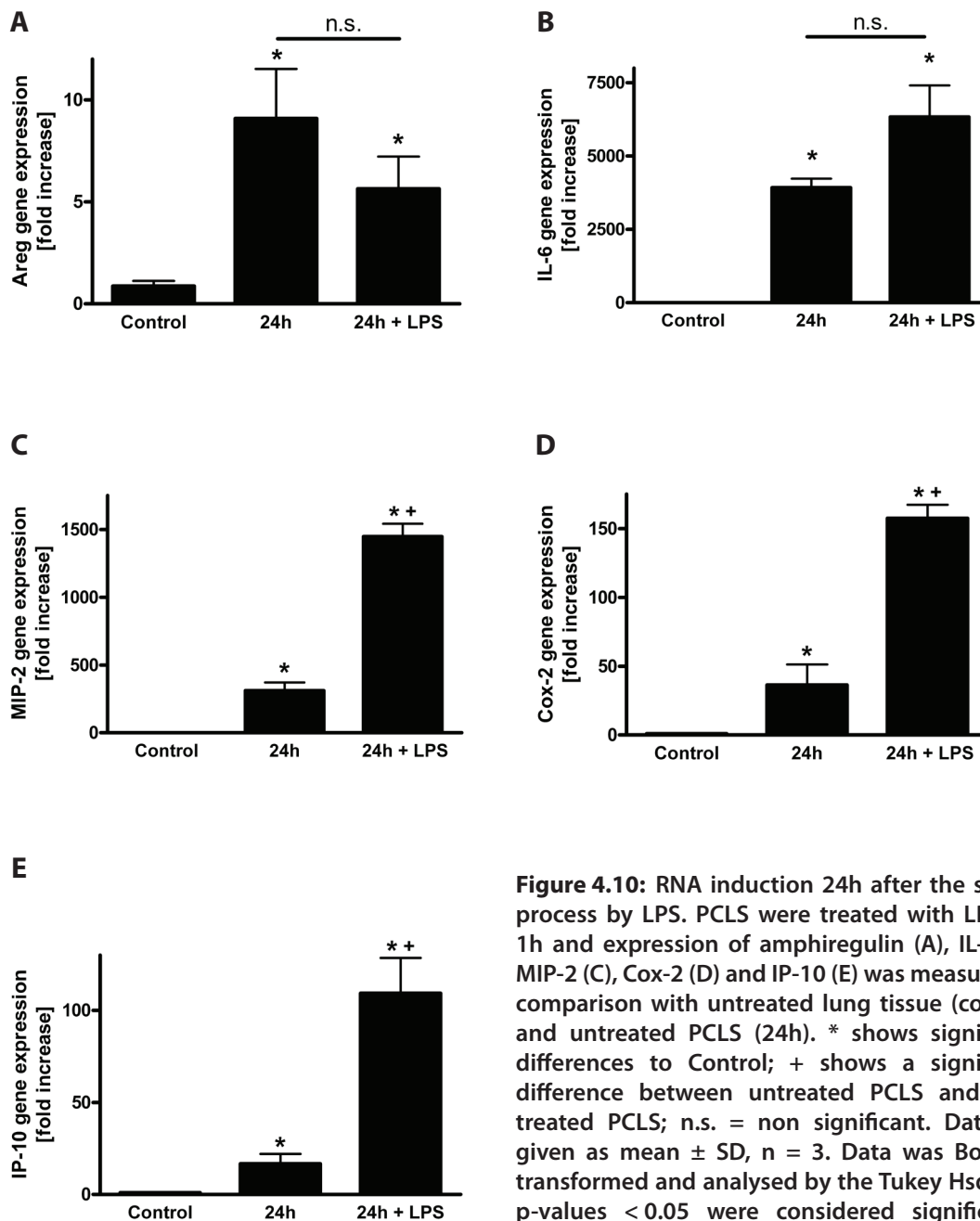

Figure 4.10: RNA induction 24h after the slicing process by LPS. PCLS were treated with LPS for 1h and expression of amphiregulin (A), IL-6 (B), MIP-2 (C), Cox-2 (D) and IP-10 (E) was measured in comparison with untreated lung tissue (control) and untreated PCLS (24h). * shows significant differences to Control; + shows a significant difference between untreated PCLS and LPS-treated PCLS; n.s. = non significant. Data are given as mean ± SD, n = 3. Data was Box-Cox transformed and analysed by the Tukey Hsd test, p-values < 0.05 were considered significantly different.

expected from IPL mouse data, LPS did not induce amphiregulin expression confirming the fact that amphiregulin is not upregulated by LPS. In fact there was a tendency of reduction in amphiregulin RNA expression after LPS treatment.

4.3.2.4. Incubation of PCLS at 4°C and 37°C

Amphiregulin, IL-6, MIP-2, Cox-2 and IP-10 were all upregulated by the slicing process. However, the maximum induction of each gene is reached after 4h to 24h incubation at cell culture conditions. To investigate the different factors which may contribute to the induction of the genes after the slicing process, we examined the effect of temperature. PCLS were kept at 4°C instead of incubating them at 37°C. Media changes were performed at 4°C. Comparison with PCLS incubated at 37°C showed no gene induction for IL-6, MIP-2, Cox-2 or IP-10, independent of the time period PCLS were kept at 4°C (4h or 24h, Fig. 4.11).
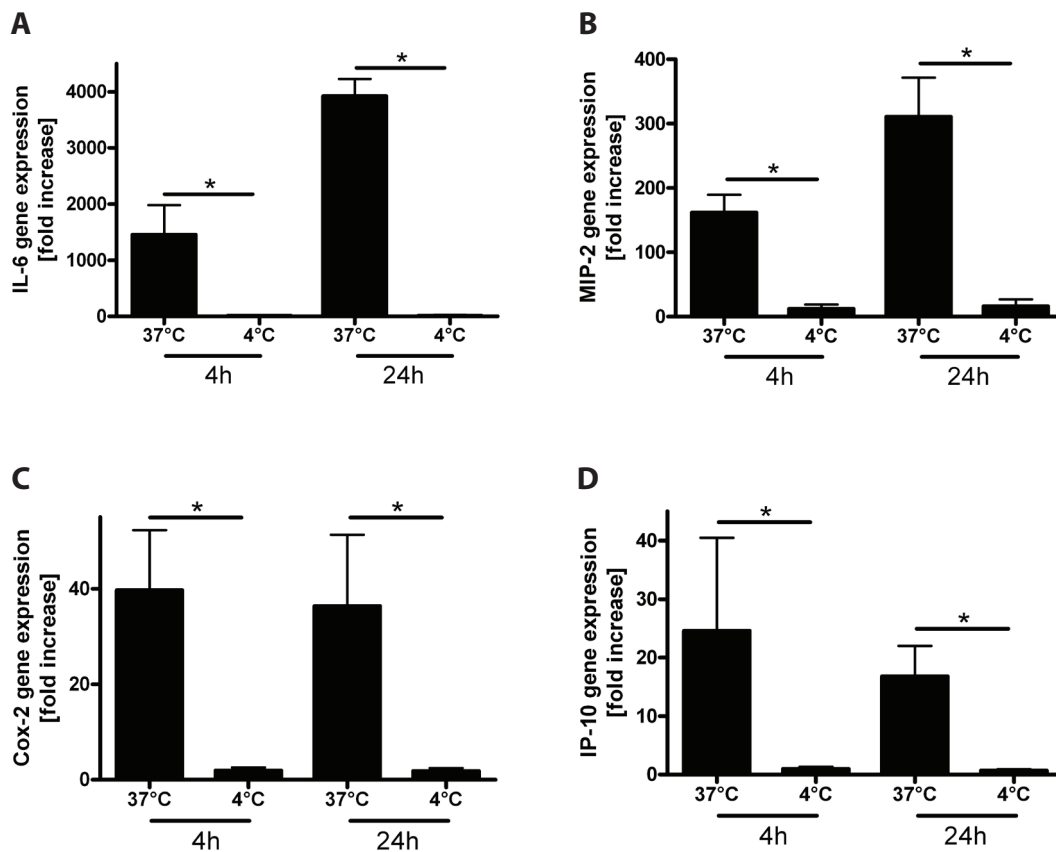

Figure 4.11: RNA expression 4h and 24h after the slicing process. PCLS were either incubated at 4°C or 37°C and induction of IL-6 (A), Mip-2 (B), Cox-2 (C) and IP-10 (D) was measured. Data are given as mean ± SD, n = 3. Data was Box-Cox transformed and analysed by the Tukey Hsd test, p-values < 0.05 were considered significantly different.

Amphiregulin induction was also measured after incubation at 4°C (Fig. 4.12). No induction was observed in PCLS incubated at 4°C after 4h and 24h. To investigate whether the maximum induction after 4h at 37°C was reduced by the 4°C incubation, PCLS were incubated at 4°C for 20h and 44h before incubation for 4h at 37°C. Incubating the PCLS for 20h at 4°C did not prevent the amphiregulin induction after 4h at 37°C, which was comparable to the induction observed in PCLS directly incubated for 4h at 37°C after the slicing process. Only PCLS incubated for 44h at 4°C showed a significant reduction in amphiregulin induction after incubation at 37°C for 4h (Fig. 4.12 B).
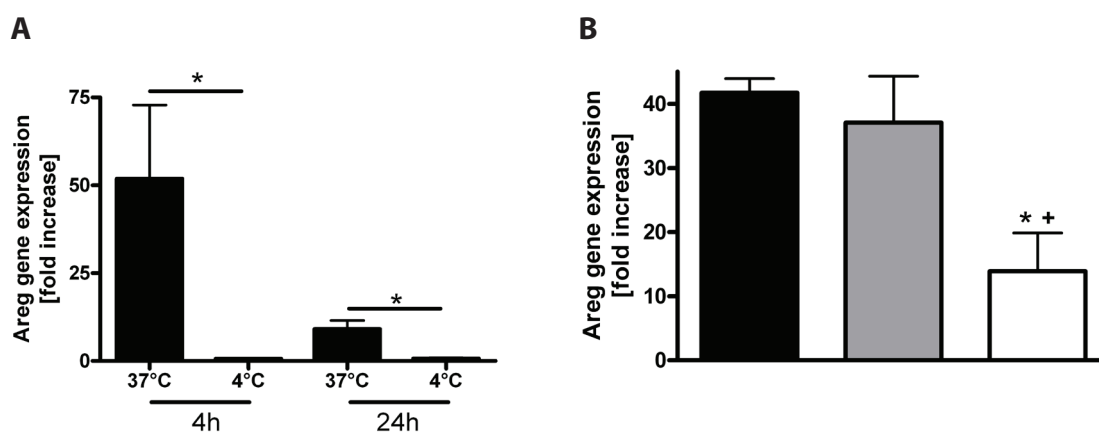

Figure 4.12: RNA expression of amphiregulin after 4h at 37°C. Panel A shows a comparison of PCLS incubated at 37°C and 4°C. Data are given as mean ± SD, n = 3. B: Amphiregulin induction after 4h at 37°C. PCLS were incubated for 0h (black column), 20h (grey column) and 44h (white column) at 4°C before they were incubated at 37°C for 4h. * shows significant differences to 0h incubated PCLS; + shows a significant difference between 0h and 44h incubated PCLS. Data are given as mean ± SD, n = 3. Data was Box-Cox transformed and analysed by the Tukey Hsd test, p-values < 0.05 were considered significantly different.

4.3.2.5. Viability of PCLS incubated at 4°C

PCLS were taken into culture at 37°C to mimic the physiological condition found in the body. To investigate whether the storage of the PCLS at 4°C had negative effects on the viability, MTT formation was measured after 24h and 48h. Incubation of PCLS at 4°C had no influence on the viability of PCLS compared to PCLS directly incubated at 37°C (Fig. 4.13).
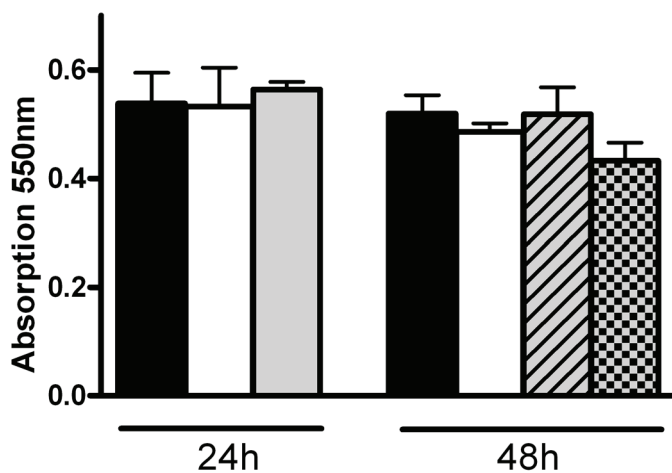

Figure 4.13: Viability of PCLS after incubation at 4°C and 37°C. Mitochondrial activity was measured 24h after the slicing process in PCLS incubated at 37°C (black column), 4°C (white column) and in PCLS incubated for 20h at 4°C and 4h at 37°C (grey column). Measurement after 48h show PCLS incubated at 37°C (black column), incubated at 4°C (white column), incubated at 4°C for 20h and 28h at 37°C (grey column with stripes) and PCLS incubated at 4°C for 44h and 4h at 37°C (checked grey column). Data are given as mean ± SD, n = 3. Data was Box-Cox transformed and analysed by the Tukey Hsd test.

4.3.2.6. Influence of agarose filling

Another parameter investigated was the agarose filling of the lung (Fig. 4.14). Although the agarose is washed out of the PCLS during the incubation at 37°C there is still a distending stimulus being filling the lung. Shortly after the slicing process no induction in the filled lung was measured. Incubation of a part of the filled lung in medium at 37°C for 4h led to an induction of IL-6, MIP-2, Cox-2, IP-10 and amphiregulin. Compared to the induction by the slicing process the expansion stimulus seems to be less intense. These data indicate that induction of genes is dependent on incubation at 37°C. The extension stimulus seems to be the first impulse leading to an upregulation of genes, while the slicing procedure may be a second cause of induction. Incubation of PCLS at 4°C after the slicing process does not prevent amphiregulin induction at 37°C; it only reduces it to a certain level if the PCLS are incubated for 44h at 4°C.
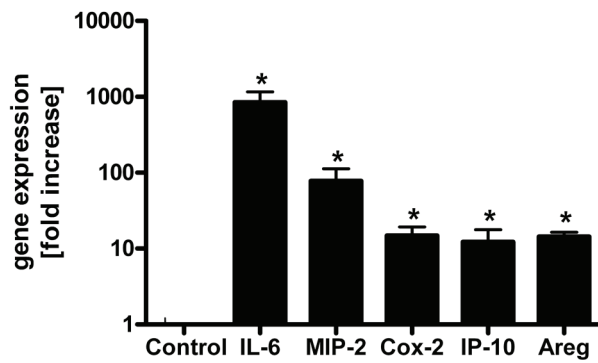
Figure 4.14: Influence of agarose filling of the lung. Lung filled with 15 ml agarose and incubated for 4h at 37°C. Gene expression of IL-6, MIP-2, Cox-2, IP-10 and amphiregulin was measured. Data are given as mean ± SD, n = 3. Data was Box-Cox transformed and analysed by ANOVA and Dunetts test, p-values < 0.05 were considered significantly different.

4.3.2.7. Inhibition of amphiregulin induction in PCLS

It was our aim to inhibit the amphiregulin induction by the slicing procedure, to differentiate a stretch specific induction by distension of the PCLS. To evaluate whether the gene induction during the preparation of the PCLS could be diminished by inhibition of the transcriptional level, different inhibitors of transcription and translation were used. Amphiregulin was the gene of special interest; because the final aim was to induce it by overexpansion of PCLS. Four different transcription inhibitors were added during the slicing process and for the next 4h. Actinomycin D,
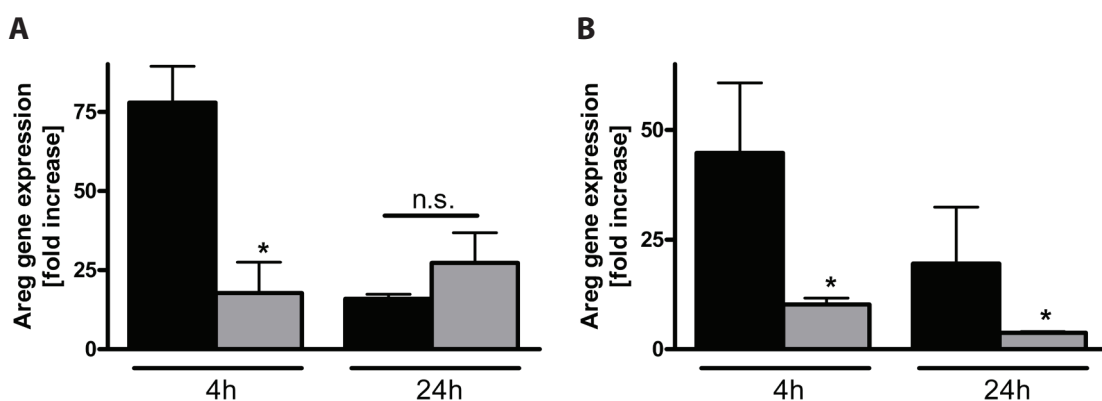
Figure 4.15: Amphiregulin RNA expression in PCLS treated with the transcription inhibitors DRB (A) or apicidin (B). Left panel shows control PCLS (black columns) compared with DRB treated PCLS (grey columns) 4h and 24h after the slicing process. Right panel shows control PCLS (black columns) compared with Apicidin treated PCLS (grey columns) 4h and 24h after the slicing process. PCLS were treated with 50 µM DRB or 2 µg/ml apicidin. Data are given as mean ± SD, n = 3. Data was Box-Cox transformed and analysed by the Tukey Hsd test, p-values < 0.05 were considered significantly different (*); n.s. = non significant.

an inhibitor of the RNA polymerase and cycloheximide, a translational inhibitor were tested alone and in combination. Preliminary experiments showed that actinomycin D almost completely blocked the amphiregulin induction for at least 24h, but slicing or stretching did not induce amphiregulin (data not shown). Cycloheximide reduced the induction only partly and after 24h the amphiregulin induction was comparable to that in untreated PCLS. The simultaneous treatment with both inhibitors resulted in the same complete inhibition as observed for actinomycin D (data not shown). Furthermore, the RNA synthesis inhibitor 5,6-Dichlorobenzimidazole riboside (DRB) and apicidin, an inhibitor of the histone deacetylase were used (Fig. 4.15). Both inhibitors were able to reduce the amphiregulin induction significantly. After 24h it tended to be increased in DRB treated PCLS compared with untreated control PCLS. Thus, DRB is only effective for 4h and subsequently it may intensify the induction. Apicidin still blocked the amphiregulin induction significantly after 24h, but it was not possible to induce amphiregulin by 4h stretch (data not shown).

In general, transcriptional and translational inhibitors were able to reduce the amphiregulin induction. Unfortunately, their effectiveness was either too strong or not long lasting.

4.3.3. Mechanisms of amphiregulin induction in PCLS

Because of the massive induction of amphiregulin in PCLS after the slicing process, different inhibitors were used to investigate the mechanism of amphiregulin induction. The highest upregulation could be observed 4h after the slicing process. Therefore inhibitors were added during the slicing process and for the next 4h of incubation. The aim was to reduce the maximum induction 4h after the slicing process to possibly diminish the overall induction of amphiregulin. Without inhibition the increase in amphiregulin after 24h is still too high to re-induce it by stretch or to differentiate stretch-induction from the basal level.

4.3.3.1. Influence of tyrosine kinases

The specific tyrosine kinase inhibitor genistein and the selective Src-tyrosine-kinase inhibitor PP2 were used to examine the influence of tyrosine kinases on amphiregulin induction (Fig. 4.16). Genistein inhibited amphiregulin induction at 4h after the slicing process. After 24h there was no difference between solvent and genistein-treated PCLS. PP2 significantly reduced amphiregulin induction after 4h compared to solvent-treated PCLS. After 24h there was no more difference between solvent-treated and PP2-treated PCLS.
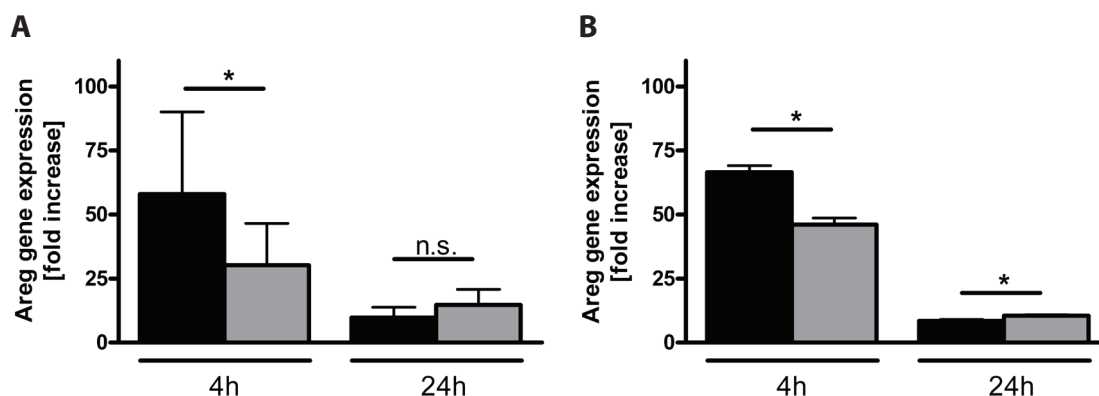
Figure 4.16: Amphiregulin expression in PCLS 4h and 24h after the slicing process treated with 100 μM of the tyrosine-kinase-inhibitor Genistein (A) and 10 μM of the Src-tyrosine-kinase inhibitor PP2 (B). Solvent-treated PCLS are illustrated as black columns and inhibitor-treated PCLS as grey columns. Data are given as mean ± SD, n = 6 – 7 (Genistein) and 3 (PP2). Data was Box-Cox transformed and analysed by the Tukey Hsd test, p-values < 0.05 were considered significantly different (*); n.s. = non significant.

These data indicate a role of tyrosine kinases in amphiregulin induction, possibly by Src-tyrosine kinases. After 4h a reduction of amphiregulin was observed, which was not seen 24h after the slicing process.

4.3.3.2. Influence of Sphingolipids

Sphingolipids, derived from the plasma membrane, are known to play an important role in the lungs (269). Acid sphingomyelinase generates ceramide, a constituent of ceramide-rich microdomains and a second messenger. Stress is well known to activate the acid sphingomyelinase, and therefore PCLS were treated with imipramine, an inhibitor of the acid sphingomyelinase pathway. Furthermore, PCLS were treated with sphingosine-1-phosphate that exerts protective effects in several insults (Fig 4.17). Again treatment was maintained during and for 4h after the slicing process. No influence of the inhibition of the acid shingomyelinase was observed, neither 4h nor 24h after the slicing process. Treatment with sphingosine-1-phosphate increased the amphiregulin induction significantly 4h after the slicing process. There may be an activating effect on amphiregulin induction by sphingosine-1 phophate, which seems to be independent from acid sphingomyelinase.
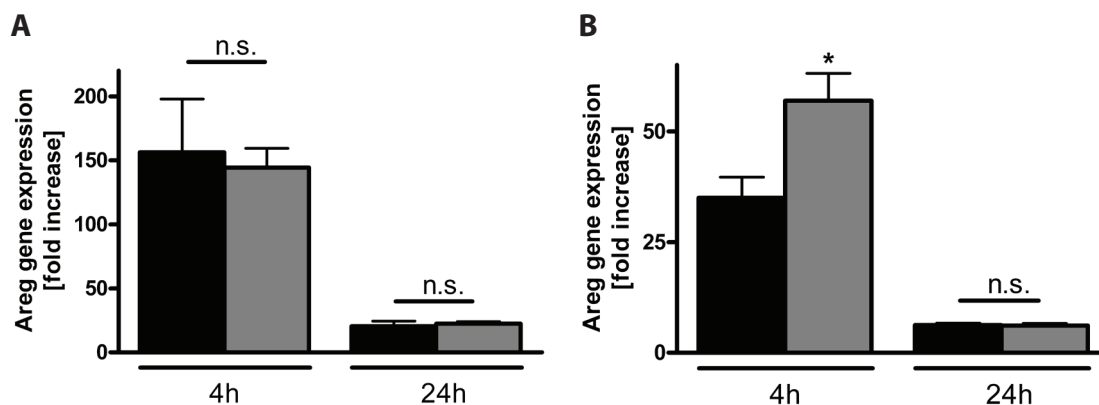
Figure 4.17: **Amphiregulin RNA expression in PCLS treated with either 10 µM imipramine (A) or 1.32 µM sphingosine-1-phosphate (B). RNA expression was measured 4h and 24h after the slicing process. Solvent-treated PCLS are illustrated as black columns and inhibitor-treated PCLS as grey columns. Data are given as mean ± SD, n = 3. Data was Box-Cox transformed and analysed by the Tukey Hsd test, p-values < 0.05 were considered significantly different (*); n.s. = non significant.**

4.3.3.3. Influence of calcium and ion-channels

Lanthanum chloride is used to block divalent cation channels, mainly calcium channels, and has been used as an unspecific inhibitor of stretch-activated ion channels (114; 227). Another selective calcium channel inhibitor is ruthenium red,

Figure 4.18: Amphiregulin induction in PCLS sliced and incubated in low calcium medium (grey columns, calcium reduced to 10 % of the normal amount) 4 and 24h after the slicing process. Control PCLS incubated in normal medium are illustrated as black columns. Data are given as mean ± SD, n = 3. Data was Box-Cox transformed and analysed by the Tukey Hsd test, n.s. = non significant.
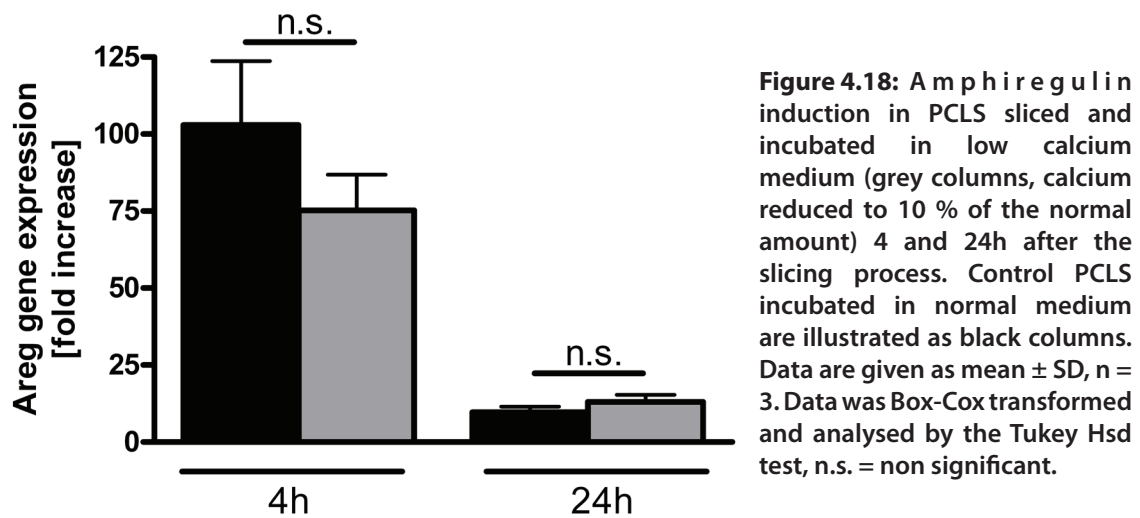
especially blocking TRPV channels and the ryanodine receptor (96; 306). As another approach, calcium in the slicing and incubation medium was reduced to 10 % of the normal amount (4.18). The treatments were applied during the slicing process and 4h thereafter. Reduced extracellular calcium slightly reduced amphiregulin induction after the slicing process, but this was not significant. 24h after the slicing process there was no difference in amphiregulin induction compared to control PCLS. No effect on amphiregulin induction was observed by treatment with lanthanum chloride (Fig. 4.19 B). Ruthenium red increased amphiregulin induction significantly 24h after the slicing process (Fig. 4.19 A).

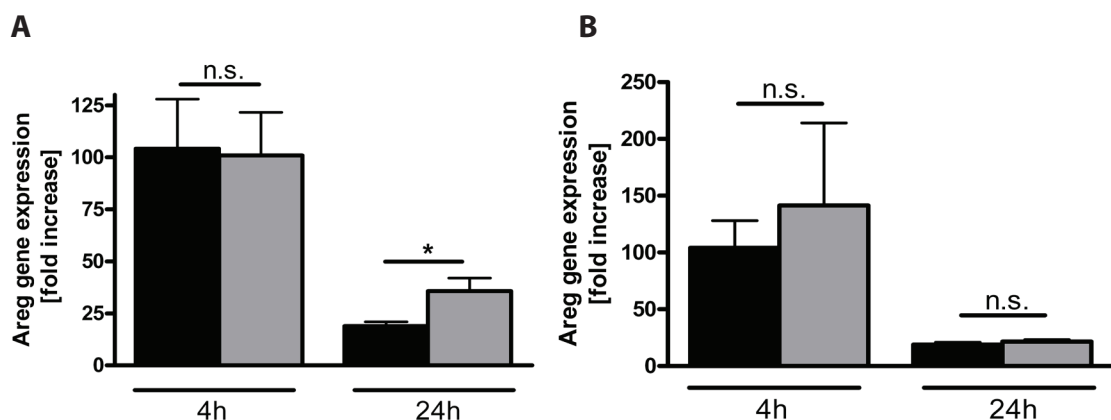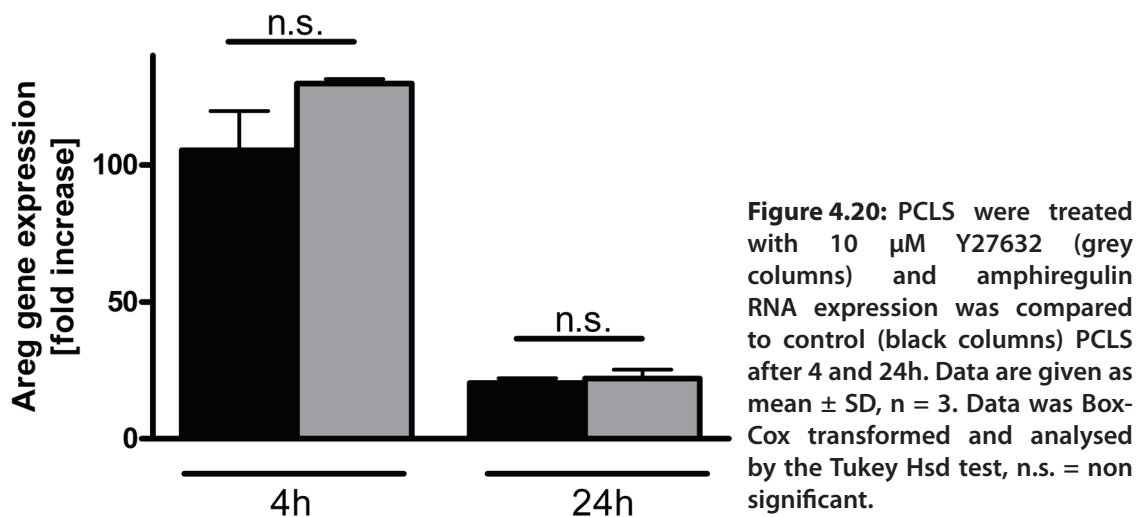**Figure 4.19:** Amphiregulin induction in PCLS sliced and incubated for 4h with either 20 μM ruthenium red (A) or 100 μM lanthanum chloride (B), shown as grey columns. Control PCLS incubated in normal medium are illustrated as black columns. Data are given as mean ± SD, n = 3. Data was Box-Cox transformed and analysed by the Tukey Hsd test, p-values < 0.05 were considered significantly different (*); n.s. = non significant.

In general reduced calcium does not appear to play a major role in amphiregulin induction, which does not seem to be mediated by store operated calcium channels, TRPV, or the ryanodine receptor.

4.3.3.4. Influence of the cytoskeleton

To investigate, whether the cytoskeleton plays a role in mediating the induction of amphiregulin, different inhibitors were used during the slicing process and 4h after it. Y27632 is an inhibitor of the rho-kinase, which is involved in the organisation of the actin cytoskeleton. Besides inhibiting the Rho-kinases, cytochalasin D, a fungal toxin, which inhibits actin polymerisation, was employed. In addition, myosin light chain phosphorylation was blocked by ML-7. No decrease in amphiregulin induction was found after treatment with Y27632 (Fig. 4.20).

Figure 4.20: PCLS were treated with 10 μM Y27632 (grey columns) and amphiregulin RNA expression was compared to control (black columns) PCLS after 4 and 24h. Data are given as mean ± SD, n = 3. Data was Box-Cox transformed and analysed by the Tukey Hsd test, n.s. = non significant.

ML-7 and cytochalasin D both inhibited the maximum induction 4h after the slicing process (Fig. 4.21). In case of ML-7 this reduction was significant. Therefore an involvement of the myosin light chain kinase and the actin filaments is probable.
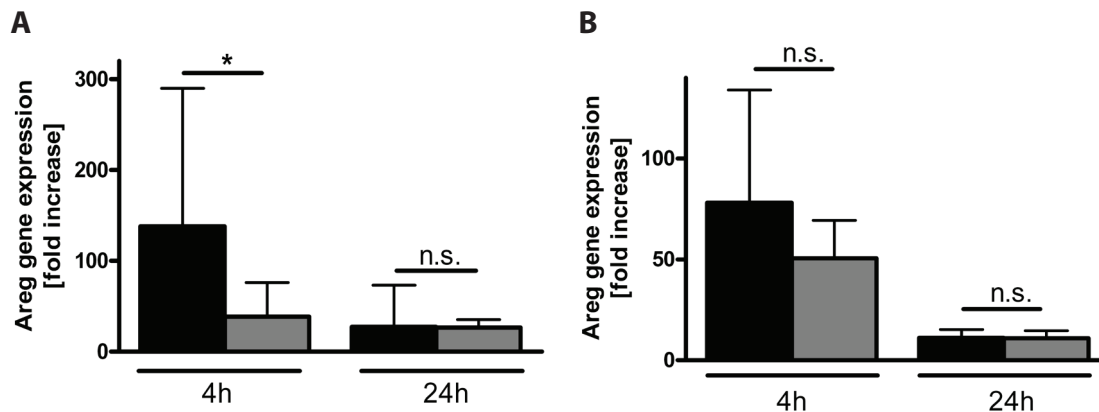
A

B

Figure 4.21: Amphiregulin RNA expression in PCLS treated with 30 µM ML-7 (A) and 1 µM cytochalasin D (B). Solvent-treated PCLS are illustrated as black columns and inhibitor-treated PCLS as grey columns. Data are given as mean ± SD, n = 6. Data was Box-Cox transformed and analysed by the Tukey Hsd test, p-values < 0.05 were considered significantly different (*); n.s. = non significant.

4.3.4. Amphiregulin induction in response to chemical substances

Amphiregulin has been shown to be induced by physical injury such as stretch or slicing. To investigate whether it is also inducible by chemical stress like allergens or reactive oxygen species, PCLS were treated with TMA, DNCB or H_2O_2 for 4h. No further induction by the substances was observed 24h after the slicing process (4.22). This could be explained by the high basal induction as observed for stretch experiments.
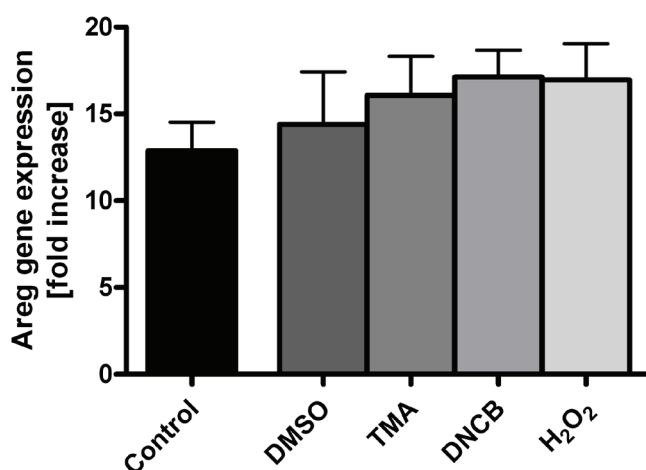

Figure 4.22: Amphiregulin induction in PCLS after treatment with 0.05 % DMSO (solvent), 1.2 µg/ml TMA, 1 µg/ml DNCB and 10 µM H_2O_2. No significant difference was found in treated PCLS compared to untreated control PCLS. Data are given as mean ± SD, n = 3. Data was Box-Cox transformed and analysed by the Tukey Hsd test.

4.4. Part IV: Distension of PCLS in a bioreactor

The bioreactor, as a pressure operated strain applicator, was first described in 2008 by Schumann et al. (232). A pressure-driven strain-applicator was developed, which uses spherical deflection of a carrier membrane to transmit tensile strain to a biological sample placed on top of it. At that time the experiments where done with test membranes serving as a physical model of biologic tissue. It was our aim to establish the distension of PCLS in the bioreactor.

4.4.1. Membranes

Evaluating the performance of the bioreactor Schumann et al. used polyurethane and latex membranes of well defined and highly reproducible material characteristics (232). To measure strain applied to lung tissue the membrane preferably would have similar characteristics to the tissue, in particular with respect to the stiffness. Furthermore, it should be flexible to allow proper dynamic deformations, yet maintain its material characteristics (no plasticity). The first membrane we tested was a thin, highly flexible silicone membrane. The membrane was placed in a plastic membrane holder and fixated by a second plastic ring by clamping it. This fixation assembly became problematic because it was impossible to clamp such a thin membrane crease-free between the two plastic rings. A second problem became apparent after distension of the membrane, which revealed its plastic deformability. To overcome the problems, the membrane concept was changed to another fixation technique and different membrane material. Polyurethane membranes were crease-free glued on a metal ring, which was placed in the membrane holder. Polyurethane membranes are much
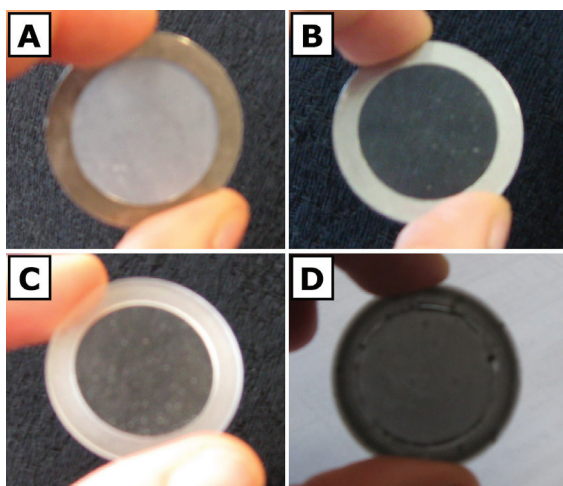
Figure 4.23: Different membranes tested in the bioreactor. (A) Polyurethane membrane glued on a metal ring, (B) PDMS membrane on a metal ring, (C) PDMS membrane on a macrolon ring, (D) Stained PDMS membrane on a macrolon ring.

thicker and therefore stiffer, but the plastic deformation was reduced. To reduce the stiffness, a third membrane material was tested. Polydimethylsiloxane (PDMS) shows a minimal plastic deformation although it is very flexible. By a spin-coating process it can be cast directly on a metal or macrolon ring with a thickness of about 30 μm. The membranes were tested with isolated rat diaphragms (9). For the above mentioned reasons, PDMS membranes were considered as the most suitable membranes to distend PCLS. Different membrane types are shown in Fig. 4.23.

4.4.2. Fixation of the lung slice

Most cell stretch devices work with cells grown directly on flexible membranes. However, PCLS did not adhere on the membranes or substrates that we tried. Therefore we attempted to glue the PCLS on top of the membrane using a tissue adhesive. Unfortunately the PCLS only properly adhered by glueing the whole undersurface of the PCLS on the membrane, which stiffened the tissue in that area completely. Hence, tissue characterics were not maintained anymore and the stiff underside of the PCLS would have interfered with strain measurements. Therefore, the new approach was the mechanical fixation of a PCLS in the bioreactor. Two macrolon discs were designed to clamp the membrane and the PCLS concentrically, leaving an aperture for the distension of the slice (Fig. 4.24). The concentrically grooved surface clamped the PCLS for 2 mm at the fringe. A space of approximately 150 μm remained between the crests to compress and fixate the PCLS. The clamped and thus damaged tissue was removed after the distension and the PCLS was used for further analysis.
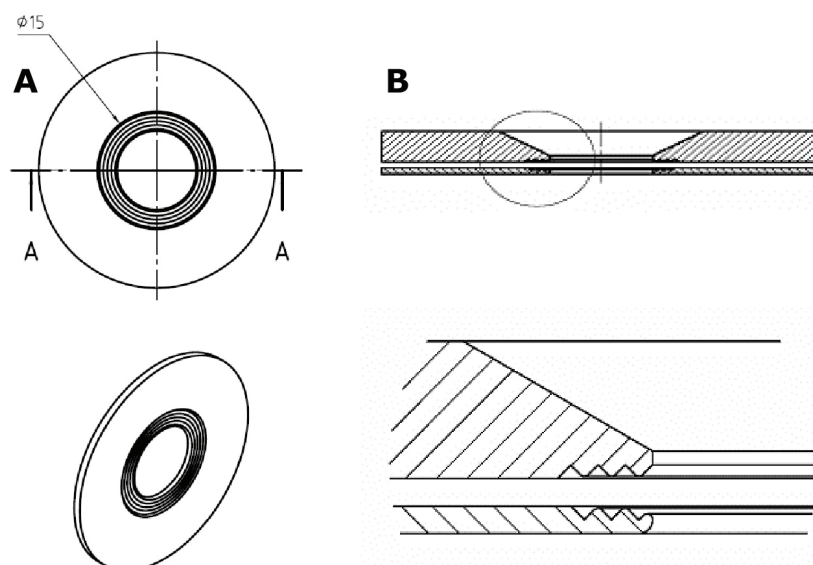

Figure 4.24: Schematic view of the clamping adapter device. The inner cogging was specifically designed to fixate very soft tissues, such as lung parenchyma. Panel A shows one macrolon disc from different points of view. In panel B the fixation clamp is shown, the circle in the upper picture is magnified below.

4.4.3. Static distension of the PCLS

4.4.3.1. Displacement readings

For static distension, pressure was increased in steps by injecting air in the lower chamber of the bioreactor. At pressures higher than 52 mbar the PCLS became disrupted, hence 52 mbar were defined as the maximum pressure. Membranes were mounted in the bioreactor as detailed below and varying pressures were applied. Displacement was measured by microscopy-based distension measurement at the center of the slices (Fig. 4.25). At 52 mbar the maximum excursion of the tip was approximately 4.5 ± 0.7 mm. Next, lung slices were mounted in the bioreactor and stretched under static conditions by applying varying pressures to the lower chamber. If lung slices were mounted onto the PDMS membranes, the excursion at pressures above 30 mbar was reduced in comparison to membranes alone and the maximum distension was about 3.5 ± 0.5 mm.
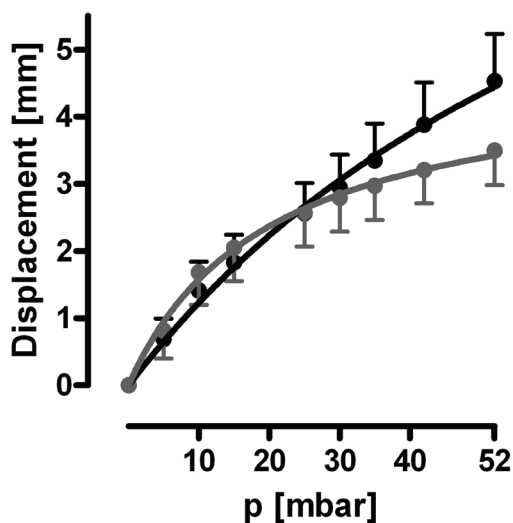

Figure 4.25: Excursion of membranes without (black) and with PCLS mounted onto them (grey). Data are given as mean ± SD, n = 11. Curves were compared by using the best-fit value of the parameters BMAX and KD by F-test, resulting in different curves for each data set.

4.4.3.2. Finite element model

To determine the strain distribution in the lung slices, the distension of the PCLS was modelled by finite elements. The numerical simulation was compared to the experimental data. The result is shown in Figure 4.26, illustrating the tip displacement of the membrane-tissue construct for varying pressures. At all pressures the numerical simulation and the experimental data were well compatible (Fig. 4.26 A). The numerically determined deformation states of the membrane tissue construct at pressures of 35 and 52 mbar are depicted in Figure 4.26 B.
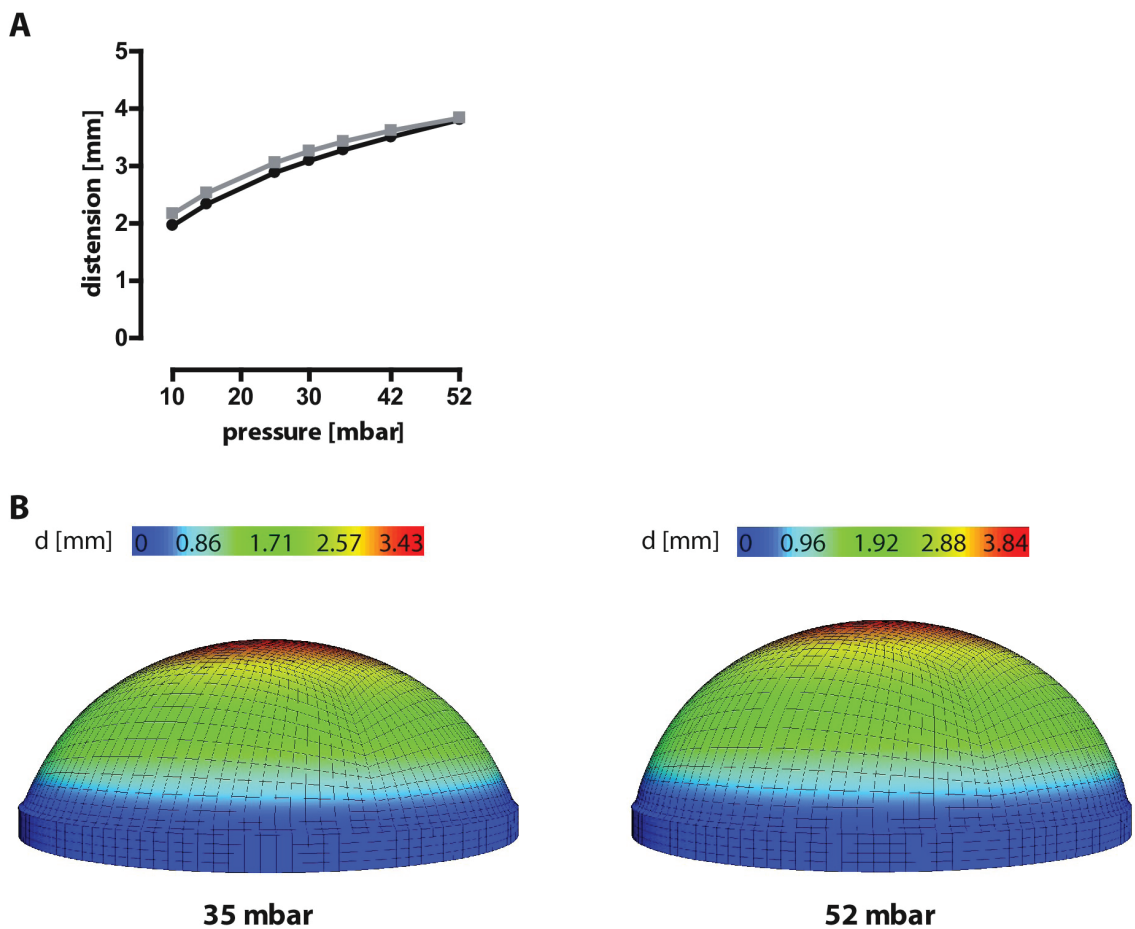
Figure 4.26: Distension of membrane-tissue construct. A: Tip displacement of the membrane-tissue construct under varying presures. The black line refers to experimentally measured deformation states, whereas the grey line represents numerical results obtained in a FE simulation. Curves were compared by F-test resulting in shared curves for each data set. B: Absolute vertical displacements d [mm] of membrane-tissue construct under a hydrostatic pressure load of 35 and 52 mbar.

Principal stretches in the longitudinal, latitudinal and transversal direction were analysed in Figure 4.27. The stretch in the latitudinal direction was up to 33 % at 35 mbar and up to 38 % at 52 mbar, with maximum values at the dome. The longitudinal stretch

of the lung tissue accounted for 22 % - 36 % at 35 mbar and between 27 % - 44 % at 52 mbar, with maximum values occurring outside the dome region. At the dome, longitudinal stretches were around 33 % at 35 mbar and 38 % at 52 mbar, hence an isotropic stretch state developed as expected. In the transversal direction the membrane became thinner by 13 % - 26 % at 35 mbar and by 20 % - 35 % at 52 mbar.

35 mbar   **52 mbar**
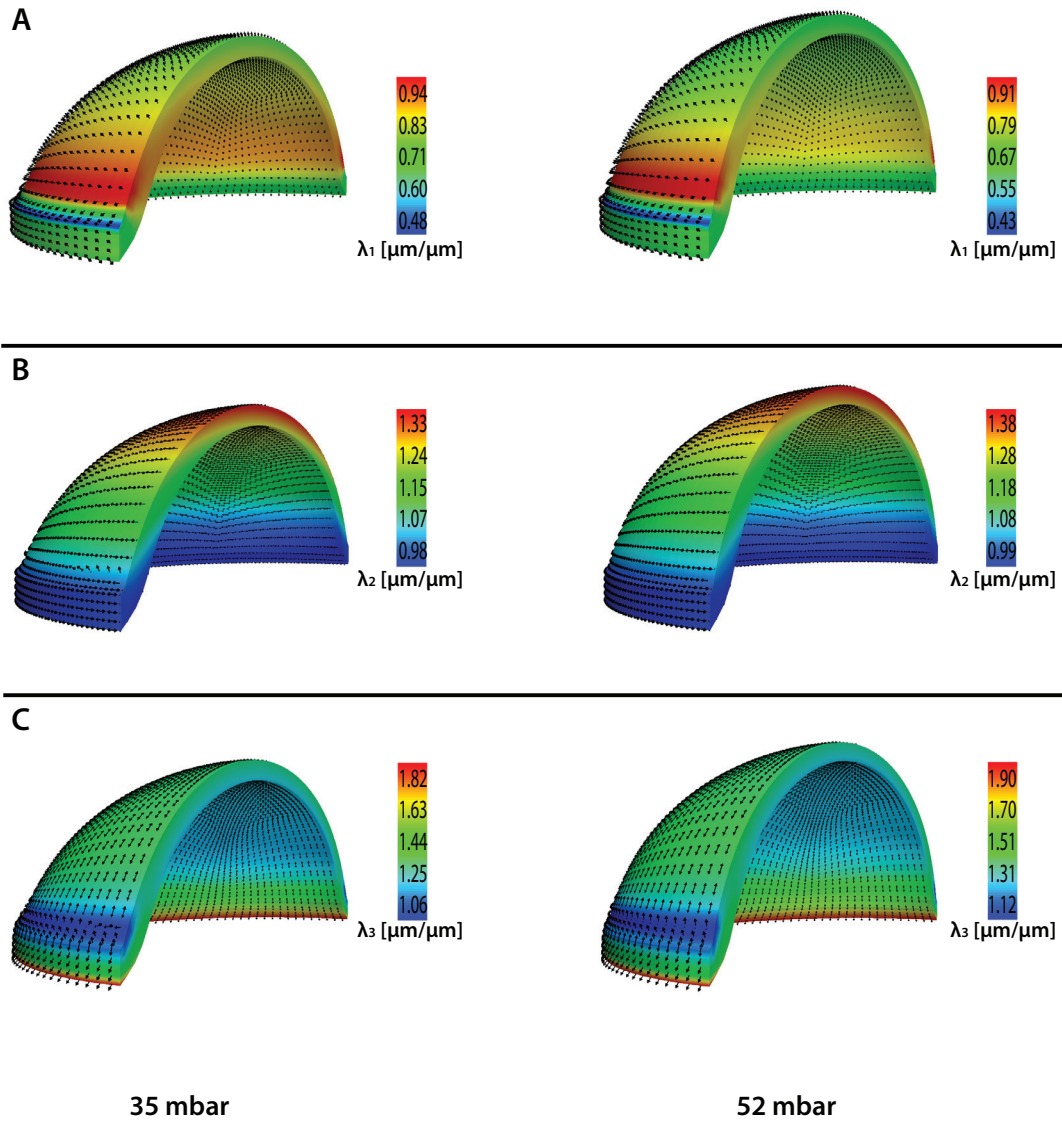
Figure 4.27: Distribution of principal stretch directions and the corresponding principal stretches at 35 (left panel) and 52 mbar (right panel). A: transverse direction. B: latitudinal direction. C: longitudinal direction.
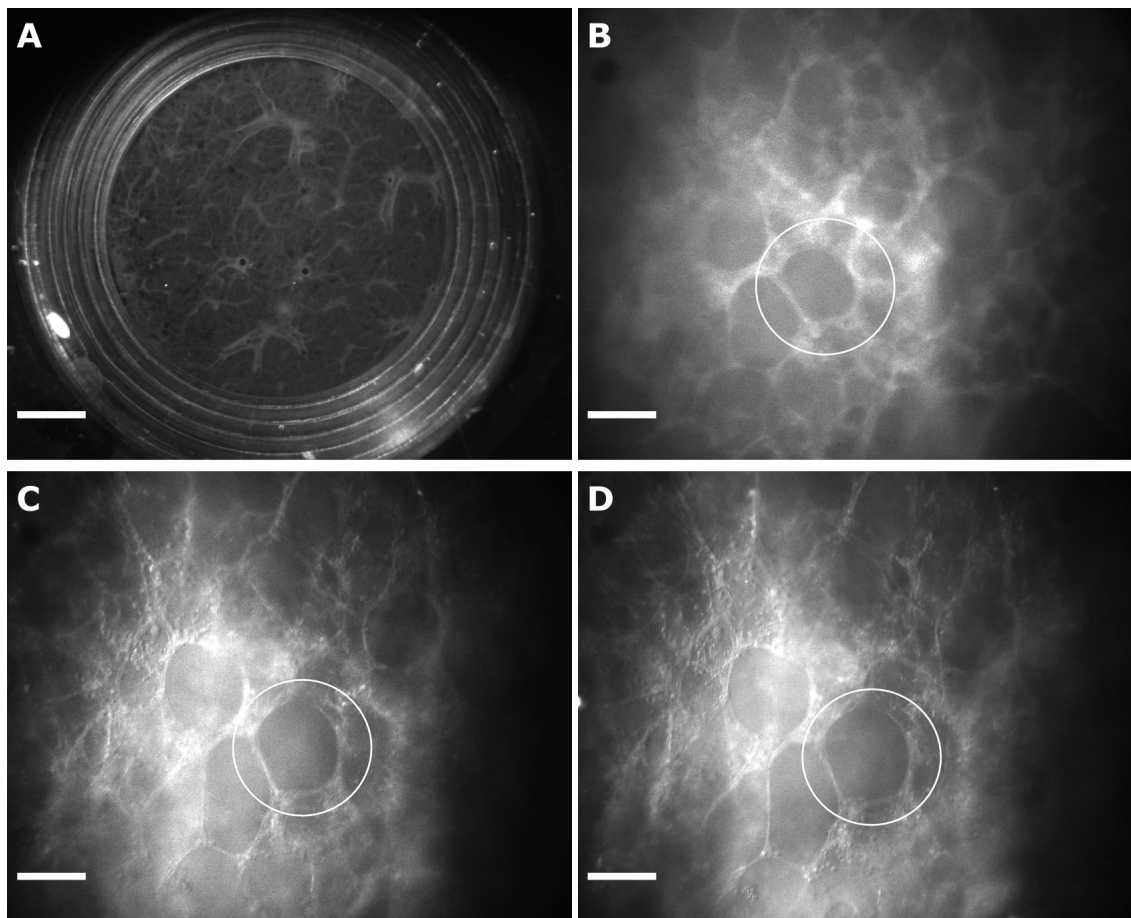
Figure 4.28: PCLS in the bioreactor under static stretch. A, B: The PCLS before stretching. Panel A shows an overview and Panel B a magnified portion of panel A. C, D: The same PCLS shown in panel B after application of 35 mbar (C) and 52 mbar (D). One single alveolus is marked. The horizontal bar corresponds to 2 mm in panel A and 0.1 mm in panels B-D.

4.4.3.3. Distension of alveoli

Lung slices stretched in the bioreactor were observed under a microscope (Fig. 4.28). Individual alveoli were marked and their perimeter and area recorded. The alveolar perimeter and area increased nearly linearly over the range of pressures and membrane excursions examined. The area of the alveoli increased up to 78 % ± 15.8. Based on the change in alveolar perimeter the mean stretch was 24.9 ± 4.1 % at 35 mbar and 35 ± 8.5 % at 52 mbar. Similar data were obtained by decreasing pressures in the same manner. No hysteresis was observed (Fig. 4.29).
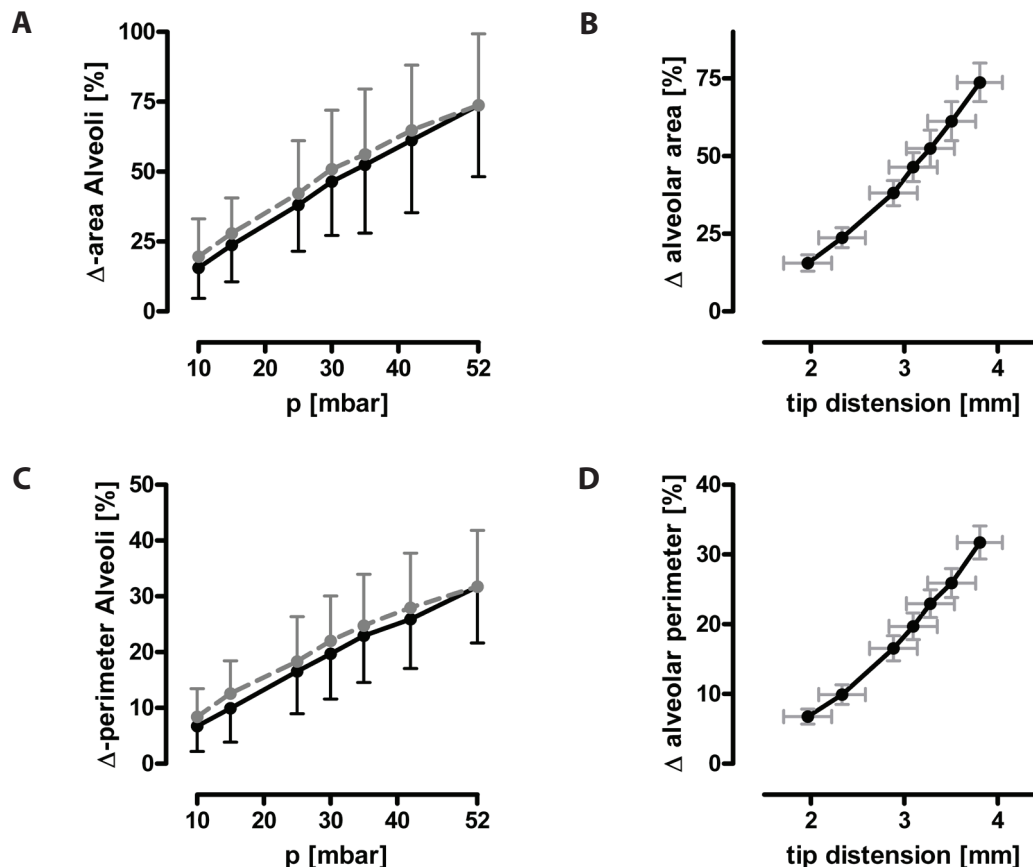
Figure 4.29: Change in alveolar area plotted against increasing (black line) and decreasing (grey line) pressure (A) and tip distension (B). Perimeter change was also plotted against increasing (black line) and decreasing (grey line) pressure (C) and tip distension (D) . Data are given as mean ± SD; n = 5 (minimum 17 PCLS).

4.4.3.4. Influence of Collagenase H

For the stress-strain relationship static distension was applied by means of displacement adjustment. PCLS were mounted in the bioreactor with a starting pressure of 5 mbar, to avoid variations at the starting point. The tip distension was statically increased by 0.5 mm steps up to 2 mm and the pressure in the lower chamber was determined. At 2 mm the pressure was at 46.8 ± 6.2 mbar. To investigate the influence of the collagen fibers, PCLS were treated with Collagenase (Fig. 4.30). Subsequently, more than 90 % of the PCLS disintegrated at a displacement of 2 mm. However, in collagenase-treated PCLS, pressures were reduced to 36.08 ± 4.57 mbar at 2 mm tip displacement. These values were close to the characteristics of the membranes, which resulted in pressures of 31.25 ± 4.4 mbar at 2 mm displacement. Interestingly, at a tip displacement of 1.5 mm and pressures of 28.9 ± 5.2 mbar, collagenase-treated PCLS were still intact (approximately 90 %).
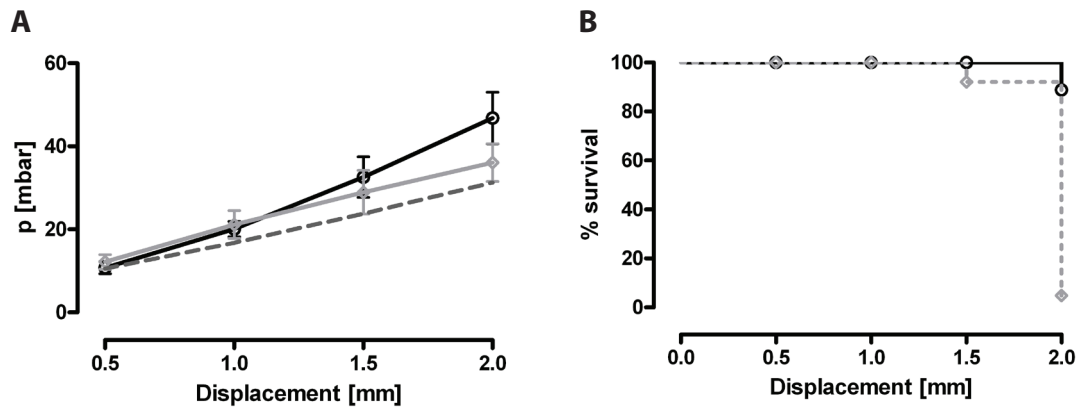
Figure 4.30: Influence of collagenase treatment to PCLS. A: Pressure curve in the lower chamber of the bioreactor after tip distension. Untreated PCLS are shown as a black curve and collagenase treated PCLS as a grey curve. Curves of untreated PCLS and collagenase treated PCLS were compared by using the best-fit value of the parameters BMAX and KD by F-test and were found to have a different slope. The dark grey dotted curve shows the membranes (mean only). Data are given as mean ± SD, n = 3. B: Survival of the same PCLS shown in panel A in percent after displacement. Again the curve of control PCLS is shown in black and the collagenase treated PCLS in grey.

Analogue experiments were performed within the same PCLS. Distension of a PCLS once, followed by incubation with collagenase and subsequent distension, resulted in a tendentially decreased pressure at 2 mm displacement (45.3 ± 6.2 vs. 41 ± 1.4 mbar) after collagenase treatment. Still the rate of disintegrated, collagenase-treated PCLS at 2 mm tip displacement was very high (more than 70 %). Incubating the PCLS with medium instead of collagenase resulted in comparable curves within one PCLS (Fig. 4.31).

Figure 4.31: Displacement of the PCLS in the bioreactor and resulting pressure curves. PCLS before (black line) and after (grey dotted line) collagenase treatment. The small inserted graph shows the survival before (black line) and after (grey dotted line) collagenase treatment. Data are given as mean ± SD, n = 3.

4.4.4. Distension of PCLS under dynamic conditions

4.4.4.1. Viability of stretched PCLS

Longitudinal stretch between 10 % and 25 % is generally considered to be relevant for stretch-induced cell activation and ventilator-induced lung injury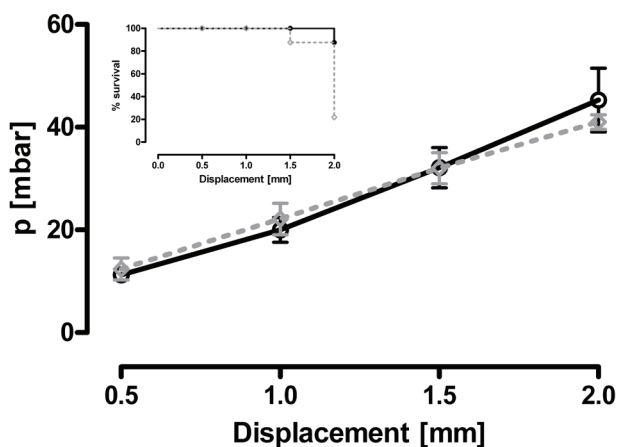. According to the static measurements this degree of stretch is obtained by applying 35 mbar in our model system. Because cyclic stretch is more relevant and also appears to be more injurious than static stretch (268) we studied the viability of PCLS stretched for 4h up to 35 mbar at 0.25 Hz. Four hours of dynamic stretch did not alter MTT reduction compared with non-stretched controls, while there was a significant decrease in MTT reduction in detergent (triton X100)-treated PCLS (Fig. 4.32).
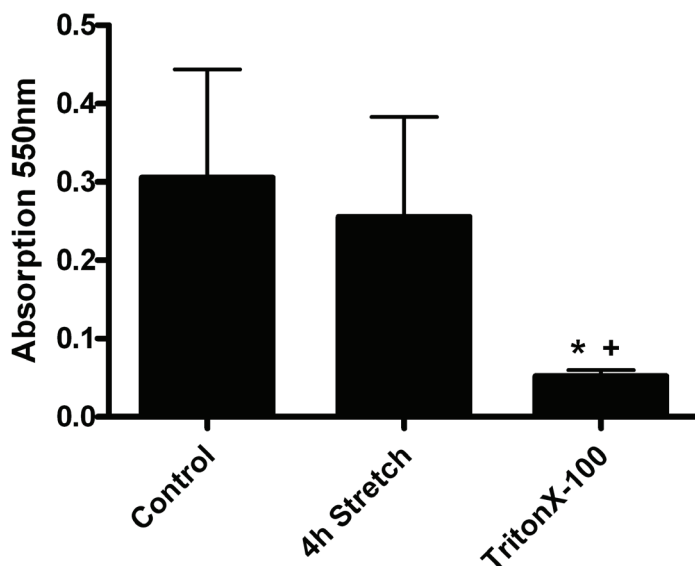
Figure 4.32: Mitochondrial activity determined by MTT-Test. MTT formation in non-stretched controls and 4h stretched PCLS is comparable while it was significantly decreased in detergent treated PCLS. Data are given as mean ± SD, n = 5. * shows a significant difference between the Control and TritonX-100 group; + shows a significant difference between the 4h Stretch and TritonX-100 group. Data was Box-Cox transformed and analysed by the Tukey Hsd test.

To further illustrate viability, PCLS were stained for dead cells with propidium iodide and pictured by confocal microscopy (Fig. 4.33 A-C)). Comparing the non-stretched control PCLS to the 4h stretched PCLS, the amount of dead cells was not significantly different. The detergent treated PCLS in contrast showed a huge amount of dead cells. However, the amount of dead cells in control and stretched PCLS was relatively high, probably because pictures were taken relatively close to the slicing area. Therefore, the same experiment was repeated with live-dead staining and examined with multi-photon microscopy (Fig. 4.33 D-F) using calcein AM as a marker of living cells and ethidium homodimer as a marker of dead cells, to gain inside into deeper layers of tissue. The overall amount of dead cells was reduced and there was again a comparable amount
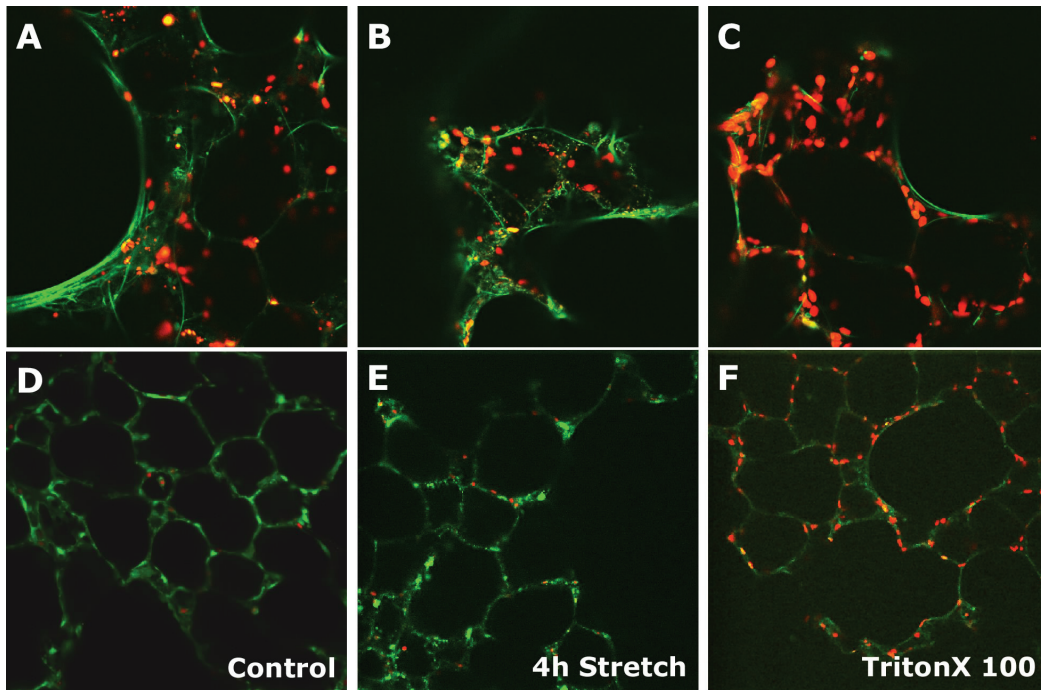
Figure 4.33: Viability of 4h stretched PCLS. A-C: PCLS were stained for dead cells (nuclei) with propidium iodide (red) and overlayed with autofluorecence (green). Non-stretched control PCLS (A) were compared to 4h stretched PCLS (B) and detergent (Triton-X 100) treated PCLS (C). Detergent treated PCLS serve as a positive control with all nuclei stained. D-E: 2 photon microscopic images of a non-stretched control PCLS (D), a 4h stretched PCLS (E) and a detergent treated PCLS (F). PCLS were treated with LIVE/DEAD staining (Calcein AM (green, cytoplasm) for living cells and ethidium homodimer (red, nuclei) for dead cells).

of dead cells in the non-stretched control and the 4h stretched PCLS. Many nuclei were stained in the detergent treated PCLS.

4.4.4.2. Amphiregulin RNA expression in stretched PCLS

Amphiregulin was shown to be upregulated specifically by overdistension of lung tissue in the isolated perfused mouse lung model (65). As a mechanosensitive protein amphiregulin is already induced by the slicing process during the preparation of PCLS. A maximum induction was found 4h after the slicing process. After 24h amphiregulin induction was reduced to a big extent, therefore we tried if it was possible to induce it by stretching the PCLS. Four hours of stretch did not induce amphiregulin RNA induction in comparison to 4h clamped but unstretched PCLS or to control PCLS. There was a trend in reduction of amphiregulin RNA expression in the stretched PCLS, possibly indicating that stretching of the PCLS may be closer to the physiological conditions of the lung than static organ culture (Fig. 4.34).
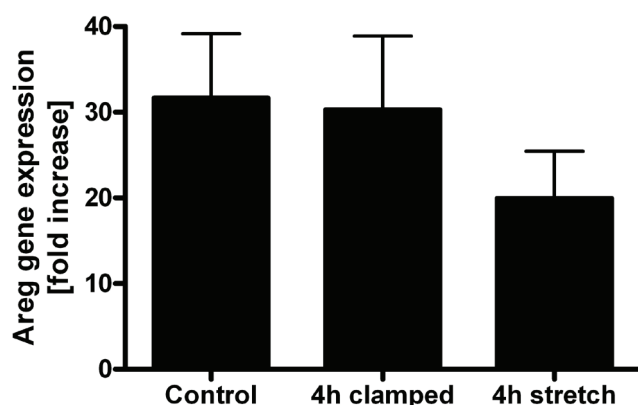
Figure 4.34: Amphiregulin RNA expression in PCLS. PCLS were cultured for 24h and dynamically stretched for 4h at 35 mbar. Stretched PCLS were compared to 4h clamped and control (PCLS in culture) PCLS. Data are given as mean ± SD, n = 3. Data was Box-Cox transformed and analysed by the Tukey Hsd test.

4.4.4.3. Treatment with ML-7

ML-7 has been shown to reduce the maximum induction of amphiregulin after the slicing process. Therefore, we treated PCLS with ML-7 during and 4h after the slicing process. 24h after the slicing process PCLS were stretched or clamped for 2h in the bioreactor and compared to non-stretched PCLS (Fig. 4.35).

The stretching period was reduced to 2h to increase the number of experiments per day. In addition, amphiregulin has been shown to be induced 1h after slicing (data not shown) and 2h after overventilation in the IPL mouse model (unpublished data, M.

Barrenschee). No difference in amphiregulin induction was found between the control and the stretched PCLS (Fig. 4.35).
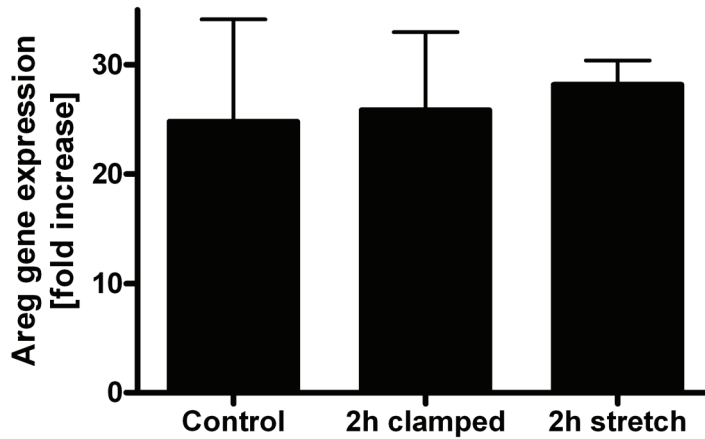
Figure 4.35: Amphiregulin RNA expression in PCLS treated with ML-7 during and 4h after the slicing process. 24h after the slicing process PCLS were either clamped or stretched for 2h at 35 mbar in the bioreactor and the amphiregulin expression was compared to control PCLS. Data are given as mean ± SD, n = 3. Data was Box-Cox transformed and analysed by the Tukey Hsd test.

4.4.4.4. Distension of PCLS after 72h

To possibly diminish the gene induction by time, experiments were performed 72h after the slicing process. Viabiliy of the PCLS was verified by MTT-test (Fig. 4.36). Compared to PCLS after 24h, amphiregulin expression in PCLS was reduced 72h after the slicing process (Fig. 4.37). Both clamping or clamping and stretching PCLS for 0.5h induced amphiregulin to a comparable amount. After 1h amphiregulin was still
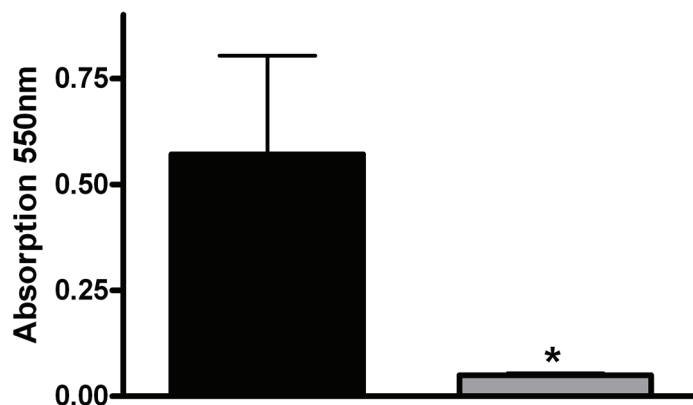
Figure 4.36: Viability of PCLS after 72h in culture measured by MTT-test. PCLS cultured for 72 h (black bar) show a significantly higher mitochondrial activity than detergent treated (grey bar) PCLS. Data are given as mean ± SD, n = 3. Data was Box-Cox transformed and analysed by the Students t-test, p-values < 0.05 were considered significantly different (*).

expressed in clamped PCLS, whereas 1h stretch significantly reduced its expression to control levels (Fig. 4.37).
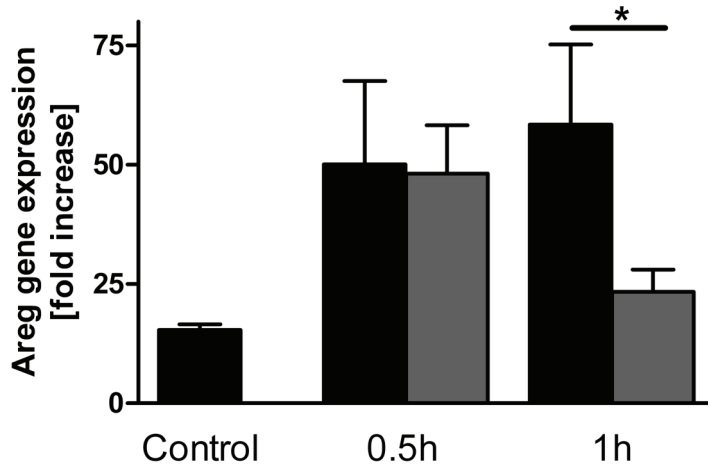
Figure 4.37: Amphiregulin RNA expression in PCLS 72h after the slicing process. Slices were clamped (black bars) or stretched dynamically (grey bars) for 0.5 and 1h in the bioreactor at 35 mbar. Data are given as mean ± SD, n = 3. Data was Box-Cox transformed and analysed by the Tukey Hsd test, p-values < 0.05 were considered significantly different (*).

4.4.4.5. Treatment with Dexamethasone

Dexamethasone is a potent anti-inflammatory and immunosuppressive agent. To exclude any effect of a possible pro-inflammatory response initiated by the slicing process, we added dexamethasone during the slicing process and during the first 4h of incubation. Viability of dexamethasone-treated PCLS was determined after 72h in culture in comparison to detergent (Triton-X 100)-treated PCLS. No difference between
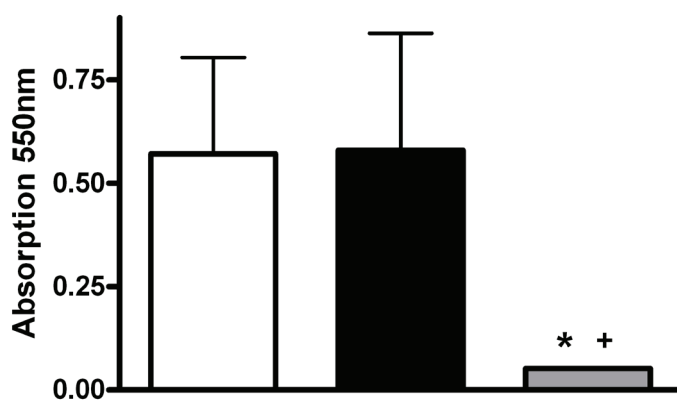
Figure 4.38: Mitochondrial activity in PCLS 72h after the slicing process. MTT formation was determined in control (white bar), dexamethasone treated (black bar) and dexamethasone + detergent treated PCLS (grey bar). Data are given as mean ± SD, n = 3. Data was Box-Cox transformed and analysed by the Tukey Hsd test. * indicates significant differences of control to detergent-treated PCLS; + indicates significant differences between dexamethasone- and detergent-treated PCLS.

dexamethasone treated and control PCLS was observed in the mitochondrial activity after 72h, indicating no influence of dexamethasone on viability of PCLS for at least 72h. In contrast, no mitochonadrial activity was observed in detergent treated PCLS (Fig. 4.38).

After 72h of incubation dexamethasone-treated PCLS were clamped or stretched in the bioreactor. Clamping and Stretching for 0.5 and 1h resulted in a comparable amphiregulin induction. No differences were observed between clamped and stretched PCLS (Fig. 4.39).
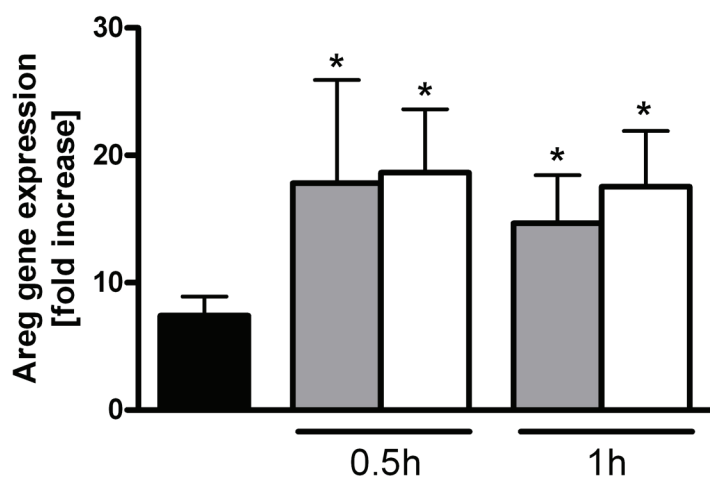
Figure 4.39: Amphiregulin RNA expression in dexamethasone treated PCLS 72h after the slicing process. PCLS were either clamped (grey) or stretched (white) for 0.5h or 1h in the bioreactor. Control dexamethasone-treated PCLS are shown as black bar. Data are given as mean ± SD, n = 4. Data was Box-Cox transformed and analysed by the Tukey Hsd test, p-values < 0.05 were considered significantly different (*).

5. Discussion

Oxygenation of the blood and removal of carbon dioxide from it is the most important function of the lung. To provide an adequate area for gas exchange, the interior surface of the lung has much larger dimensions than its outer surface area. Although the lung is situated inside the body, most of it is permanently in contact with the enviroment. On such a large surface, many kinds of stresses can occur and damage the lung. Stress can appear chemically in terms of toxins or allergens, or it can appear in form of physical damage, by overstretching the tissue. At the same time the lung is a very complex organ with more than 40 different cell types. Most stress models are either too complex, considering the whole organ, or too simple by studying only one cell type. Using precision-cut lung slices as a stress model has several advantages. They provide a relatively intact microanatomy of many different cell types and possess an extracellular matrix. Originally developed for toxicological research, lung slices have recently become an important tool for pharmacological and mechanistic studies. The advantage that many slices can be prepared from a single donor lung is associated with the possibility to prepare PCLS of different parts of the lung. It is possible to prepare PCLS with focus on large or small airways or vessels, and it is also possible to prepare tissue slices of different sizes. At present, PCLS with a diameter of up to 14 mm can be prepared with a Krumdieck tissue slicer. Another fact which makes PCLS attractive is the possibility to prepare them from different species. Amongst others, this provides the opportunity to compare animal tissue to that of human lungs. Comparison between different species has been realised mostly to study airway pharmacology (218) with good prospects to apply this also for other studies. Another advantage is the possibility to compare PCLS to *in vivo* experiments of the same species in order to reduce the number of *in vivo* experiments. Promising results have been shown in mouse PCLS by comparison of pulmonary resistance *in vivo* and maximum contraction *in vitro* (110).

In this study PCLS were used as a model for different kinds of stress in the lungs. Stress was applied in form of chemical allergens and in form of tissue injury by slicing and stretching. In general two aspects were adressed in this work. Firstly, two new methods were developed. Sheep PCLS were introduced as a model to study pharmacology of broncho- and vasoconstriction. This study also established and characterised a new stretch model adressing overexpansion of lung tissue during mechanical ventilation. To this end, PCLS were stretched in a bioreactor to study mechanical and biological consequences. Finally, PCLS were used to measure responses like bronchoconstriction and gene expression to stress stimuli, such as chemical allergen challenge or slicing.

5.1. The model of sheep PCLS

Sheep are considered a useful model in lung research. Sheep have been used as models for asthma, COPD or cystic fibrosis (3). In addition, several studies of ALI or ARDS have been performed in sheep (223; 285). A specific model of lung research is represented by the sheep pulmonary adenomatosis model, which studies retrovirus-associated lung cancer (192). Studies on preterm sheep were done especially in the context of chorioamnionitis, a risk factor for bronchopulmonary dysplasia in preterm infants (40). In the present study we describe the establishment and characterisation of sheep PCLS, prepared from agarose-filled lungs with a Krumdieck tissue slicer. Before, only one other study was published in 1967 describing the preparation of sheep lung slices from lung explants (44). In that study, slices were cultured for only 3h, and used to measure acetate incorporation into phospholipids and fatty acids. Other studies with sheep were accomplished *in vivo* or by using *in vitro* experimental set-ups, such as bronchial- and tracheal rings or lung parenchymal strips (165; 178; 236). Mehta et al. investigated the effect of xanthine derivatives on tracheal rings of preterm lambs. Interestingly, caffeine and theophylline had differential effects on preterm sheep airway smooth muscle cells. In contrast to precontracted adult airway smooth muscle cells, which are relaxed by addition of xanthine derivatives, only theophylline had a relaxing effect on preterm sheep airway smooth muscle cells (165). Others used tracheal strips and bronchial rings in the organ bath technique, to determine contractile responses of large and small ovine airways to thiopental (178). Functional innervation of sheep airway smooth muscle cells was measured in tracheal segments, bronchial rings and lung parenchymal strips (236). This is the first study to exam airway and pulmonary vascular responses in sheep in PCLS. Our aim was to establish sheep precision-cut lung slices to study single airway and vessel pharmacology in this species. In contrast to isolated trachea or lung strips the microanatomy around the smooth muscle is mostly preserved, which stabilises the airway and makes it unnecessary to apply an external preload to the lung slice. Therefore the smooth muscle can contract in a way more physiological way than isolated tracheal- or bronchial rings, because preload directly influences the contractility. Non-laboratory animals with body weights in the range of humans are often considered to be more relevant to the human pathophysiology than smaller animals. Additionally, the maturation of sheep lungs is more similar to the maturation of human lungs than are rodent lungs. That favors this species especially for the examination of preterm animals. In the present study, sheep PCLS of preterm and adult sheep were compared. This would be difficult in rodents, because preterm rodent lungs are too small to yield PCLS. The use of preterm sheep limits the supply with lungs, because sheep are seasonal breeders and give birth only once a year, usually in spring. Therefore, in the present study, only a limited number of PCLS could be tested.

PCLS of adult and preterm sheep were viable up to 72h in culture, as assessed by mitochondrial activity. However, preterm sheep PCLS showed a significantly higher mitochondrial activity than adult sheep PCLS. The airway size in both adult and preterm sheep was comparable, in the same way than the size of the PCLS themselves. Therefore, we had age-related size differences, because smaller airways were prepared from adult sheep than from preterm ones, in order to measure airways of comparable size. Preparing PCLS from different parts of the lungs may have influenced the mitochondrial activity. Another reason could be a general higher mitochondrial activity in preterm sheep lungs. During transition from fetal to neonatal life cellular energy requirements are at maximal rates. Brown adipose tissue is enriched during gestation, which is rich of mitochondria, especially at the time of birth (175; 195). MTT formation is dependent on mitochondrial activity which may explain the higher reduction rates in the preterm sheep.

5.1.1. Airway responses of sheep PCLS

Sheep have been used as an asthma model because of several similarities to humans. This includes the immune status, airway inflammation after allergen challenge, the airway response and the AHR (3). Six different mediators which are known to act as bronchoconstrictors, were used to characterise bronchoconstriction in sheep PCLS (217). Compared to other species, the reactivity to methacholine was in the same range as observed in human and guinea pig PCLS (Table 5.1). In contrast to human PCLS, sheep PCLS showed responsiveness to serotonin. The EC_{50} value for serotonin of 122 nM was in the same range as in guinea pig PCLS (69 nM). *In vivo,* ED_{50} values of methacholine and serotonin in anaesthesised guinea pigs are 3 mM and 7 µM, respectively (121). The in vivo setup measures whole lung responses by pulmonary inflation pressure while in PCLS single airways are measured directly. Additionally, the form of application – inhaled versus solution – differs in the experimental setups. Therefore a comparison of the absolute values is not reasonable. Interestingly, methacholine is more effective than serotonin *in vivo,* whereas in PCLS serotonin was the more potent mediator compared to methacholine. Surprisingly, sheep PCLS - just as mouse airways - did not react to histamine, while airways in guinea pig and human PCLS respond to histamine. *In vivo*, sheep airway responsiveness to histamine was observed (3). *In vitro*, sheep airway smooth muscle strips and bronchial rings also reacted to histamine, but dependent on airway size. Only large airways contracted, smaller airways even relaxed in response to histamine (178; 236). Because we studied only PCLS with relatively small airways, this could explain the unresponsiveness in PCLS compared to *in vivo* and *in vitro* experiments. Endothelin-1 EC_{50} values of guinea pig, rat, mouse and sheep PCLS were comparable (Table 5.1). In contrast to guinea pig and human PCLS, the response

of sheep PCLS to leukotriene D_4 was rather weak with contractions starting at 100 nM. Also the response to U46619 in sheep showed a weak contraction at concentrations of 10 µM in sheep PCLS. Taken together, the airway response pattern of small airways of sheep PCLS to endogenous mediators differs from that of human airways studied under comparable conditions (218). *In vivo* a response to leukotriene D_4 and histamine was observed. Like in guinea pig PCLS there was a response to serotonin, which is not observed in human PCLS (218). As with mouse and rat PCLS (108; 304), the response to histamine and leukotriene D_4 was either not observed or only weak. Preterm birth may have effects on airway function, because the lung is not fully maturated. Snibson et al. found that preterm sheep had a higher baseline pulmonary resistance and a greater airway response to bronchoconstrictors than normal sheep (242). This is the first time that bronchoconstriction of preterm and adult sheep airways in response to bronchoconstrictors was compared. We found different EC_{50} values for methacholine and serotonin. In contrast to the *in vivo* study by Snibson et al. preterm sheep airways were less reactive than adult ones to both mediators. This may be explained by a different contractile response of newborn airway smooth muscle cells. In *in vitro* experiments, isolated adult airway smooth muscle cells show a faster maximum shortening velocity than cells from newborn sheep (139).

Responsiveness to endothelin-1 showed no difference between adult and preterm sheep PCLS. In isolated airway smooth muscle cells the influence of ageing was dependent on the species investigated. Whereas the endothelin-1 response was influenced by the age of the donor in rabbit and rat cells, guinea pig cells showed no difference by ageing (92; 204). EC_{50} values of guinea pig and sheep PCLS were also comparable (Table 5.1), indicating similar responses to endothelin-1 in both species. With the exception of the response to leukotriene D_4, where preterm sheep PCLS showed a higher maximum contraction, they responded generally weaker than adult sheep PCLS (Table 5.1). This difference could be due to the age-related size difference of the airways of preterm and adult sheep. This is consistent with the different airway size related responses which were demonstrated in rat PCLS before (155).

Table 5.1: EC_{50} values of mediators in PCLS of different species.

	Adult sheep	Newborn sheep	Human (218)	Guinea pig (218)	Rat (12; 153; 155)	Mouse (108)
Methacholine	70 nM	187 nM	234 nM	231 nM	640 nM	1500 nM
Serotonin	122 nM	377 nM	unresponsive	69 nM	100 nM	2000 nM
Endothelin-1	16 nM	16 nM	-	9.6 nM	22 nM	50 nM
Histamine	unresponsive	unresponsive	2170 nM	217 nM	-	unresponsive

5.1.2. Vascular responses of sheep PCLS

Another advantage of the PCLS model is the possibility to study the response of airways and vessels in one slice. Pulmonary arteries are located close to the airways and can be observed at the same time. As with airway responses there was no difference in the response of adult and preterm pulmonary arteries to endothelin-1, which contracted with an EC_{50} value of 19 nM. The constriction was therefore in same range as the airway response. These EC_{50} values are comparable with those in guinea pig PCLS (218). Responses to endothelin-1 in isolated pulmonary vessels of adult sheep, fetal and newborn sheep have been studied before by Toga et al. (259). They found a dose-dependent contraction to concentrations of 1 nM to 1 µM endothelin-1 in vessel rings. Both, arteries and veins of adult sheep lungs were more sensitive to endothelin-1 than those of fetal and newborn sheep. Additionally, they found a greater sensitivity of veins to endothelin-1, compared with arteries (259). In adult and preterm sheep PCLS, we observed contractions of pulmonary arteries in the same range of endothelin-1 concentrations, but no differences between adult and preterm sheep PCLS were found. This could be a result of the different models used. Toga et al. isolated vessel rings whereas we used PCLS with relatively intact tissue around the vessel. Additionally, we observed only pulmonary arteries. In the study of Toga et al. the arteries were less responsive than veins (259).

In contrast to airway responses, adult and newborn sheep vessels responded likewise to U46619, while there was no response to leukotriene D_4, apart from a slight reaction of preterm sheep PCLS. U46619 was used as a precontracting agent *ex vivo* in lambs, especially with regard to pulmonary hypertension (260; 289). *In vivo*, the age-dependent response to leukotriene D_4 was investigated in lambs of different ages. This was tested via bolus injection of 0.01-1 µg/kg leukotriene D_4 into the main pulmonary artery while pulmonary blood flow as well as aortic, pulmonary artery, left and right ventricle pressures were monitored. A vasoconstriction increasing with age, was observed for leukotriene D_4 (50). These results were not found in PCLS, which showed, if at all, a rather weak response of preterm sheep arteries. This could have different reasons. Firstly, no preterm sheep arteries were examined in the study mentioned above (70), only lambs at the age of 1.5 days and 7 days. Secondly, the contraction was measured indirectly via vessel pressures and blood flow. Those in vivo studies may therefore provide other physiological characteristics than the PCLS model.

Taken together, the sheep PCLS provide a novel and useful model to measure vascular responses of single vessels in response to different vasoconstrictors.

5.2. Effect of allergens to mouse PCLS

The knowledge of potential toxicants, among them potential allergens, is quite limited and has received new awareness by the European Union Regulation REACH (Regulation, Evaluation, Authorisation and restriction of CHemicals), which was released in 2006 (74). REACH addresses the production and use of chemical substances, and their potential impact on both human health and the enviroment. Companies that manufacture or import substances in quantities of one ton or more per year have to register them in the European Union. This increases the need for easy-to-handle screening methods in animals, which should account for the 3R (replace, reduce, refine) concept (226).

Our experiments were accomplished in mouse PCLS, because murine models are well studied and characterised. TMA and DNCB were used as examples of typical respiratory and dermal sensitisers, respectively. Both substances have been used in various studies before and are therefore well characterised with respect to their allergic potential. In general both substances induced a Th2 dependent IL-4 expression, which was more distinct in TMA sensitised mice (14). The cytokine profile induced in lymph node assays was different for both, TMA and DNCB, with a mixed induction of a Th1 and Th2 response (60). An increase in serum IgE was found in TMA and in DNCB sensitised mice (93; 278), with a stronger induction in TMA sensitised mice (14). The sensitisation with TMA and DNCB in our experiments was successful as approved by the determination of IgE serum concentrations. The present study was realised in collaboration with the group of A. Braun (ITEM, Hannover), who measured IgE concentrations in the serum of sensitised mice and lung functions *in vivo*. The results are in line with the studies mentioned above (93; 278), also displaying an increase in IgE serum concentrations (Figure 5.1.).

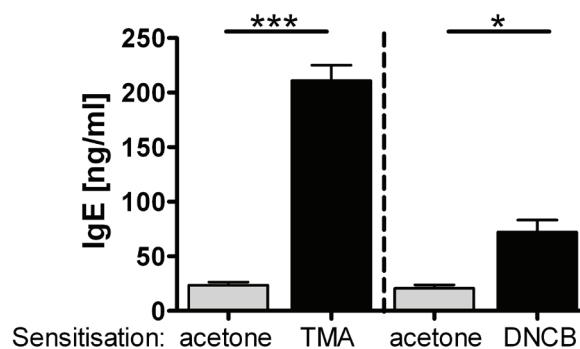**Figure 5.1:** Total IgE serum levels determined in blood samples collected by retroorbital bleeding on day 13 after the start of sensitisation. Mice were sensitised by TMA, DNCB or acetone as vehicle control. Experiments were performed by Maja Henjakovich (Hannover). Data are given as mean ± SEM; n = 5 –15. Data was compared by the two-sided, unpaired t-test. The data are taken from Reference (110).

The dermal application route was chosen because it is the relevant route of sensitisation. Former studies demonstrated the development of a respiratory allergy with a typical Th2 immune response in mice after dermal exposure and respiratory challenge with TMA (14; 61). Furthermore, the sensitisation in humans with TMA may originate in dermal exposure (18).

In the present study we compared invasive *in vivo* lung function measurements with bronchoconstriction *ex vivo* in PCLS. The aim was to establish PCLS as an alternative method to *in vivo* experiments. In agreement with the 3R concept, the use of PCLS avoids stress for the individual animal, since experiments are performed *ex vivo* and it allows reducing animal numbers by using several slices from one animal. At least 10 ideally cut PCLS can be obtained from one mouse lung (108; 111), which, in addition to construction of full dose-response curves for airway contraction, allows the comparison to control PCLS from the same animals. It is assumed that animal numbers can be reduced by a factor of 3 to 10 compared to full *in vivo* studies (110). Our results indicate that PCLS and *in vivo* data do concur well.

5.2.1. Early allergic response in TMA and DNCB sensitised mice

TMA and DNCB sensitised mice have been shown to exhibit an EAR after challenge with TMA and DNCB (278). In the present study neither *in vivo* nor *ex vivo* an EAR was observed. Vanoirbeek et al. measured the EAR *in vivo* by the obsolete PenH method (278), in contrast to the invasive method we used (87). PenH is no reliable measurement of lung resistance and does not distinguish between the upper and the lower airways, which becomes relevant with regard to allergic rhinitis. Humans who inhaled TMA dust developed allergic rhinitis (90), suggesting a reason for altered responses with the PenH method. It is impossible to correlate airway resistance with PenH measurements (128; 147; 166). In principle, the detection of EAR in invasive pulmonary function tests in mice is possible, as it was shown for Aspergillus fumigates antigen sensitised mice (72; 87). However, preexisting inflammation in the lung seems to be a requirement for EAR in mice, so possibly a single TMA provocation is not sufficient to induce an EAR. In publications dealing with ovalbumin sensitised mice, an EAR is also lacking after single provocations (183; 314). Other species, such as the guinea pig, show an EAR even in non-sensitised animals in response to inhaled TMA dust (138). This may be another example for the notion that guinea pigs may reflect humans better than rodents (218). We used allergen doses which were not toxic in PCLS. Our doses were 10-fold lower than doses in other studies (278), excluding any irritant toxic effects by the allergen itself. This may also explain the absence of stronger inflammation and EAR in comparison to other studies.

5.2.2. Airway hyperresponsiveness in TMA and DNCB sensitised mice

The *in vivo* and *ex vivo* responsiveness to methacholine 24h or 16h after allergen challenge was significantly increased in TMA-sensitised mice and in PCLS from those animals, demonstrating that TMA caused a marked AHR. DNCB-sensitised animals and lung slices from DNCB-treated mice did not show clear signs of AHR. Although the nominal differences between TMA and DNCB groups to their vehicle control were similar, only the difference between TMA and control reached statistical significance. Therefore, this method may not be suitable for the differentiation between skin and respiratory sensitsers at this stage of development. Because the AHR occured *in vitro*, the influx of inflammatory cells can be excluded as a contributing factor, which, amongst other mechanisms, is thought to play a role (149). Resident mast cells, eosinophils and neutrophils are possible mediators of the AHR. Another potential mechanism may result from smooth muscle priming leading to a direct contraction (109; 110). It has been reported before that TMA sensitisation leads to an increased methacholine responsiveness in mice while DNCB sensitisation results in diminished AHR compared to TMA or does not lead to a response at all (278). This is in line with studies demonstrating that DNCB sensitisation does not result in respiratory allergenicity and is defined mostly by a Th1 response (62). At least the influx of T lymphocytes seem to be not essential for AHR, judged by the absence of these cells in the *ex vivo* experiments. An influence of T lymphocytes could only result from preliminarily migrated cells.
In summary, the EAR and AHR *in vivo* correlated well with those in PCLS obtained from sensitised animals. We were able to show that TMA induces allergic sensitisation, inflammation of the respiratory tract and airway responsiveness to methacholine *in vivo* and *ex vivo*. In general, airway sensitising effects of LMW allergens may be studied in PCLS.

5.3. Stretching of PCLS in the bioreactor

We describe a new experimental *in vitro* model for studying mechanostimulation of lung tissue with relatively intact microanatomy under cell culture conditions. We have shown that PDMS is a suitable material to support PCLS. In the bioreactor lung tissue can be stretched cyclically by about 30 % longitudinally and latitudinally for at least 4h without causing cell death. 70 µM below the surface of the slices, multi-photon microscopy showed a comparable amount of dead cells in control and stretched slices. In contrast, confocal microscopic images showed relatively high numbers of dead cells in stretched and control PCLS (Fig. 4.32). The confocal images were recorded in a depth of approximal 40 to 50 µm. Dead cells may therefore be due to the relatively close distance to the surface. The difference between the two methods may also be

explained by the different stainings. However, the difference to completely dead PCLS shown by detergent treated PCLS is obvious and the viability of stretched PCLS was confirmed by mitochondrial activity.

To study PCLS in the bioreactor, several modifications of the bioreactor were necessary. The dimensions of rat lungs permit a maximum PCLS diameter of 14 mm only, which mandated downsizing the bioreactor inserts from the 30 mm that were used in the original version of the bioreactor (232). To support the tissue in the bioreactor, we used 30 µm thick PMDS-membranes, which are about a factor 3 to 6 more pliant than polyurethane or latex membranes employed originally in the bioreactor (232).

Others have used the Flexercell system to stretch cells in culture (15), where silicon membranes with a thickness of 250 µm are used. In contrast to the Flexercell set-up, there is no frictional energy dissipation inside the bioreactor (depending on the viscous properties of the membrane). This allows a precise control of the deflection amplitude and thus of the strain which is applied to the tissue or the cells under investigation. In addition, in its present form the Flexercell system does not allow to mount living slices. Stretched PCLS as an *in vitro* model have several advantages. First, the slices can be viewed under the microscope, which allows studying of alveolar regions during the stretching process. In combination with multi-photon microscopy this will allow to image the stretched lung tissue in 3D and to follow critical signalling responses such as calcium fluxes. Secondly, up to 20 usable slices can be prepared from one rat lung. Since the slices are of a defined diameter and thickness experimental conditions can be adjusted individually. Third, PCLS are viable for at least three days (218) which will permit to study the effects of different ventilation strategies on lung tissue over time. Fourth, PCLS provide an intact microanatomy consisting of different lung cell types and extracellular matrix which is lost in cell culture models consisting of only one cell type. Fifth, PCLS can also be prepared from human tissue (218; 303) which will offer the unique opportunity to study the response of human tissue to various degrees of stretch.

5.3.1. Applied stretch in our model

Material properties applied in the FE model were selected to fit the directly measured displacements (Fig. 4.26). The FE simulation allowed quantifying the associated strain distribution in the lung slices (Fig. 4.27). In the longitudinal direction, the stretch distribution seems to be remarkably homogeneous. Latitudinal stretches of the membrane-tissue construct were continuously increasing from the periphery towards the center (about 35 %). The FEM data compare rather well to the increase in perimeter of single alveoli close to the center that were determined by direct measurement under the microscope. At 35 mbar, the combination of longitudinal and latitudinal stretch was

24.9 ± 4.1 %, a degree of stretch that is generally considered to be relevant for possible side effects caused by mechanical ventilation (198). It should be noted though that the baseline stretch of the slice mounted on the membrane to which the stretch is normalised is not exactly defined; however, once the agarose has been washed out the only forces in the slices that are keeping the alveoli open are the tethering forces of the tissue. Therefore, it seems reasonable to assume that the unstretched lung slices correspond to a deflated lung, although the degree of deflation is not known.

Recently, Perlman and Bhattacharya demonstrated that the perimeter of superficial alveoli 20 μm below the rat lung surface increased by about 14 % if the lung volume was increased from 50 % TLC at 5 mbar up to 85 % TLC at 20 mbar (198). Thus, in terms of perimeter increase the compliance in two dimensions was 14 % / 15 mbar = 0.93 % / mbar. Calculation of the slope in Fig. 4.29 D yields in 0.69 % / mbar. This may suggests that mechanical lung properties in both settings are comparable, although there are several caveats. First, the mechanics of tissue distension in two and three dimensions is different. Second, it is not clear which level of lung volume is represented by the mounted slices at baseline (0 mbar). However, as long as the relation between alveolar pressure and perimeter is linear (as it was in this study and in (198), the slope should be independent of any particular lung volume. And third, our model lacks surface tension, although this would not alter the strain state but only the inner stress state of the tissue. Taken together, it remains to be determined whether the comparable slope of the pressure/perimeter relationship in the slices and in the intact organ is a coincidence or reveals a typical behaviour of lung tissue.

In the past, calculations of the strain that is generated during distension of lung tissue have been based either on the analysis of fixated lung tissue specimen (267), of superficial lung regions (198) or on cells in culture (15; 54). All these methods have their specific advantages and shortcomings. Tissue fixation is prone to fixation artefacts and provides images of dead tissue only. The analysis of superficial alveolar regions offers problems with identifying the factual imaging plane and can only analyse the special case of subpleural alveoli; here the present work suggests that the mechanical behaviour of those superficial alveoli is representative for alveoli in general (see above). And finally, lung cells in culture – although easy to stretch and study – do only partly reflect the properties of real lung tissue with its many different cell types and its extracellular matrix. In comparison to the models discussed above, one advantage of the present model is that it uses viable lung tissue with a relatively intact microanatomy that is not derived from the lung surface. Thus, this model complements the already available methods. A wide variety of techniques are available to study responses in precision-cut lung slices including videomicroscopy to study airway smooth muscle responses (153), ciliary beating (303), alveolar distension (this study), calcium fluxes (20), as well as gene expression and cytokine signalling (154). Thus, in a next step, this

model will allow to establish a quantitative relationship between mechanical forces and cellular response in the lung.

A comparable model has been described with neonatal tissue explants and has yielded important insights into understanding the processes of the lung expansion at birth (275). However, that model was based on the ability of the neonatal tissue to grow into and adhere to a medical sponge material. Experiments with precision-cut lung slices showed that adult tissue is not capable of making contact with sponge materials in the same manner and therefore the lung tissue needed to be fixated mechanically. In addition, experiments where the tissue was glued to the membrane resulted in a non homogeneous extension of the tissue and may activate cells in the tissue.

Hysteresis was not observed in our model which may have different reasons. Firstly, we eliminated the air-liquid interface by covering the PCLS in the bioreactor with medium. Incubation also depleted the surfactant from the PCLS. Secondly, we did our displacement measurements statically, which could have eliminated hysteresis.
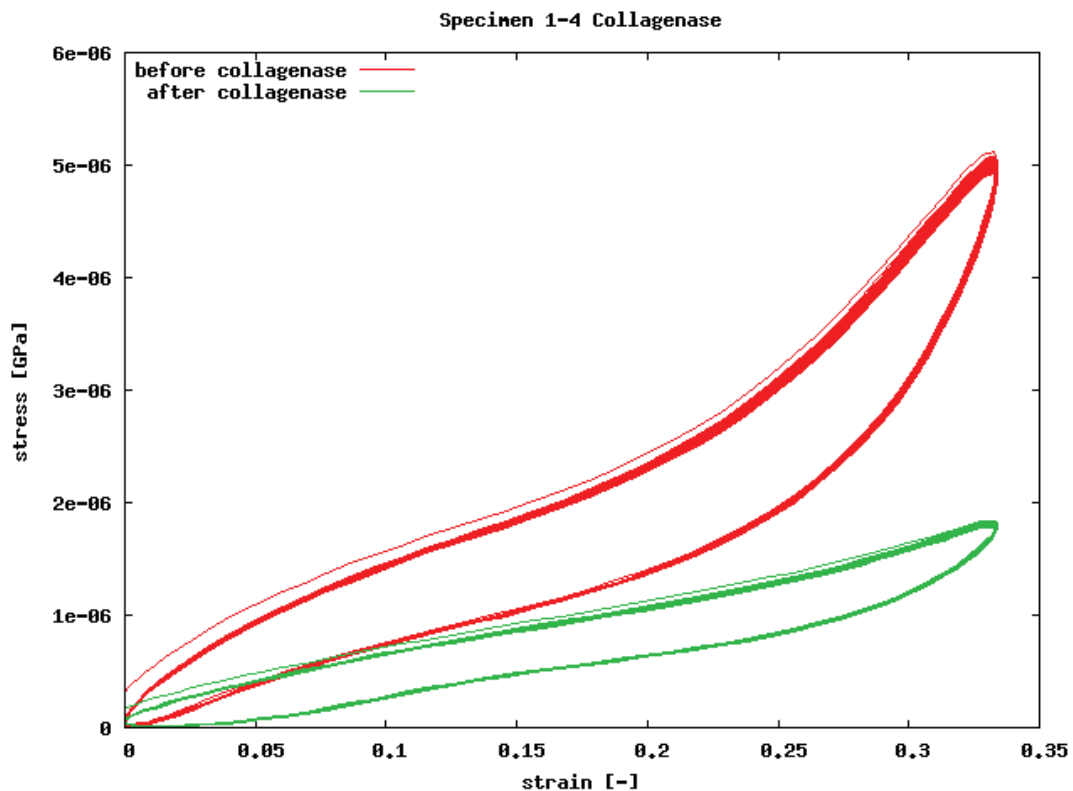
Figure 5.2: Strain-stress curve of a PCLS stretched in a tension machine. PCLS was measured before (red) and after (green) collagenase treatment. Experiment was performed by S. Rausch (München).

5.3.2. Influence of collagen

Lung tissue exhibits linear viscoelastic and nonlinear behaviour, dependent on several structural components, such as collagen. Collagen fibers in the extracellular matrix give lung tissue its tensile strength. It is thought to limit lung extensibility at high

volumes, therefore protecting the lung against overdistension (161). Strain-stress curves of lung parenchyma normally show a linear interval at low strains passing into a nonlinear region, probably defined by the tensile strengh of the collagen fibers, at higher strains. After collagenase treatment, the strain-stress curves show a right shift of the curve resulting in a softer tissue (310). Without collagen, no tensile strength limits the distension of the tissue. Hence, the slope and the elastic modulus after collagenase treatment must be smaller.

This was confirmed by the group of W. Wall (München) by stretching PCLS in a tension machine (Fig. 5.2).

In the bioreactor we observed a shift towards the membrane curve at a displacement of 2 mm. Most of the PCLS ripped between a displacement of 1.5 and 2 mm, indicating rather a disintegration of the PCLS before the altered material properties of the tissue become apparent. Disintegration of the PCLS in such a small range indicates that the stretch applied is greater or at least the strain in the bioreactor is different from the one applied in the tension machine. The stretch applied in the bioreactor is biaxial, which complicates the comparison with the uniaxial tension applied by the tension machine. However, our method concerning displacement readings may not be as sensitive as tissue stretched in a tension machine.

Regarding to the stretch distributions, the bioreactor applies stretch inhomogeneously, which may reflect the *in vivo* situation closer than homogeneous stretch. Taken together, these data demonstrate that tissue properties are altered by collagenase treatment. However, the current technical equipment of the strain-stress measurements is not ideal to measure material properties following collagenase treatment.

5.4. Gene induction in PCLS

5.4.1. Amphiregulin induction in PCLS

We exposed PCLS to mechanical stress by stretching them in the bioreactor. To investigate the biological consequences of the stretch, we examined gene induction in stretched PCLS. The most favoured gene was amphiregulin, which has been proven to be a promising candidate gene in mouse IPL experiments (65). Its induction specifically by stretch and not by LPS makes it an ideal stretch marker. Unfortunately, amphiregulin was already upregulated by the slicing process, which obviously acts as mechanical stress as well. Amphiregulin has been shown to be stress sensitive before, an upregulation can be triggered for example by mechanical compression of bronchial

epithelial cells (47). It has been also shown to participate in wound healing in colonic mucosa cells (117), which could be also its function in sliced lung tissue.

To measure amphiregulin expression especially induced by stretch, it was our aim to decrease its basal expression induced by the slicing process. One idea was to culture PCLS at 37℃ for longer time periods (up to 72h) to reduce the basal expression. However, also the expression of amphiregulin decreased during the incubation, even after 3 days it could not be induced by stretch in the bioreactor. One explanation could be that the PCLS were held in static culture. Stretch of 1h even seemed to reduce the amphiregulin induction, which may be due to the fact, that the lung in its normal environment is stretched all the time. Therefore the static culture conditions may be a stress factor for the PCLS itself. This could be solved by the adjustment of culture conditions, for example by culturing them in the roller culture system described before (153). In that system the PCLS are held at the air-liquid interface and are moved constantly. This could be further improved by a basic stretch tonus applied to the PCLS during culture, mimicking the *in vivo* situation.

Another idea was to keep the PCLS at 4℃ after the slicing process, to avoid activation on transcriptional level and thus reduce the initial gene induction triggered by the slicing process. We incubated PCLS for different time spans at 4℃ and investigated the induction at 37℃ afterwards. Twenty hours at 4℃ did not reduce the induction, but 44h had a significant influence. This indicates a "memory" of the PCLS, the induction is only delayed. Longer incubation periods at 4℃ may contribute to a degradation of inflammatory mediators released during the slicing process and therefore reduce the inflammatory response after 44h at 4℃. However, the induction was still comparably pronounced to the 24h induction after normal incubation.

PCLS were also treated with different inhibitors of transcription, translation and signalling pathways. Aside from trying to reduce the basal amphiregulin induction, it was our aim to get more information about the mechanism by which amphiregulin is upregulated by the slicing process. Actinomycin D, DRB and cycloheximide are known inhibitors of transcriptional processes (41; 100; 256). All of them were able to inhibit the RNA induction. Actinomycin D, DRB and apicidin are known to affect the RNA synthesis directly by intercalating into the DNA, inhibiting the casein kinase 2 and inhibiting the histone deacetylase, respectively. Apicidin seems to act irreversible (100), which was also observed with actinomycin D, but not with DRB. Interestingly cycloheximide also reduced amphiregulin induction, although it is a translational inhibitor and should not influence RNA levels (188). An explanation could be a feedback mechanism, by the newly synthesised amphiregulin protein. However, a feedback mechanism of amphiregulin has not been described up to now.

The tyrosine kinase signalling system has been shown to be important in the induction of amphiregulin (235), as confirmed in our system. In addition we found an influence of the cytoskeleton, namely by inhibition of the MLCK. Both MLCK and tyrosine kinases

seem to play an important role in endothelial cells in cytoskeletal rearrangements after shear stress (23), another type of mechanical stress. Also airway smooth muscle cells, which are subjected to mechanical stretch exhibit increased MLCK quantities (241). Consequently, MLCK and tyrosine kinases play a role in responses to mechanical stretch in different cell types and may therefore also be important for the mechanical stress induced upregulation of amphiregulin in PCLS. Inhibition of ROCK had no effect on amphiregulin; therefore it is very unlikely to be involved in amphiregulin induction. However, models of lung imflammation and lung injury showed an activation of ROCK and preventive effects of Y27632 (26; 130; 168). Blocking of the MLCK pathway looks promising; therefore it could be interesting to add both inhibitors, ML-7 and Y27632, looking for a synergistic effect. Another major molecule, which may be involved in mechanotransduction, is calcium. It has been shown to be involved in signalling by stretch-activated ion channels (96). In lung fetal alveolar epithelial cells calcium mobilisation seems to be a key molecule to activate early response genes after mechanical stretch (54). Calcium may play a role in the amphiregulin induction. We reduced calcium in the medium during the slicing process and for 4h after it. There was a small reduction in the amphiregulin induction at 0h and 4h after the slicing process. Because calcium is a fast acting mediator which is elevated during seconds in the cytoplasm our method may not be significant. Firstly, we did not deplete the calcium in the medium, which means there could be still enough calcium left for signalling. Secondly, the direct measurement of calcium for example by multi photon microscopy would be more adequate. However, neither the partial depletion of calcium nor blocking of calcium channels did reduce amphiregulin expression.

The acid sphingomyelinase pathway has received attention in many pulmonary diseases, such as COPD, cystic fibrosis and ALI. As initiator of ceramide-mediated signal transduction it may also play a role in stress-induced cell death (240). Especially sphingosine-1-phosphate, a mediator of the acid sphingomyelinase pathway, has been shown to be barrier protective on the alveolar and vascular level in murine lungs subjected to mechanical stress (160; 196). Sphingosine-1-phosphate may enhance amphiregulin induction which could be also a solvent effect. The solvent reduced the amphiregulin induction 4h after the slicing process. Compared to control PCLS there is no effect of sphingosine-1-phosphate. This is in line with the fact, that imipramine, an inhibitor of the acid sphingomyelinase, did not affect the induction of amphiregulin, suggesting the acid sphingomyelinase is not involved in this process.

Taken together, neither the reduction of temparature during incubation or at later time points nor the addition of inhibitors resulted in a satisfying reduction of the amphiregulin expression that is induced by the slicing process. A combination of inhibitors may be promising, possibly with storage of the PCLS at 4°C for at least 44h. The mechanism by which amphiregulin induction is regulated by mechanical stress seems to be dependent on tyrosine kinases and the cytoskeleton.

5.4.2. Amphiregulin RNA expression by other stress factors

To investigate amphiregulin induction by stress other than slicing and stretching, we treated PCLS with TMA, DNCB and H_2O_2 (Fig. 4.22). TMA and DNCB cause chemical stress in the lungs and have been shown to induce allergic reactions in murine airways (110). Oxidative stress, as one contributing stress factor to bronchopulmonary dysplasia was investigated by Wagenaar et al., who found an upregulation of amphiregulin in response to hyperoxia in neonatal rat lungs (284). We observed no further amphiregulin induction by treatment with these substances. Again, this might be due to the massive induction by the slicing process. Additionally, we used PCLS from adult rat lungs, which may not be comparable to the neonatal rat lungs used by Wagenaar et al. or the murine airways that showed allergic reactions to DNCB and TMA.
However, we could not definitely exclude an effect because the induction could be too weak to be distinguished from the slicing effect.

Taken together, there is a massive amphiregulin induction triggered by the preparation process of the PCLS. Others have examined the role of amphiregulin in wound healing processes after injury. Amphiregulin seems to be involved in liver fibrosis in mice, and it is upregulated after hypoxia in rat gastric mucosal cells (126; 199). Further studies support a role of amphiregulin in wound healing processes in damaged human colonic mucosa cells (118). Those studies show an involvement of amphiregulin in regenerative processes after different stress factors.
Our data may also suggest a role for amphiregulin in wound healing, probably in response to the slicing stimulus, which seems to be stronger than the induction triggered by stretch or other stress factors, such as chemicals.

5.4.3. Induction of immune response genes in PCLS

A gene array was performed to reveal information about upregulated genes by stretching the PCLS in the bioreactor, in order to find other candidate genes by screening. PCLS were stretched in the bioreactor for 2h and 4h and compared to PCLS which were clamped for the same time period. Stretched and clamped slices were compared to untreated control PCLS and to untreated lung tissue. A relatively huge amount of RNA was needed for the gene array; therefore the RNA was pooled from 6 animals, which reduced the final experiment to one analysis per group. In addition, only two bioreactor prototypes to stretch the tissue mean some time limitation. Consequently, a statistical evaluation of the data could only be handled with care and had to be verified by RTq-PCR. An obvious upregulation of inflammatory genes could be found by the untreated PCLS in comparison with untreated tissue. The pattern of

the upregulated genes shows a reaction to the mechanical stimulus and seems to react with repair mechanisms such as wound healing (Serpine1) and inflammatory processes (Il6). Stretched tissue in comparison with clamped controls did not reveal many genes specifically upregulated. Genes which appeared upregulated by stretch in the microarray could not be verified by RTq-PCR (data not shown).

The induction of genes triggered by the production process of the PCLS was investigated using RTq-PCR. One interesting fact was that the filling of the lung contributed partly to the induction of inflammatory mRNA. A completely filled lung lobe was incubated at 37°C for 4h, which means they were not sliced. The stimulus is therefore directly associated to the expansion of the lung. However, the stress factor which induces the main part of the inflammatory gene expression seems to be the slicing procedure. Several immune response genes were upregulated in PCLS. Mechanical stress and injury of cells during the slicing process as an activator of early immediated genes has been adressed in PCLS before (154). Martin et al. investigated Cox-2 as representative immediate early gene directly after the slicing process and over time. They observed that the induction could be abolished by media changes after the slicing process, probably due to the removal of inflammatory mediators released by the slicing process (154). We found a significant upregulation of different immune response genes after the slicing process, such as IL-6, MIP-2 and IP-10, and also including Cox-2. All of them are known to be involved in inflammatory processes, however, Cox-2 was not induced in PCLS after the slicing procedure and incubation in previous studies (154). Explanation for these different results may be: (i) we did not use the roller culture incubation system, so-called dynamic incubation, that was used by Martin et al., but did cultivate the PCLS in a static culture system (150; 218), (ii) the Krumdieck tissue slicer we used was an older model which may produce slices of non-ideal quality, and (iii) we directly quantified the cDNA by SYBR Green intercalation, which may be more sensitive than quantification by semi-quantitative PCR that was used before.

Proinflammatory cytokines are known to be released after tissue injury. During the innate immune response cytokines are produced for example by macrophages. Recruited T cells, belonging to the adapted immune response release additional cytokines enhancing the inflammatory response (150; 177). IL-6 and MIP-2 upregulation was highest 24h after the slicing process. Not much is known about RNA levels in rat tissue over time during inflammation, however, we found that IL-6, IP-10 and MIP-2 are produced to a high extend up to 24h after the slicing process. For IL-6 it was shown that mRNA expression in endothelial cells and serum levels were at maximum 4h after the onset of inflammation (142; 311). The prolonged IL-6 production in PCLS in comparison to endothelial cells and serum may be explained by the media changes carried out every 30 minutes during the first 4h (142; 311). Inflammatory responses are enhanced by positive feedback loops induced by the released mediators. Removal of

released mediators may have delayed the inflammatory process and prolonged the maximum cytokine production to 24h after the slicing process.

Cox-2 was upregulated to a certain extent and did not change the expression for the next 48h. This could be due to an enhanced basal expression. A long lasting release of proinflammatory mediators has been shown for example in sepsis (222).

The amphiregulin response to mechanical stress seems to be maximally upregulated after the slicing process. To investigate, wether the inflammatory response may be at a maximum too, we treated PCLS with LPS for 4h. LPS is known to upregulate early immediate genes, therefore we incubated PCLS with LPS to evalute whether IL-6, MIP-2, Cox-2 and IP-10 could be induced furthermore. LPS treatment has been applied in PCLS by Martin et al., who found an upregulation of Cox-2 expression after LPS treatment (154). We observed an induction of IL-6, MIP-2, Cox-2 and IP-10 after LPS treatment, which means that the slicing process does not induce the mRNA maximally and that slicing and LPS act additively on RNA induction. Although, the induction was not significant for IL-6.

The induction of IL-6, MIP-2, Cox-2 and IP-10 could only be prevented by storage of the PCLS at 4°C. Normally, PCLS are incubated at 37°C to mimick the body temperature. The absolute prevention of mRNA induction showed the importance of temperature for the transcriptional system.

Taken together, there is an inflammatory response induced by the slicing process. Unlike amphiregulin, different inflammatory cytokines could be further induced by the treatment with LPS. However, the ongoing inflammation was only partly reduced after 48h.

5.5. Conclusions

PCLS serve as a model for different clinical problems, such as asthma or overventilation. In addition to the use as a method to investigate airway and vascular pharmacology in different species, including human material, here we show that they can also be used for studying chemical and mechanical stress.

This is the first time PCLS were prepared from sheep lungs. Sheep PCLS offer the possibility to study differences in adult and preterm sheep. The bronchoconstriction to various mediators showed different results from adult and preterm sheep and may therefore provide a new model to investigate age-dependent stress responses.

We also show that PCLS as a model to investigate chemical stress is useful to study respiratory allergens as required in the REACH (Regulation, Evaluation, Authorisation and restriction of CHemicals) process. The specification of EAR and AHR to chemical allergens in mice is a promising method to predict the response *in vivo*.

Furthermore PCLS can be used as a new experimental model for studying mechanical stress in lung tissue of animals under well defined conditions. PCLS can be stretched in the bioreactor for at least 4h without significant cell death. We were able to determine stretches applied in our model during the stretching process. A gene induction of specific stretch markers in response to the applied stretch was not found in our model, probably because of the upregulation of stress genes by the slicing procedure. Stretching of precision-cut lung slices represents a link between *in vivo* and cell culture models designed to examine the biomechanical consequences of lung stretch. The new model will be useful to further investigate pulmonary sequelae of overdistension of lung tissue as may occur during mechanical ventilation. It is planned to extend this time span to up to three days, the time that PCLS can survive without cell death or loss of biological function (153; 303) and to apply this method to the study of human lung slices (218; 303).

6. Summary

Lungs are exposed to different forms of stress such as chemical substances, allergens or in the form of direct tissue injury. This study examined whether precision-cut lung slices are suitable as a model for studying different types of stress. We established the use of PCLS from sheep to study the response of airways and vessels to mediators. According to *in vivo* experiments sheep are thought to represent the human pathophysiology better than rodents. We therefore established the use of sheep PCLS and showed that methacholine, serotonin and endothelin-1 lead to a bronchoconstriction, while the response to leukotriene and thromboxane was rather weak. PCLS were also produced from preterm sheep and compared to adult sheep, which revealed a decreased reagibility to methacholine and serotonin in preterm sheep. Comparison of the bronchoconstriction of sheep PCLS with bronchoconstriction data from human PCLS revealed a less satisfactory accordance than the one seen *in vivo*. Although sheep PCLS may not represent the characteristics of human PCLS completely, the results presented in this thesis indicate that they are closer to human PCLS than PCLS from rodents.

Another kind of stress that we examined was chemical stress. This study also aimed at studying the usefulness of PCLS to study respiratory allergens as required in the REACH (Regulation, Evaluation, Authorisation and restriction of CHemicals) process. Bronchoconstriction in PCLS as response to chemical allergen was investigated and compared to bronchoconstriction *in vivo*. For this purpose a well established sensitisation protocol with TMA, a respiratory allergen and DNCB, a dermal allergen, was used. The early allergic response and airway hyperresponsiveness in mouse PCLS was investigated and compared to data from *in vivo* invasive measurements. Acquired measurements were comparable suggesting PCLS as a reasonable alternative to invasive lung function measurements. Hence, stress-related bronchoconstriction to chemical allergens may be a suitable predictability for *in vivo* experiments.

Several *in vivo* and cell culture models have been developed to study the pulmonary responses to mechanical stretch. While providing extremely useful information, these models do also suffer from limitations in being either too complex for detailed mechanical or mechanistic studies, or being devoid of the full complexity present *in vivo* (e.g. different cell types and interstitial matrix). Therefore, we developed a new model, based on the biaxial stretching of precision-cut lung slices. Single PCLS were mounted on a thin and flexible carrier membrane of PDMS in a bioreactor and the membrane was stretched by applying varying pressures under static conditions. A gene array revealed a general upregulation of immune response and wound healing genes by the slicing process. Stretch markers like amphiregulin were upregulated in PCLS by the slicing process. This upregulation was dependent on tyrosin kinases and

the cytoskeleton, but could not be blocked sufficiently, which made it complicated to differentiate a stretch response from the basal increase.

Distension of the PCLS was modelled via finite element simulation. According to this analysis, lung tissue was stretched by up to 38 % in the latitudinal and by up to 44 % in the longitudinal direction resulting in alveolar distension similar to what has been described in intact lungs. Lung slices were stretched dynamically with a frequency of 0.25 Hz for 4h, without causing cell injury. This indicates that the distension of PCLS in the bioreactor may not be suitable to study gene expression but allow the calculation of deformation and occurring forces of the PCLS during the stretching process.

PCLS are a suitable model for studying different forms of stress in the lung and allows the investigation of different pathophysiological situations. Additionally, PCLS may serve as a link between different species.

7. Deutsche Zusammenfassung

Die Lunge, die der Atmung dient, ist durch ihre Lage und Funktion vielen verschiedenen Stressfaktoren ausgesetzt. Diese können in Form von chemischen Substanzen, wie zum Beispiel Allergenen und Mediatoren auftreten, oder zu einer direkten Verletzung des Lungengewebes führen. In dieser Arbeit wurde untersucht, ob und inwiefern sich präzisions-geschnittene Lungenschnitte (PCLS) als Stressmodell eignen.

Ein Teil der vorliegenden Arbeit befasst sich mit der Etablierung des Lungenschnitt-Modells aus Schafslungen und die Wirkung von Mediatoren auf die Atemwege und Blutgefäße. Viele Tiermodelle spiegeln das Krankheitsbild des humanen Asthma bronchiale nur unzulänglich wider. *In vivo* weisen Schafe sehr viele Merkmale des humanen Krankheitsbildes auf, deswegen wurde in dieser Arbeit das Modell der Schaf-PCLS für die Messung der Bronchokonstriktion in Atemwegen und der Vasokonstriktion in Blutgefäßen etabliert. Während die Mediatoren Metacholin, Serotonin und Endothelin-1 zu einer starken Konstriktion der Atemwege in Schaf- PCLS führten, war die Reaktion auf Leukotriene und Thromboxane vergleichsweise schwach.

Neben PCLS aus adulten Tieren wurden auch Lungenschnitte aus frühgeborenen Lämmern hergestellt und mit den adulten Schaf-PCLS verglichen. Atemwege aus frühgeborenen Schafen zeigten eine abgeschwächte Konstriktion im Vergleich mit denen aus adulten Tieren. Vergleicht man die Bronchokonstriktion der Schaf-PCLS mit den Literaturdaten humaner Lungenschnitte, so zeigt sich eine weniger gute Übereinstimmung der Daten als die *in vivo* beobachtete Übereinstimmung der Asthma-Charakteristika in Menschen und Schafen. Trotzdem bietet das Schaf-PCLS-Modell einige Vorteile gegenüber dem Nagermodell, zum Beispiel den Vergleich von Lungenschnitten aus adulten mit frühgeborenen Schafen. Weiterhin wurde die Bronchokonstriktion als Reaktion auf chemische Allergene in PCLS mit der Reaktion *in vivo* verglichen. Hierfür wurde ein bekanntes Maus-Sensibilisierungsprotokoll mit dem respiratorischen Allergen TMA, und dem dermalen Allergen DNCB als Modell genutzt. Die allergische Frühphase und die Atemwegshyperreagibilität wurden *in vitro* in Maus-präzisionsgeschnittenen Lungenschnitten gemessen und mit *in vivo* Daten aus invasiven Experimenten verglichen. Durch die gute Übereinstimmung der Ergebnisse lassen sich PCLS als mögliche Alternative für *in vivo* Lungenfunktionsmessungen in Betracht ziehen. Stress-bedingte Bronchokonstriktion in PCLS durch chemische Allergene könnte als Vorhersage für *in vivo* Experimente dienen und damit für die Identifikation von chemischen Allergenen im Zuge der REACH (Regulation, Evaluation, Authorisation and restriction of CHemicals)-Richtlinien von Vorteil sein.

Neben Stress durch chemische Substanzen kann die Lunge auch durch physische Stimuli in Form von Überdehnung des Gewebes Schaden nehmen, wie z. B. bei der künstlichen Beatmung. Zahlreiche *in vivo*- und Zellkultur-Modelle wurden entwickelt, um die

Auswirkungen von mechanischem Stress auf das Lungenparenchym zu untersuchen. Obwohl durch diese Modelle schon viele wichtige Fragen beantwortet wurden, weisen sie immer noch einige Defizite auf. Während *in vivo*- Modelle oft zu komplex sind, um mechanische Eigenschaften adequat messen zu können, sind Zellkultur-Modelle oftmals zu einfach, um die Zusammenhänge der *in vivo*-Situation zu erfassen (beispielsweise verschiedene Zelltypen und die interstitielle Matrix). Deswegen haben wir ein neues Modell entwickelt, mit dem präzisions-geschnittene Lungenschnitte biaxial gedehnt werden können. Einzelne PCLS wurden auf einer dünnen, flexiblen Polydimethylsiloxan- Membran in den Bioreaktor eingespannt und durch Anlegen unterschiedlich hohen Druckes statisch ausgelenkt. Durch einen Genarray konnten wir weiterhin herausfinden, dass das Schneiden der Lunge an sich schon als physischer Stimulus wirkt und eine Anzahl von Genen hochreguliert. Bekannte Dehnungsmarker, wie zum Beispiel Amphiregulin, wurden durch den Schneideprozess hochreguliert. Bei dieser Induktion scheinen besonders Tyrosinkinasen und das Zytoskelett beteiligt zu sein, allerdings ließ sich die Hochregulation nicht vollständig blockieren. Daher war es uns nicht möglich, eine spezifisch durch Dehnung im Bioreaktor ausgelöste Amphiregulin-Induktion von der basalen Induktion abzugrenzen. Die Dehnung wurde mit Hilfe eines Finite-Element Modells untersucht. Dabei zeigte sich eine Dehnung von bis zu 38 % in der Breite und bis zu 44 % in der Längsrichtung. Diese Daten entsprechen Literaturdaten, die in intakten Lungen erhoben wurden. Die PCLS wurden außerdem dynamisch mit einer Frequenz von 0.25 Hz für 4 Stunden im Bioreaktor gedehnt, ohne die Zellstruktur zu verletzen.

Die Anwendung von präzisions-geschnittenen Lungenschnitten als Modell für Stress in der Lunge hat sich als erfolgreich erwiesen. Verschiedene pathophysiologische Situationen der Lunge konnten in den Lungenschnitten untersucht werden. Speziesunterschiede stellen immer noch eine Problematik bei der Übertragung von Daten aus Tiermodellen auf die humane Situation dar. Daher eignen sich präzision-geschnittene Lungenschnitte besonders, die pulmonalen Reaktionen in verschiedenen Spezies zu untersuchen.

8. Reference List

1. Randomized, placebo-controlled trial of lisofylline for early treatment of acute lung injury and acute respiratory distress syndrome. *Crit Care Med* 30: 1-6, 2002.

2. Ventilation with lower tidal volumes as compared with traditional tidal volumes for acute lung injury and the acute respiratory distress syndrome. The Acute Respiratory Distress Syndrome Network. *N Engl J Med* 342: 1301-1308, 2000.

3. **Abraham WM**. Modeling of asthma, COPD and cystic fibrosis in sheep. *Pulm Pharmacol Ther* 21: 743-754, 2008.

4. **Abraham WM, Delehunt JC, Yerger L and Marchette B**. Characterization of a late phase pulmonary response after antigen challenge in allergic sheep. *Am Rev Respir Dis* 128: 839-844, 1983.

5. **Abraham WM and Perruchoud AP**. Role of arachidonic acid metabolites in allergen-induced late responses. *Respiration* 56: 48-56, 1989.

6. **Adissu HA and Schuller HM**. Antagonistic growth regulation of cell lines derived from human lung adenocarcinomas of Clara cell and aveolar type II cell lineage: Implications for chemoprevention. *Int J Oncol* 24: 1467-1472, 2004.

7. **Amato MB, Barbas CS, Medeiros DM, Magaldi RB, Schettino GP, Lorenzi-Filho G, Kairalla RA, Deheinzelin D, Munoz C, Oliveira R, Takagaki TY and Carvalho CR**. Effect of a protective-ventilation strategy on mortality in the acute respiratory distress syndrome. *N Engl J Med* 338: 347-354, 1998.

8. **Anzueto A, Baughman RP, Guntupalli KK, Weg JG, Wiedemann HP, Raventos AA, Lemaire F, Long W, Zaccardelli DS and Pattishall EN**. Aerosolized surfactant in adults with sepsis-induced acute respiratory distress syndrome.

Exosurf Acute Respiratory Distress Syndrome Sepsis Study Group. *N Engl J Med* 334: 1417-1421, 1996.

9. **Armbruster C, Schneider M, Schumann S, Gamerdinger K, Cuevas M, Rausch S, Baaken G and Guttmann J**. Characteristics of highly flexible PDMS membranes for long-term mechanostimulation of biological tissue (in press). *Journal of Biomedical Materials Research* 2009.

10. **Arold SP, Wong JY and Suki B**. Design of a new stretching apparatus and the effects of cyclic strain and substratum on mouse lung epithelial-12 cells. *Ann Biomed Eng* 35: 1156-1164, 2007.

11. **Arts JH and Kuper CF**. Animal models to test respiratory allergy of low molecular weight chemicals: a guidance. *Methods* 41: 61-71, 2007.

12. **Bai Y and Sanderson MJ**. The contributions of Ca2+ signaling and Ca2+ sensitivity to the regulation of airway smooth muscle contraction is different in rats and mice. *Am J Physiol Lung Cell Mol Physiol* 2009.

13. **Bailey TC, Martin EL, Zhao L and Veldhuizen RA**. High oxygen concentrations predispose mouse lungs to the deleterious effects of high stretch ventilation. *J Appl Physiol* 94: 975-982, 2003.

14. **Ban M and Hettich D**. Relationship between IgE positive cell numbers and serum total IgE levels in mice treated with trimellitic anhydride and dinitrochlorobenzene. *Toxicol Lett* 118: 129-137, 2001.

15. **Banes AJ, Gilbert J, Taylor D and Monbureau O**. A new vacuum-operated stress-providing instrument that applies static or variable duration cyclic tension or compression to cells in vitro. *J Cell Sci* 75: 35-42, 1985.

16. **Bartz RR**. What is the role of high-frequency ventilation in adult respiratory distress syndrome? *Respir Care Clin N Am* 10: 329-39, vi, 2004.

17. **Baur X and Czuppon A**. Diagnostic validation of specific IgE antibody concentrations, skin prick testing, and challenge tests in chemical workers with symptoms of sensitivity to different anhydrides. *J Allergy Clin Immunol* 96: 489-494, 1995.

18. **Beck LA and Leung DY**. Allergen sensitization through the skin induces systemic allergic responses. *J Allergy Clin Immunol* 106: S258-S263, 2000.

19. **Belperio JA, Keane MP, Burdick MD, Londhe V, Xue YY, Li K, Phillips RJ and Strieter RM**. Critical role for CXCR2 and CXCR2 ligands during the pathogenesis of ventilator-induced lung injury. *J Clin Invest* 110: 1703-1716, 2002.

20. **Bergner A and Sanderson MJ**. Acetylcholine-induced calcium signaling and contraction of airway smooth muscle cells in lung slices. *J Gen Physiol* 119: 187-198, 2002.

21. **Bernard GR, Luce JM, Sprung CL, Rinaldo JE, Tate RM, Sibbald WJ, Kariman K, Higgins S, Bradley R, Metz CA and .** High-dose corticosteroids in patients with the adult respiratory distress syndrome. *N Engl J Med* 317: 1565-1570, 1987.

22. **Bingham CO, III and Austen KF**. Mast-cell responses in the development of asthma. *J Allergy Clin Immunol* 105: S527-S534, 2000.

23. **Birukov KG, Birukova AA, Dudek SM, Verin AD, Crow MT, Zhan X, DePaola N and Garcia JG**. Shear stress-mediated cytoskeletal remodeling and cortactin translocation in pulmonary endothelial cells. *Am J Respir Cell Mol Biol* 26: 453-464, 2002.

24. **Bischof RJ, Snibson K, Shaw R and Meeusen EN**. Induction of allergic inflammation in the lungs of sensitized sheep after local challenge with house dust mite. *Clin Exp Allergy* 33: 367-375, 2003.

25. **Bjorck T and Dahlen SE**. Leukotrienes and histamine mediate IgE-dependent contractions of human bronchi: pharmacological evidence obtained with tissues from asthmatic and non-asthmatic subjects. *Pulm Pharmacol* 6: 87-96, 1993.

26. **Bogatcheva NV, Adyshev D, Mambetsariev B, Moldobaeva N and Verin AD**. Involvement of microtubules, p38, and Rho kinases pathway in 2-methoxyestradiol-induced lung vascular barrier dysfunction. *Am J Physiol Lung Cell Mol Physiol* 292: L487-L499, 2007.

27. **Bradley BL, Azzawi M, Jacobson M, Assoufi B, Collins JV, Irani AM, Schwartz LB, Durham SR, Jeffery PK and Kay AB**. Eosinophils, T-lymphocytes, mast cells, neutrophils, and macrophages in bronchial biopsy specimens from atopic subjects with asthma: comparison with biopsy specimens from atopic subjects without asthma and normal control subjects and relationship to bronchial hyperresponsiveness. *J Allergy Clin Immunol* 88: 661-674, 1991.

28. **Brochard L, Roudot-Thoraval F, Roupie E, Delclaux C, Chastre J, Fernandez-Mondejar E, Clementi E, Mancebo J, Factor P, Matamis D, Ranieri M, Blanch L, Rodi G, Mentec H, Dreyfuss D, Ferrer M, Brun-Buisson C, Tobin M and Lemaire F**. Tidal volume reduction for prevention of ventilator-induced lung injury in acute respiratory distress syndrome. The Multicenter Trail Group on Tidal Volume reduction in ARDS. *Am J Respir Crit Care Med* 158: 1831-1838, 1998.

29. **Brower RG, Lanken PN, MacIntyre N, Matthay MA, Morris A, Ancukiewicz M, Schoenfeld D and Thompson BT**. Higher versus lower positive end-expiratory pressures in patients with the acute respiratory distress syndrome. *N Engl J Med* 351: 327-336, 2004.

30. **Brower RG, Shanholtz CB, Fessler HE, Shade DM, White P, Jr., Wiener CM, Teeter JG, Dodd-o JM, Almog Y and Piantadosi S**. Prospective, randomized, controlled clinical trial comparing traditional versus reduced tidal volume ventilation in acute respiratory distress syndrome patients. *Crit Care Med* 27: 1492-1498, 1999.

31. **Brown TD**. Techniques for mechanical stimulation of cells in vitro: a review. *J Biomech* 33: 3-14, 2000.

32. **Buckley TL and Nijkamp FP**. Mucosal exudation associated with a pulmonary delayed-type hypersensitivity reaction in the mouse. Role for the tachykinins. *J Immunol* 153: 4169-4178, 1994.

33. **Carlon GC, Howland WS, Ray C, Miodownik S, Griffin JP and Groeger JS**. High-frequency jet ventilation. A prospective randomized evaluation. *Chest* 84: 551-559, 1983.

34. **Carney DE, Bredenberg CE, Schiller HJ, Picone AL, McCann UG, Gatto LA, Bailey G, Fillinger M and Nieman GF**. The Mechanism of Lung Volume Change during Mechanical Ventilation. *Am J Respir Crit Care Med* 160: 1697-1702, 1999.

35. **Castell JV, Donato MT and Gomez-Lechon MJ**. Metabolism and bioactivation of toxicants in the lung. The in vitro cellular approach. *Exp Toxicol Pathol* 57 Suppl 1: 189-204, 2005.

36. **Cavanaugh KJ, Jr. and Margulies SS**. Measurement of stretch-induced loss of alveolar epithelial barrier integrity with a novel in vitro method. *Am J Physiol Cell Physiol* 283: C1801-C1808, 2002.

37. **Cavanaugh KJ, Jr., Oswari J and Margulies SS**. Role of stretch on tight junction structure in alveolar epithelial cells. *Am J Respir Cell Mol Biol* 25: 584-591, 2001.

38. **Cepkova M and Matthay MA**. Pharmacotherapy of acute lung injury and the acute respiratory distress syndrome. *J Intensive Care Med* 21: 119-143, 2006.

39. **Chapman KE, Sinclair SE, Zhuang D, Hassid A, Desai LP and Waters CM**. Cyclic mechanical strain increases reactive oxygen species production in pulmonary epithelial cells. *Am J Physiol Lung Cell Mol Physiol* 289: L834-L841, 2005.

40. **Cheah FC, Pillow JJ, Kramer BW, Polglase GR, Nitsos I, Newnham JP, Jobe AH and Kallapur SG**. Airway inflammatory cell responses to intra-amniotic lipopolysaccharide in a sheep model of chorioamnionitis. *Am J Physiol Lung Cell Mol Physiol* 296: L384-L393, 2009.

41. **Chen H, Liu X and Patel DJ**. DNA bending and unwinding associated with actinomycin D antibiotics bound to partially overlapping sites on DNA. *J Mol Biol* 258: 457-479, 1996.

42. **Chen J, Fabry B, Schiffrin EL and Wang N**. Twisting integrin receptors increases endothelin-1 gene expression in endothelial cells. *Am J Physiol Cell Physiol* 280: C1475-C1484, 2001.

43. **Cheng KC, Zhang H, Lin CY and Slutsky AS**. Ventilation with negative airway pressure induces a cytokine response in isolated mouse lung. *Anesth Analg* 94: 1577-82, table, 2002.

44. **Chida N and Adams FH**. Incorporation of acetate into fatty acids and lecithin by lung slices from fetal and newborn lambs. *J Lipid Res* 8: 335-341, 1967.

45. **Chokki M, Mitsuhashi H and Kamimura T**. Metalloprotease-dependent amphiregulin release mediates tumor necrosis factor-alpha-induced IL-8 secretion in the human airway epithelial cell line NCI-H292. *Life Sci* 78: 3051-3057, 2006.

46. **Choudhury S, Wilson MR, Goddard ME, O'Dea KP and Takata M**. Mechanisms of early pulmonary neutrophil sequestration in ventilator-induced lung injury in mice. *Am J Physiol Lung Cell Mol Physiol* 287: L902-L910, 2004.

47. **Chu EK, Foley JS, Cheng J, Patel AS, Drazen JM and Tschumperlin DJ**. Bronchial epithelial compression regulates epidermal growth factor receptor family ligand expression in an autocrine manner. *Am J Respir Cell Mol Biol* 32: 373-380, 2005.

48. **Chu EK, Whitehead T and Slutsky AS**. Effects of cyclic opening and closing at low- and high-volume ventilation on bronchoalveolar lavage cytokines. *Crit Care Med* 32: 168-174, 2004.

49. **Citri A and Yarden Y**. EGF-ERBB signalling: towards the systems level. *Nat Rev Mol Cell Biol* 7: 505-516, 2006.

50. **Coe JY, Olley PM and Coceani F**. A fetal-instrumented model to study age-specific responses to leukotriene D4 and prostaglandin D2 in unsedated newborn lambs. *Can J Physiol Pharmacol* 67: 587-593, 1989.

51. **Coffman RL and Hessel EM**. Nonhuman primate models of asthma. *J Exp Med* 201: 1875-1879, 2005.

52. **Cooper PR, McParland BE, Mitchell HW, Noble PB, Politi AZ, Ressmeyer AR and West AR**. Airway mechanics and methods used to visualize smooth muscle dynamics in vitro. *Pulm Pharmacol Ther* 2008.

53. **Cooper PR and Panettieri RA, Jr.** Steroids completely reverse albuterol-induced beta(2)-adrenergic receptor tolerance in human small airways. *J Allergy Clin Immunol* 122: 734-740, 2008.

54. **Copland IB and Post M**. Stretch-activated signaling pathways responsible for early response gene expression in fetal lung epithelial cells. *J Cell Physiol* 210: 133-143, 2007.

55. **Correa-Meyer E, Pesce L, Guerrero C and Sznajder JI**. Cyclic stretch activates ERK1/2 via G proteins and EGFR in alveolar epithelial cells. *Am J Physiol Lung Cell Mol Physiol* 282: L883-L891, 2002.

56. **Cross AS, Opal SM, Sadoff JC and Gemski P**. Choice of bacteria in animal models of sepsis. *Infect Immun* 61: 2741-2747, 1993.

57. **De KR, De Jager MH, Draaisma AL, Jurva JU, Olinga P, Meijer DK and Groothuis GM**. Drug-metabolizing activity of human and rat liver, lung, kidney and intestine slices. *Xenobiotica* 32: 349-362, 2002.

58. **De KR, Monshouwer M, Draaisma AL, De Jager MH, de G, I, Proost JH, Meijer DK and Groothuis GM**. Prediction of whole-body metabolic clearance of drugs through the combined use of slices from rat liver, lung, kidney, small intestine and colon. *Xenobiotica* 34: 229-241, 2004.

59. **Dearman RJ, Basketter DA and Kimber I**. Selective induction of type 2 cytokines following topical exposure of mice to platinum salts. *Food Chem Toxicol* 36: 199-207, 1998.

60. **Dearman RJ, Moussavi A, Kemeny DM and Kimber I**. Contribution of CD4+ and CD8+ T lymphocyte subsets to the cytokine secretion patterns induced in mice during sensitization to contact and respiratory chemical allergens. *Immunology* 89: 502-510, 1996.

61. **Dearman RJ, Warbrick EV, Humphreys IR and Kimber I**. Characterization in mice of the immunological properties of five allergenic acid anhydrides. *J Appl Toxicol* 20: 221-230, 2000.

62. **Dearman RJ, Warbrick EV, Skinner R and Kimber I**. Cytokine fingerprinting of chemical allergens: species comparisons and statistical analyses. *Food Chem Toxicol* 40: 1881-1892, 2002.

63. **Deng L, Fairbank NJ, Fabry B, Smith PG and Maksym GN**. Localized mechanical stress induces time-dependent actin cytoskeletal remodeling and stiffening in cultured airway smooth muscle cells. *Am J Physiol Cell Physiol* 287: C440-C448, 2004.

64. **Derksen FJ, Robinson NE, Armstrong PJ, Stick JA and Slocombe RF**. Airway reactivity in ponies with recurrent airway obstruction (heaves). *J Appl Physiol* 58: 598-604, 1985.

65. **Dolinay T, Kaminski N, Felgendreher M, Kim HP, Reynolds P, Watkins SC, Karp D, Uhlig S and Choi AM**. Gene expression profiling of target genes in ventilator-induced lung injury. *Physiol Genomics* 26: 68-75, 2006.

66. **dos Santos CC, Han B, Andrade CF, Bai X, Uhlig S, Hubmayr R, Tsang M, Lodyga M, Keshavjee S, Slutsky AS and Liu M**. DNA microarray analysis of gene expression in alveolar epithelial cells in response to TNFalpha, LPS, and cyclic stretch. *Physiol Genomics* 19: 331-342, 2004.

67. **dos Santos CC and Slutsky AS**. Invited review: mechanisms of ventilator-induced lung injury: a perspective. *J Appl Physiol* 89: 1645-1655, 2000.

68. **dos Santos CC and Slutsky AS**. The contribution of biophysical lung injury to the development of biotrauma. *Annu Rev Physiol* 68: 585-618, 2006.

69. **Dreyfuss D and Saumon G**. Ventilator-induced lung injury: lessons from experimental studies. *Am J Respir Crit Care Med* 157: 294-323, 1998.

70. **Ebsen M, Mogilevski G, Anhenn O, Maiworm V, Theegarten D, Schwarze J and Morgenroth K**. Infection of murine precision cut lung slices (PCLS) with respiratory syncytial virus (RSV) and chlamydophila pneumoniae using the Krumdieck technique. *Pathol Res Pract* 198: 747-753, 2002.

71. **Edwards YS, Sutherland LM and Murray AW**. NO protects alveolar type II cells from stretch-induced apoptosis. A novel role for macrophages in the lung. *Am J Physiol Lung Cell Mol Physiol* 279: L1236-L1242, 2000.

72. **Erpenbeck VJ, Ziegert M, Cavalet-Blanco D, Martin C, Baelder R, Glaab T, Braun A, Steinhilber W, Luettig B, Uhlig S, Hoymann HG, Krug N and Hohlfeld JM**. Surfactant protein D inhibits early airway response in Aspergillus fumigatus-sensitized mice. *Clin Exp Allergy* 36: 930-940, 2006.

73. **Escolar JD and Escolar A**. Lung hysteresis: a morphological view. *Histol Histopathol* 19: 159-166, 2004.

74. **European Parliament and Council**. Regulation (EC) No 1907/2006: Regulation concerning the Registration, Evaluation, Authorisation and Restriction of Chemicals (REACH), establishing a European Chemicals Agency. *Official journal of the European Union* 2006.

75. **Fisher JL, Levitan I and Margulies SS**. Plasma membrane surface increases with tonic stretch of alveolar epithelial cells. *Am J Respir Cell Mol Biol* 31: 200-208, 2004.

76. **Fisher JL and Margulies SS**. Na(+)-K(+)-ATPase activity in alveolar epithelial cells increases with cyclic stretch. *Am J Physiol Lung Cell Mol Physiol* 283: L737-L746, 2002.

77. **Fisher RL, Smith MS, Hasal SJ, Hasal KS, Gandolfi AJ and Brendel K**. The use of human lung slices in toxicology. *Hum Exp Toxicol* 13: 466-471, 1994.

78. **Fox-Dewhurst R, Alberts MK, Kajikawa O, Caldwell E, Johnson MC, Skerrett SJ, Goodman RB, Ruzinski JT, Wong VA, Chi EY and Martin TR**. Pulmonary and systemic inflammatory responses in rabbits with gram-negative pneumonia. *Am J Respir Crit Care Med* 155: 2030-2040, 1997.

79. **Frank JA and Matthay MA**. Science review: mechanisms of ventilator-induced injury. *Crit Care* 7: 233-241, 2003.

80. **Frank L, Bucher JR and Roberts RJ**. Oxygen toxicity in neonatal and adult animals of various species. *J Appl Physiol* 45: 699-704, 1978.

81. **Freeman BA and O'Neil JJ**. Tissue slices in the study of lung metabolism and toxicology. *Environ Health Perspect* 56: 51-60, 1984.

82. **Garssen J, Nijkamp FP, Van D, V and Van LH**. T-cell-mediated induction of airway hyperreactivity in mice. *Am Rev Respir Dis* 144: 931-938, 1991.

83. **Garssen J, Nijkamp FP, Wagenaar SS, Zwart A, Askenase PW and Van LH**. Regulation of delayed-type hypersensitivity-like responses in the mouse lung, determined with histological procedures: serotonin, T-cell suppressor-inducer factor and high antigen dose tolerance regulate the magnitude of T-cell dependent inflammatory reactions. *Immunology* 68: 51-58, 1989.

84. **Garssen J, Van LH, Van D, V, Bot H and Nijkamp FP**. T cell-mediated induction of airway hyperresponsiveness and altered lung functions in mice are independent of increased vascular permeability and mononuclear cell infiltration. *Am Rev Respir Dis* 147: 307-313, 1993.

85. **Gasser TC, Ogden RW and Holzapfel GA**. Hyperelastic modelling of arterial layers with distributed collagen fibre orientations. *Journal of the Royal Society Interface* 3: 15-35, 2006.

86. **Gentleman RC, Carey VJ, Bates DM, Bolstad B, Dettling M, Dudoit S, Ellis B, Gautier L, Ge Y, Gentry J, Hornik K, Hothorn T, Huber W, Iacus S, Irizarry R, Leisch F, Li C, Maechler M, Rossini AJ, Sawitzki G, Smith C, Smyth G, Tierney L, Yang JY and Zhang J**. Bioconductor: open software development for computational biology and bioinformatics. *Genome Biol* 5: R80, 2004.

87. **Glaab T, Mitzner W, Braun A, Ernst H, Korolewitz R, Hohlfeld JM, Krug N and Hoymann HG**. Repetitive measurements of pulmonary mechanics to inhaled cholinergic challenge in spontaneously breathing mice. *J Appl Physiol* 97: 1104-1111, 2004.

88. **Goris K, Uhlenbruck S, Schwegmann-Wessels C, Kohl W, Niedorf F, Stern M, Hewicker-Trautwein M, Bals R, Taylor G, Braun A, Bicker G, Kietzmann M and Herrler G**. Differential sensitivity of differentiated epithelial cells to respiratory viruses reveals different viral strategies of host infection. *J Virol* 83: 1962-1968, 2009.

89. **Gram TE**. Chemically reactive intermediates and pulmonary xenobiotic toxicity. *Pharmacol Rev* 49: 297-341, 1997.

90. **Grammer LC, Shaughnessy MA, Henderson J, Zeiss CR, Kavich DE, Collins MJ, Pecis KM and Kenamore BD**. A clinical and immunologic study of workers with trimellitic-anhydride-induced immunologic lung disease after transfer to low exposure jobs. *Am Rev Respir Dis* 148: 54-57, 1993.

91. **Greene KE, Wright JR, Steinberg KP, Ruzinski JT, Caldwell E, Wong WB, Hull W, Whitsett JA, Akino T, Kuroki Y, Nagae H, Hudson LD and Martin TR**. Serial changes in surfactant-associated proteins in lung and serum before and after onset of ARDS. *Am J Respir Crit Care Med* 160: 1843-1850, 1999.

92. **Grunstein MM, Rosenberg SM, Schramm CM and Pawlowski NA**. Mechanisms of action of endothelin 1 in maturing rabbit airway smooth muscle. *Am J Physiol* 260: L434-L443, 1991.

93. **Guo TL, Zhang XL, Leffel EK, Peachee VL, Karrow NA, Germolec DR and White KL, Jr.** Differential stimulation of IgE production, STAT activation and cytokine and CD86 expression by 2,4-dinitrochlorobenzene and trimellitic anhydride. *J Appl Toxicol* 22: 397-403, 2002.

94. **Hager DN, Krishnan JA, Hayden DL and Brower RG**. Tidal volume reduction in patients with acute lung injury when plateau pressures are not high. *Am J Respir Crit Care Med* 172: 1241-1245, 2005.

95. **Halbertsma FJ, Vaneker M, Scheffer GJ and van der Hoeven JG**. Cytokines and biotrauma in ventilator-induced lung injury: a critical review of the literature. *Neth J Med* 63: 382-392, 2005.

96. **Hamanaka K, Jian MY, Weber DS, Alvarez DF, Townsley MI, Al-Mehdi AB, King JA, Liedtke W and Parker JC**. TRPV4 initiates the acute calcium-dependent permeability increase during ventilator-induced lung injury in isolated mouse lungs. *Am J Physiol Lung Cell Mol Physiol* 293: L923-L932, 2007.

97. **Hammerschmidt S, Kuhn H, Grasenack T, Gessner C and Wirtz H**. Apoptosis and necrosis induced by cyclic mechanical stretching in alveolar type II cells. *Am J Respir Cell Mol Biol* 30: 396-402, 2004.

98. **Hammerschmidt S, Kuhn H, Sack U, Schlenska A, Gessner C, Gillissen A and Wirtz H**. Mechanical stretch alters alveolar type II cell mediator release toward a proinflammatory pattern. *Am J Respir Cell Mol Biol* 33: 203-210, 2005.

99. **Han B, Lodyga M and Liu M**. Ventilator-induced lung injury: role of protein-protein interaction in mechanosensation. *Proc Am Thorac Soc* 2: 181-187, 2005.

100. **Han JW, Ahn SH, Park SH, Wang SY, Bae GU, Seo DW, Kwon HK, Hong S, Lee HY, Lee YW and Lee HW**. Apicidin, a histone deacetylase inhibitor, inhibits proliferation of tumor cells via induction of p21WAF1/Cip1 and gelsolin. *Cancer Res* 60: 6068-6074, 2000.

101. **Hanlon N, Coldham N, Sauer MJ and Ioannides C**. Modulation of rat pulmonary carcinogen-metabolising enzyme systems by the isothiocyanates erucin and sulforaphane. *Chem Biol Interact* 177: 115-120, 2009.

102. **Harrigan JA, McGarrigle BP, Sutter TR and Olson JR**. Tissue specific induction of cytochrome P450 (CYP) 1A1 and 1B1 in rat liver and lung following in vitro (tissue slice) and in vivo exposure to benzo(a)pyrene. *Toxicol In Vitro* 20: 426-438, 2006.

103. **Harrigan JA, Vezina CM, McGarrigle BP, Ersing N, Box HC, Maccubbin AE and Olson JR**. DNA adduct formation in precision-cut rat liver and lung slices exposed to benzo[a]pyrene. *Toxicol Sci* 77: 307-314, 2004.

104. **Hart PH**. Regulation of the inflammatory response in asthma by mast cell products. *Immunol Cell Biol* 79: 149-153, 2001.

105. **Hayashi M, Higashi K, Kato H and Kaneko H**. Assessment of preferential Th1 or Th2 induction by low-molecular-weight compounds using a reverse transcription-polymerase chain reaction method: comparison of two mouse strains, C57BL/6 and BALB/c. *Toxicol Appl Pharmacol* 177: 38-45, 2001.

106. **Hays AM, Lantz RC and Witten ML**. Correlation between in vivo and in vitro pulmonary responses to jet propulsion fuel-8 using precision-cut lung slices and a dynamic organ culture system. *Toxicol Pathol* 31: 200-207, 2003.

107. **Held HD, Boettcher S, Hamann L and Uhlig S**. Ventilation-induced chemokine and cytokine release is associated with activation of nuclear factor-kappaB and is blocked by steroids. *Am J Respir Crit Care Med* 163: 711-716, 2001.

108. **Held HD, Martin C and Uhlig S**. Characterization of airway and vascular responses in murine lungs. *Br J Pharmacol* 126: 1191-1199, 1999.

109. **Held HD and Uhlig S**. Mechanisms of endotoxin-induced airway and pulmonary vascular hyperreactivity in mice. *Am J Respir Crit Care Med* 162: 1547-1552, 2000.

110. **Henjakovic M, Martin C, Hoymann HG, Sewald K, Ressmeyer AR, Dassow C, Pohlmann G, Krug N, Uhlig S and Braun A**. Ex vivo lung function measurements in precision-cut lung slices (PCLS) from chemical allergen-sensitized mice represent a suitable alternative to in vivo studies. *Toxicol Sci* 106: 444-453, 2008.

111. **Henjakovic M, Sewald K, Switalla S, Kaiser D, Muller M, Veres TZ, Martin C, Uhlig S, Krug N and Braun A**. Ex vivo testing of immune responses in precision-cut lung slices. *Toxicol Appl Pharmacol* 231: 68-76, 2008.

112. **Hickling KG**. Reinterpreting the pressure-volume curve in patients with acute respiratory distress syndrome. *Curr Opin Crit Care* 8: 32-38, 2002.

113. **Hirshman CA, Malley A and Downes H**. Basenji-Greyhound dog model of asthma: reactivity to Ascaris suum, citric acid, and methacholine. *J Appl Physiol* 49: 953-957, 1980.

114. **Huettner JE, Stack E and Wilding TJ**. Antagonism of neuronal kainate receptors by lanthanum and gadolinium. *Neuropharmacology* 37: 1239-1247, 1998.

115. **Hukkanen J, Pelkonen O, Hakkola J and Raunio H**. Expression and regulation of xenobiotic-metabolizing cytochrome P450 (CYP) enzymes in human lung. *Crit Rev Toxicol* 32: 391-411, 2002.

116. **Imai Y, Parodo J, Kajikawa O, de PM, Fischer S, Edwards V, Cutz E, Liu M, Keshavjee S, Martin TR, Marshall JC, Ranieri VM and Slutsky AS**. Injurious mechanical ventilation and end-organ epithelial cell apoptosis and organ dysfunction in an experimental model of acute respiratory distress syndrome. *JAMA* 289: 2104-2112, 2003.

117. **Inatomi O, Andoh A, Yagi Y, Bamba S, Tsujikawa T and Fujiyama Y**. Regulation of amphiregulin and epiregulin expression in human colonic subepithelial myofibroblasts. *Int J Mol Med* 18: 497-503, 2006.

118. **Inatomi O, Andoh A, Yagi Y, Bamba S, Tsujikawa T and Fujiyama Y**. Regulation of amphiregulin and epiregulin expression in human colonic subepithelial myofibroblasts. *Int J Mol Med* 18: 497-503, 2006.

119. **Ishida T, Takahashi M, Corson MA and Berk BC**. Fluid shear stress-mediated signal transduction: how do endothelial cells transduce mechanical force into biological responses? *Ann N Y Acad Sci* 811: 12-23, 1997.

120. **Joad JP, Kott KS, Bric JM, Peake JL and Pinkerton KE**. Effect of perinatal secondhand tobacco smoke exposure on in vivo and intrinsic airway structure/ function in non-human primates. *Toxicol Appl Pharmacol* 234: 339-344, 2009.

121. **Johnson A and Broadley KJ**. Airway reactivity to inhaled spasmogens 18-24 h after antigen-challenge in sensitized anaesthetized guinea-pigs. *J Pharm Pharmacol* 49: 1062-1066, 1997.

122. **Johnston JB, Navaratnam S, Pitz MW, Maniate JM, Wiechec E, Baust H, Gingerich J, Skliris GP, Murphy LC and Los M**. Targeting the EGFR pathway for cancer therapy. *Curr Med Chem* 13: 3483-3492, 2006.

123. **Jones JC, Lane K, Hopkinson SB, Lecuona E, Geiger RC, Dean DA, Correa-Meyer E, Gonzales M, Campbell K, Sznajder JI and Budinger S**. Laminin-6 assembles into multimolecular fibrillar complexes with perlecan and participates in mechanical-signal transduction via a dystroglycan-dependent, integrin-independent mechanism. *J Cell Sci* 118: 2557-2566, 2005.

124. **Kamikawa Y and Shimo Y**. Adenosine selectively inhibits noncholinergic transmission in guinea pig bronchi. *J Appl Physiol* 66: 2084-2091, 1989.

125. **Kasper M, Seidel D, Knels L, Morishima N, Neisser A, Bramke S and Koslowski R**. Early signs of lung fibrosis after in vitro treatment of rat lung slices with CdCl2 and TGF-beta1. *Histochem Cell Biol* 121: 131-140, 2004.

126. **Katada K, Naito Y, Mizushima K, Takagi T, Handa O, Kokura S, Ichikawa H, Yoshida N, Matsui H and Yoshikawa T**. Gene expression profiles on hypoxia and reoxygenation in rat gastric epithelial cells: a high-density DNA microarray analysis. *Digestion* 73: 89-100, 2006.

127. **Kelly LJ, Undem BJ and Adams GK, III**. Antigen-induced contraction of guinea pig isolated pulmonary arteries and lung parenchyma. *J Appl Physiol* 74: 1563-1569, 1993.

128. **Kirschvink N, Vincke G, Onclinx C, Peck MJ and Gustin P**. Comparison between pulmonary resistance and Penh in anaesthetised rats with tracheal diameter reduction and after carbachol inhalation. *J Pharmacol Toxicol Methods* 51: 123-128, 2005.

129. **Koike K, Moore FA, Moore EE, Poggetti RS, Tuder RM and Banerjee A**. Endotoxin after gut ischemia/reperfusion causes irreversible lung injury. *J Surg Res* 52: 656-662, 1992.

130. **Koksel O, Yildirim C, Tiftik RN, Kubat H, Tamer L, Cinel L, Kaplan MB, Degirmenci U, Ozdulger A and Buyukafsar K**. Rho-kinase (ROCK-1 and ROCK-2) upregulation in oleic acid-induced lung injury and its restoration by Y-27632. *Eur J Pharmacol* 510: 135-142, 2005.

131. **Krumdieck CL, dos Santos JE and Ho KJ**. A new instrument for the rapid preparation of tissue slices. *Anal Biochem* 104: 118-123, 1980.

132. **Kuebler WM, Uhlig U, Goldmann T, Schael G, Kerem A, Exner K, Martin C, Vollmer E and Uhlig S**. Stretch activates nitric oxide production in pulmonary vascular endothelial cells in situ. *Am J Respir Crit Care Med* 168: 1391-1398, 2003.

133. **Kummer W, Wiegand S, Akinci S, Schinkel AH, Wess J, Koepsell H, Haberberger RV and Lips KS**. Role of acetylcholine and muscarinic receptors in serotonin-induced bronchoconstriction in the mouse. *J Mol Neurosci* 30: 67-68, 2006.

134. **Kummer W, Wiegand S, Akinci S, Wessler I, Schinkel AH, Wess J, Koepsell H, Haberberger RV and Lips KS**. Role of acetylcholine and polyspecific cation transporters in serotonin-induced bronchoconstriction in the mouse. *Respir Res* 7: 65, 2006.

135. **Lachmann B, Robertson B and Vogel J**. In vivo lung lavage as an experimental model of the respiratory distress syndrome. *Acta Anaesthesiol Scand* 24: 231-236, 1980.

136. **Lake BG, Meredith C, Scott MP, Renwick AB and Price RJ**. Use of cultured precision-cut rat lung slices to study the in vitro induction of pulmonary cytochrome P450 forms. *Xenobiotica* 33: 691-702, 2003.

137. **Lanes S, Stevenson JS, Codias E, Hernandez A, Sielczak MW, Wanner A and Abraham WM**. Indomethacin and FPL-57231 inhibit antigen-induced airway hyperresponsiveness in sheep. *J Appl Physiol* 61: 864-872, 1986.

138. **Larsen CP and Regal JF**. Trimellitic anhydride (TMA) dust induces airway obstruction and eosinophilia in non-sensitized guinea pigs. *Toxicology* 178: 89-99, 2002.

139. **Laudadio RE, Wolfson MR, Shaffer TH and Driska SP**. Developmental differences in the contractile response of isolated ovine tracheal smooth muscle cells. *Pediatr Pulmonol* 44: 602-612, 2009.

140. **Le PE, Vaz E, Bion A, Dionnet F and Morin JP**. Toxicity of diesel engine exhausts in an in vitro model of lung slices in biphasic organotypic culture: induction of a proinflammatory and apoptotic response. *Arch Toxicol* 74: 460-466, 2000.

141. **Leguillette R**. Recurrent airway obstruction--heaves. *Vet Clin North Am Equine Pract* 19: 63-86, vi, 2003.

142. **Lehrke M, Broedl UC, Biller-Friedmann IM, Vogeser M, Henschel V, Nassau K, Goke B, Kilger E and Parhofer KG**. Serum concentrations of cortisol, interleukin 6, leptin and adiponectin predict stress induced insulin resistance in acute inflammatory reactions. *Crit Care* 12: R157, 2008.

143. **Lewis JF and Jobe AH**. Surfactant and the adult respiratory distress syndrome. *Am Rev Respir Dis* 147: 218-233, 1993.

144. **Li LF, Liao SK, Lee CH, Tsai YH, Huang CC and Quinn DA**. Ventilation-induced neutrophil infiltration and apoptosis depend on apoptosis signal-regulated kinase 1 pathway. *Crit Care Med* 33: 1913-1921, 2005.

145. **Li LF, Ouyang B, Choukroun G, Matyal R, Mascarenhas M, Jafari B, Bonventre JV, Force T and Quinn DA**. Stretch-induced IL-8 depends on c-Jun NH2-terminal and nuclear factor-kappaB-inducing kinases. *Am J Physiol Lung Cell Mol Physiol* 285: L464-L475, 2003.

146. **Lionetti V, Lisi A, Patrucco E, De GP, Milazzo MG, Ceci S, Wymann M, Lena A, Gremigni V, Fanelli V, Hirsch E and Ranieri VM**. Lack of phosphoinositide 3-kinase-gamma attenuates ventilator-induced lung injury. *Crit Care Med* 34: 134-141, 2006.

147. **Lundblad LK, Irvin CG, Hantos Z, Sly P, Mitzner W and Bates JH**. Penh is not a measure of airway resistance! *Eur Respir J* 30: 805, 2007.

148. **Mack PJ, Kaazempur-Mofrad MR, Karcher H, Lee RT and Kamm RD**. Force-induced focal adhesion translocation: effects of force amplitude and frequency. *Am J Physiol Cell Physiol* 287: C954-C962, 2004.

149. **MacLean JA, Sauty A, Luster AD, Drazen JM and De Sanctis GT**. Antigen-induced airway hyperresponsiveness, pulmonary eosinophilia, and chemokine expression in B cell-deficient mice. *Am J Respir Cell Mol Biol* 20: 379-387, 1999.

150. **Martin C**. Study of pharmacological and inflammatory responses in precision cut lung slices. 1997.

151. **Martin C, Goggel R, Dal P, V, Vergelli C, Giovannoni P, Ernst M and Uhlig S**. Airway relaxant and anti-inflammatory properties of a PDE4 inhibitor with low affinity for the high-affinity rolipram binding site. *Naunyn Schmiedebergs Arch Pharmacol* 365: 284-289, 2002.

152. **Martin C, Goggel R, Ressmeyer AR and Uhlig S**. Pressor responses to platelet-activating factor and thromboxane are mediated by Rho-kinase. *Am J Physiol Lung Cell Mol Physiol* 287: L250-L257, 2004.

153. **Martin C, Uhlig S and Ullrich V**. Videomicroscopy of methacholine-induced contraction of individual airways in precision-cut lung slices. *Eur Respir J* 9: 2479-2487, 1996.

154. **Martin C, Uhlig S and Ullrich V**. Cytokine-induced bronchoconstriction in precision-cut lung slices is dependent upon cyclooxygenase-2 and thromboxane receptor activation. *Am J Respir Cell Mol Biol* 24: 139-145, 2001.

155. **Martin C, Ullrich V and Uhlig S**. Effects of the thromboxane receptor agonist U46619 and endothelin-1 on large and small airways. *Eur Respir J* 16: 316-323, 2000.

156. **Matthay MA, Bhattacharya S, Gaver D, Ware LB, Lim LH, Syrkina O, Eyal F and Hubmayr R**. Ventilator-induced lung injury: in vivo and in vitro mechanisms. *Am J Physiol Lung Cell Mol Physiol* 283: L678-L682, 2002.

157. **Matute-Bello G, Frevert CW, Kajikawa O, Skerrett SJ, Goodman RB, Park DR and Martin TR**. Septic shock and acute lung injury in rabbits with peritonitis: failure of the neutrophil response to localized infection. *Am J Respir Crit Care Med* 163: 234-243, 2001.

158. **Matute-Bello G, Frevert CW and Martin TR**. Animal models of acute lung injury. *Am J Physiol Lung Cell Mol Physiol* 295: L379-L399, 2008.

159. **McBryan J, Howlin J, Napoletano S and Martin F**. Amphiregulin: role in mammary gland development and breast cancer. *J Mammary Gland Biol Neoplasia* 13: 159-169, 2008.

160. **McVerry BJ, Peng X, Hassoun PM, Sammani S, Simon BA and Garcia JG**. Sphingosine 1-phosphate reduces vascular leak in murine and canine models of acute lung injury. *Am J Respir Crit Care Med* 170: 987-993, 2004.

161. **MEAD J**. Mechanical properties of lungs. *Physiol Rev* 41: 281-330, 1961.

162. **Meade MO, Cook DJ, Guyatt GH, Slutsky AS, Arabi YM, Cooper DJ, Davies AR, Hand LE, Zhou Q, Thabane L, Austin P, Lapinsky S, Baxter A, Russell J, Skrobik Y, Ronco JJ and Stewart TE**. Ventilation strategy using low tidal volumes, recruitment maneuvers, and high positive end-expiratory pressure for acute lung injury and acute respiratory distress syndrome: a randomized controlled trial. *JAMA* 299: 637-645, 2008.

163. **Meduri GU, Headley S, Kohler G, Stentz F, Tolley E, Umberger R and Leeper K**. Persistent elevation of inflammatory cytokines predicts a poor outcome in ARDS. Plasma IL-1 beta and IL-6 levels are consistent and efficient predictors of outcome over time. *Chest* 107: 1062-1073, 1995.

164. **Mehendale HM, Angevine LS and Ohmiya Y**. The isolated perfused lung--a critical evaluation. *Toxicology* 21: 1-36, 1981.

165. **Mehta PN, Panitch HB, Wolfson MR and Shaffer TH**. Dissociation between the effects of theophylline and caffeine on premature airway smooth muscles. *Pediatr Res* 29: 446-448, 1991.

166. **Mitzner W and Tankersley C**. Interpreting Penh in mice. *J Appl Physiol* 94: 828-831, 2003.

167. **Modelska K, Pittet JF, Folkesson HG, Courtney B, V and Matthay MA**. Acid-induced lung injury. Protective effect of anti-interleukin-8 pretreatment on alveolar epithelial barrier function in rabbits. *Am J Respir Crit Care Med* 160: 1450-1456, 1999.

168. **Mong PY and Wang Q**. Activation of Rho kinase isoforms in lung endothelial cells during inflammation. *J Immunol* 182: 2385-2394, 2009.

169. **Monteil C, Le PE, Buisson S, Morin JP, Guerbet M and Jouany JM**. Acrolein toxicity: comparative in vitro study with lung slices and pneumocytes type II cell line from rats. *Toxicology* 133: 129-138, 1999.

170. **Montgomery AB, Stager MA, Carrico CJ and Hudson LD**. Causes of mortality in patients with the adult respiratory distress syndrome. *Am Rev Respir Dis* 132: 485-489, 1985.

171. **Moore BB and Hogaboam CM**. Murine models of pulmonary fibrosis. *Am J Physiol Lung Cell Mol Physiol* 294: L152-L160, 2008.

172. **Moreno L, Perez-Vizcaino F, Harrington L, Faro R, Sturton G, Barnes PJ and Mitchell JA**. Pharmacology of airways and vessels in lung slices in situ: role of endogenous dilator hormones. *Respir Res* 7: 111, 2006.

173. **Morris AH, Wallace CJ, Menlove RL, Clemmer TP, Orme JF, Jr., Weaver LK, Dean NC, Thomas F, East TD, Pace NL and .** Randomized clinical trial of

pressure-controlled inverse ratio ventilation and extracorporeal CO2 removal for adult respiratory distress syndrome. *Am J Respir Crit Care Med* 149: 295-305, 1994.

174. **Moses BL and Spaulding GL**. Chronic bronchial disease of the cat. *Vet Clin North Am Small Anim Pract* 15: 929-948, 1985.

175. **Mostyn A, Pearce S, Stephenson T and Symonds ME**. Hormonal and nutritional regulation of adipose tissue mitochondrial development and function in the newborn. *Exp Clin Endocrinol Diabetes* 112: 2-9, 2004.

176. **Murakami M, Austen KF and Arm JP**. The immediate phase of c-kit ligand stimulation of mouse bone marrow-derived mast cells elicits rapid leukotriene C4 generation through posttranslational activation of cytosolic phospholipase A2 and 5-lipoxygenase. *J Exp Med* 182: 197-206, 1995.

177. **Murphy KM, Travers P and Walport M**. Janeway`s immunobiology. *Taylor & Francis, 7th revised edition* 2008.

178. **Mustafa S, Thulesius L and Thulesius O**. The contractile response of thiopental in large and small ovine airways. *Acta Anaesthesiol Scand* 38: 499-504, 1994.

179. **Mutschler E, Geisslinger G, Kroemer HK, Ruth P and Schäfer-Korting M**. Mutschler Arzneimittelwirkungen. *Wissenschaftliche Verlagsges* 2009.

180. **Navajas D, Maksym GN and Bates JH**. Dynamic viscoelastic nonlinearity of lung parenchymal tissue. *J Appl Physiol* 79: 348-356, 1995.

181. **Nave R, Fisher R and McCracken N**. In vitro metabolism of beclomethasone dipropionate, budesonide, ciclesonide, and fluticasone propionate in human lung precision-cut tissue slices. *Respir Res* 8: 65, 2007.

182. **Nave R, Fisher R and Zech K**. In Vitro metabolism of ciclesonide in human lung and liver precision-cut tissue slices. *Biopharm Drug Dispos* 27: 197-207, 2006.

183. **Neuhaus-Steinmetz U, Glaab T, Daser A, Braun A, Lommatzsch M, Herz U, Kips J, Alarie Y and Renz H**. Sequential development of airway hyperresponsiveness and acute airway obstruction in a mouse model of allergic inflammation. *Int Arch Allergy Immunol* 121: 57-67, 2000.

184. **Niimi A, Amitani R, Suzuki K, Tanaka E, Murayama T and Kuze F**. Eosinophilic inflammation in cough variant asthma. *Eur Respir J* 11: 1064-1069, 1998.

185. **Ning QM and Wang XR**. Activations of mitogen-activated protein kinase and nuclear factor-kappaB by mechanical stretch result in ventilation-induced lung injury. *Med Hypotheses* 68: 356-360, 2007.

186. **Ning QM and Wang XR**. Response of alveolar type II epithelial cells to mechanical stretch and lipopolysaccharide. *Respiration* 74: 579-585, 2007.

187. **Norris Reinero CR, Decile KC, Berghaus RD, Williams KJ, Leutenegger CM, Walby WF, Schelegle ES, Hyde DM and Gershwin LJ**. An experimental model of allergic asthma in cats sensitized to house dust mite or bermuda grass allergen. *Int Arch Allergy Immunol* 135: 117-131, 2004.

188. **Obrig TG, Culp WJ, McKeehan WL and Hardesty B**. The mechanism by which cycloheximide and related glutarimide antibiotics inhibit peptide synthesis on reticulocyte ribosomes. *J Biol Chem* 246: 174-181, 1971.

189. **Ogden RW**. Large Deformation Isotropic Elasticity - Correlation of Theory and Experiment for Incompressible Rubberlike Solids. *Proceedings of the Royal Society of London Series A-Mathematical and Physical Sciences* 326: 565-&, 1972.

190. **Osborne ML, Evans TW, Sommerhoff CP, Chung KF, Hirshman CA, Boushey HA and Nadel JA**. Hypotonic and isotonic aerosols increase bronchial reactivity in basenji-greyhound dogs. *Am Rev Respir Dis* 135: 345-349, 1987.

191. **Paddenberg R, Konig P, Faulhammer P, Goldenberg A, Pfeil U and Kummer W**. Hypoxic vasoconstriction of partial muscular intra-acinar pulmonary arteries in murine precision cut lung slices. *Respir Res* 7: 93, 2006.

192. **Palmarini M, Fan H and Sharp JM**. Sheep pulmonary adenomatosis: a unique model of retrovirus-associated lung cancer. *Trends Microbiol* 5: 478-483, 1997.

193. **Papaiahgari S, Yerrapureddy A, Hassoun PM, Garcia JG, Birukov KG and Reddy SP**. EGFR-activated signaling and actin remodeling regulate cyclic stretch-induced NRF2-ARE activation. *Am J Respir Cell Mol Biol* 36: 304-312, 2007.

194. **Parrish AR, Gandolfi AJ and Brendel K**. Precision-cut tissue slices: applications in pharmacology and toxicology. *Life Sci* 57: 1887-1901, 1995.

195. **Pearce S, Mostyn A, ves-Guerra MC, Pecqueur C, Miroux B, Webb R, Stephenson T and Symond ME**. Prolactin, prolactin receptor and uncoupling proteins during fetal and neonatal development. *Proc Nutr Soc* 62: 421-427, 2003.

196. **Peng X, Hassoun PM, Sammani S, McVerry BJ, Burne MJ, Rabb H, Pearse D, Tuder RM and Garcia JG**. Protective effects of sphingosine 1-phosphate in murine endotoxin-induced inflammatory lung injury. *Am J Respir Crit Care Med* 169: 1245-1251, 2004.

197. **Pepe PE, Hudson LD and Carrico CJ**. Early application of positive end-expiratory pressure in patients at risk for the adult respiratory-distress syndrome. *N Engl J Med* 311: 281-286, 1984.

198. **Perlman CE and Bhattacharya J**. Alveolar expansion imaged by optical sectioning microscopy. *J Appl Physiol* 103: 1037-1044, 2007.

199. **Perugorria MJ, Latasa MU, Nicou A, Cartagena-Lirola H, Castillo J, Goni S, Vespasiani-Gentilucci U, Zagami MG, Lotersztajn S, Prieto J, Berasain C and Avila MA**. The epidermal growth factor receptor ligand amphiregulin participates in the development of mouse liver fibrosis. *Hepatology* 48: 1251-1261, 2008.

200. **Pfaff M, Powaga N, Akinci S, Schutz W, Banno Y, Wiegand S, Kummer W, Wess J and Haberberger RV**. Activation of the SPHK/S1P signalling pathway is coupled to muscarinic receptor-dependent regulation of peripheral airways. *Respir Res* 6: 48, 2005.

201. **Pinhu L, Whitehead T, Evans T and Griffiths M**. Ventilator-associated lung injury. *Lancet* 361: 332-340, 2003.

202. **Piper PJ**. Leukotrienes: possible mediators in bronchial asthma. *Eur J Respir Dis Suppl* 129: 45-64, 1983.

203. **Plotz FB, Slutsky AS, van Vught AJ and Heijnen CJ**. Ventilator-induced lung injury and multiple system organ failure: a critical review of facts and hypotheses. *Intensive Care Med* 30: 1865-1872, 2004.

204. **Preuss JM, Rigby PJ and Goldie RG**. Ageing and epithelial integrity as modulators of airway smooth muscle responsiveness to endothelin-1. *Naunyn Schmiedebergs Arch Pharmacol* 361: 391-396, 2000.

205. **Price RJ, Renwick AB, Beamand JA, Esclangon F, Wield PT, Walters DG and Lake BG**. Comparison of the metabolism of 7-ethoxycoumarin and coumarin in precision-cut rat liver and lung slices. *Food Chem Toxicol* 33: 233-237, 1995.

206. **Price RJ, Renwick AB, Walters DG, Young PJ and Lake BG**. Metabolism of nicotine and induction of CYP1A forms in precision-cut rat liver and lung slices. *Toxicol In Vitro* 18: 179-185, 2004.

207. **Price RJ, Renwick AB, Wield PT, Beamand JA and Lake BG**. Toxicity of 3-methylindole, 1-nitronaphthalene and paraquat in precision-cut rat lung slices. *Arch Toxicol* 69: 405-409, 1995.

208. **Price RJ, Walters DG, Hoff C, Mistry H, Renwick AB, Wield PT, Beamand JA and Lake BG**. Metabolism of [ring-U-14C] agaritine by precision-cut rat, mouse and human liver and lung slices. *Food Chem Toxicol* 34: 603-609, 1996.

209. **Pugin J**. Molecular mechanisms of lung cell activation induced by cyclic stretch. *Crit Care Med* 31: S200-S206, 2003.

210. **Pushparajah DS, Umachandran M, Nazir T, Plant KE, Plant N, Lewis DF and Ioannides C**. Up-regulation of CYP1A/B in rat lung and liver, and human liver precision-cut slices by a series of polycyclic aromatic hydrocarbons; association with the Ah locus and importance of molecular size. *Toxicol In Vitro* 22: 128-145, 2008.

211. **Pushparajah DS, Umachandran M, Plant KE, Plant N and Ioannides C**. Evaluation of the precision-cut liver and lung slice systems for the study of induction of CYP1, epoxide hydrolase and glutathione S-transferase activities. *Toxicology* 231: 68-80, 2007.

212. **Pushparajah DS, Umachandran M, Plant KE, Plant N and Ioannides C**. Differential response of human and rat epoxide hydrolase to polycyclic aromatic hydrocarbon exposure: studies using precision-cut tissue slices. *Mutat Res* 640: 153-161, 2008.

213. **Pushparajah DS, Umachandran M, Plant KE, Plant N and Ioannides C**. Up-regulation of the glutathione S-transferase system in human liver by polycyclic

aromatic hydrocarbons; comparison with rat liver and lung. *Mutagenesis* 23: 299-308, 2008.

214. **Quinn D, Tager A, Joseph PM, Bonventre JV, Force T and Hales CA**. Stretch-induced mitogen-activated protein kinase activation and interleukin-8 production in type II alveolar cells. *Chest* 116: 89S-90S, 1999.

215. **Ranieri VM, Suter PM, Tortorella C, De TR, Dayer JM, Brienza A, Bruno F and Slutsky AS**. Effect of mechanical ventilation on inflammatory mediators in patients with acute respiratory distress syndrome: a randomized controlled trial. *JAMA* 282: 54-61, 1999.

216. **Reinero CR, Declue AE and Rabinowitz P**. Asthma in humans and cats: Is there a common sensitivity to aeroallegens in shared environments? *Environ Res* 2009.

217. **Ressmeyer AR**. Mechanisms of bronchoconstriction in the early allergic response. 2006.

218. **Ressmeyer AR, Larsson AK, Vollmer E, Dahlen SE, Uhlig S and Martin C**. Characterisation of guinea pig precision-cut lung slices: comparison with human tissues. *Eur Respir J* 28: 603-611, 2006.

219. **Ricard JD, Dreyfuss D and Saumon G**. Production of inflammatory cytokines in ventilator-induced lung injury: a reappraisal. *Am J Respir Crit Care Med* 163: 1176-1180, 2001.

220. **Ricciardolo FL, Nijkamp F, De R, V and Folkerts G**. The guinea pig as an animal model for asthma. *Curr Drug Targets* 9: 452-465, 2008.

221. **Richter E, Friesenegger S, Engl J and Tricker AR**. Use of precision-cut tissue slices in organ culture to study metabolism of 4-(methylnitrosamino)-1-(3-

pyridyl)-1-butanone (NNK) and 4-(methylnitrosamino)-1-(3-pyridyl)-1-butanol (NNAL) by hamster lung, liver and kidney. *Toxicology* 144: 83-91, 2000.

222. **Rittirsch D, Hoesel LM and Ward PA**. The disconnect between animal models of sepsis and human sepsis. *J Leukoc Biol* 81: 137-143, 2007.

223. **Robertson B**. Surfactant inactivation and surfactant replacement in experimental models of ARDS. *Acta Anaesthesiol Scand Suppl* 95: 22-28, 1991.

224. **Rose F, Zwick K, Ghofrani HA, Sibelius U, Seeger W, Walmrath D and Grimminger F**. Prostacyclin enhances stretch-induced surfactant secretion in alveolar epithelial type II cells. *Am J Respir Crit Care Med* 160: 846-851, 1999.

225. **Russell JA**. Responses of isolated canine airways to electric stimulation and acetylcholine. *J Appl Physiol* 45: 690-698, 1978.

226. **Russell WM and Burch RI**. *Principles of Human Experimental Technique*. 1992.

227. **Saad MH and Burka JF**. Role of calcium in arachidonic acid-induced contractions of guinea pig airways. *Eur J Pharmacol* 100: 13-20, 1984.

228. **Sahin U, Weskamp G, Kelly K, Zhou HM, Higashiyama S, Peschon J, Hartmann D, Saftig P and Blobel CP**. Distinct roles for ADAM10 and ADAM17 in ectodomain shedding of six EGFR ligands. *J Cell Biol* 164: 769-779, 2004.

229. **Sakuma T, Takahashi K, Ohya N, Kajikawa O, Martin TR, Albertine KH and Matthay MA**. Ischemia-reperfusion lung injury in rabbits: mechanisms of injury and protection. *Am J Physiol* 276: L137-L145, 1999.

230. **Salerno FG, Fust A and Ludwig MS**. Stretch-induced changes in constricted lung parenchymal strips: role of extracellular matrix. *Eur Respir J* 23: 193-198, 2004.

231. **Schachter EN, Zuskin E, Goswami S, Castranova V, Siegel P, Whitmer M and Gadgil A**. Pharmacologic effects of tobacco dust extract on isolated Guinea pig trachea. *Chest* 123: 862-868, 2003.

232. **Schumann S, Stahl CA, Moller K, Schneider M, Metzke R, Wall WA, Priebe HJ and Guttmann J**. Contact-free determination of material characteristics using a newly developed pressure-operated strain-applying bioreactor. *J Biomed Mater Res B Appl Biomater* 86B: 483-492, 2008.

233. **Schuster DP**. ARDS: clinical lessons from the oleic acid model of acute lung injury. *Am J Respir Crit Care Med* 149: 245-260, 1994.

234. **Selg E, Andersson M, Lastbom L, Ryrfeldt A and Dahlen SE**. Two different mechanisms for modulation of bronchoconstriction in guinea-pigs by cyclooxygenase metabolites. *Prostaglandins Other Lipid Mediat* 88: 101-110, 2009.

235. **Shao J, Evers BM and Sheng H**. Prostaglandin E2 synergistically enhances receptor tyrosine kinase-dependent signaling system in colon cancer cells. *J Biol Chem* 279: 14287-14293, 2004.

236. **Sheller JR and Brigham KL**. Bronchomotor responses of isolated sheep airways to electrical field stimulation. *J Appl Physiol* 53: 1088-1093, 1982.

237. **Siminski JT, Kavanagh TJ, Chi E and Raghu G**. Long-term maintenance of mature pulmonary parenchyma cultured in serum-free conditions. *Am J Physiol* 262: L105-L110, 1992.

238. **Simoen V and Christophe B**. Effect of levocetirizine on the contraction induced by histamine on isolated rabbit bronchioles from precision-cut lung slices. *Pharmacology* 78: 61-65, 2006.

239. **Slutsky AS and Tremblay LN**. Multiple system organ failure. Is mechanical ventilation a contributing factor? *Am J Respir Crit Care Med* 157: 1721-1725, 1998.

240. **Smith EL and Schuchman EH**. The unexpected role of acid sphingomyelinase in cell death and the pathophysiology of common diseases. *FASEB J* 22: 3419-3431, 2008.

241. **Smith PG, Roy C, Dreger J and Brozovich F**. Mechanical strain increases velocity and extent of shortening in cultured airway smooth muscle cells. *Am J Physiol* 277: L343-L348, 1999.

242. **Snibson KJ, Bischof RJ, Koumoundouros E, McMurtrie LS, Cock M and Harding R**. Altered airway responsiveness in adult sheep born prematurely: effects of allergen exposure. *Exp Lung Res* 32: 215-228, 2006.

243. **Snibson KJ, Bischof RJ, Slocombe RF and Meeusen EN**. Airway remodelling and inflammation in sheep lungs after chronic airway challenge with house dust mite. *Clin Exp Allergy* 35: 146-152, 2005.

244. **Soler M, Sielczak M and Abraham WM**. Separation of late bronchial responses from airway hyperresponsiveness in allergic sheep. *J Appl Physiol* 70: 617-623, 1991.

245. **Springer J and Fischer A**. Substance P-induced pulmonary vascular remodelling in precision cut lung slices. *Eur Respir J* 22: 596-601, 2003.

246. **Springer J, Groneberg DA, Dinh QT, Quarcoo D, Hamelmann E, Braun-Dullaeus RC, Geppetti P, Anker SD and Fischer A**. Neurokinin-1 receptor activation induces reactive oxygen species and epithelial damage in allergic airway inflammation. *Clin Exp Allergy* 37: 1788-1797, 2007.

247. **Springer J, Wagner S, Subramamiam A, McGregor GP, Groneberg DA and Fischer A**. BDNF-overexpression regulates the reactivity of small pulmonary arteries to neurokinin A. *Regul Pept* 118: 19-23, 2004.

248. **Stefaniak MS and Brendel K**. Biochemical and histological characterization of agar-filled precision-cut rat lung slices in dynamic organ culture as an in vitro tool. 2009.

249. **Steinberg KP, Hudson LD, Goodman RB, Hough CL, Lanken PN, Hyzy R, Thompson BT and Ancukiewicz M**. Efficacy and safety of corticosteroids for persistent acute respiratory distress syndrome. *N Engl J Med* 354: 1671-1684, 2006.

250. **Stewart TE, Meade MO, Cook DJ, Granton JT, Hodder RV, Lapinsky SE, Mazer CD, McLean RF, Rogovein TS, Schouten BD, Todd TR and Slutsky AS**. Evaluation of a ventilation strategy to prevent barotrauma in patients at high risk for acute respiratory distress syndrome. Pressure- and Volume-Limited Ventilation Strategy Group. *N Engl J Med* 338: 355-361, 1998.

251. **Struckmann N, Schwering S, Wiegand S, Gschnell A, Yamada M, Kummer W, Wess J and Haberberger RV**. Role of muscarinic receptor subtypes in the constriction of peripheral airways: studies on receptor-deficient mice. *Mol Pharmacol* 64: 1444-1451, 2003.

252. **Stuber F, Wrigge H, Schroeder S, Wetegrove S, Zinserling J, Hoeft A and Putensen C**. Kinetic and reversibility of mechanical ventilation-associated pulmonary and systemic inflammatory response in patients with acute lung injury. *Intensive Care Med* 28: 834-841, 2002.

253. **Sturton RG, Trifilieff A, Nicholson AG and Barnes PJ**. Pharmacological characterization of indacaterol, a novel once daily inhaled 2 adrenoceptor agonist, on small airways in human and rat precision-cut lung slices. *J Pharmacol Exp Ther* 324: 270-275, 2008.

254. **Suki B, Barabasi AL, Hantos Z, Petak F and Stanley HE**. Avalanches and power-law behaviour in lung inflation. *Nature* 368: 615-618, 1994.

255. **Tanaka R and Ludwig MS**. Changes in viscoelastic properties of rat lung parenchymal strips with maturation. *J Appl Physiol* 87: 2081-2089, 1999.

256. **te Poele RH, Okorokov AL and Joel SP**. RNA synthesis block by 5, 6-dichloro-1-beta-D-ribofuranosylbenzimidazole (DRB) triggers p53-dependent apoptosis in human colon carcinoma cells. *Oncogene* 18: 5765-5772, 1999.

257. **Tee RD, Cullinan P, Welch J, Burge PS and Newman-Taylor AJ**. Specific IgE to isocyanates: a useful diagnostic role in occupational asthma. *J Allergy Clin Immunol* 101: 709-715, 1998.

258. **ter Horst SA, Walther FJ, Poorthuis BJ, Hiemstra PS and Wagenaar GT**. Inhaled nitric oxide attenuates pulmonary inflammation and fibrin deposition and prolongs survival in neonatal hyperoxic lung injury. *Am J Physiol Lung Cell Mol Physiol* 293: L35-L44, 2007.

259. **Toga H, Ibe BO and Raj JU**. In vitro responses of ovine intrapulmonary arteries and veins to endothelin-1. *Am J Physiol* 263: L15-L21, 1992.

260. **Toga H, Usha RJ, Hillyard R, Ku B and Anderson J**. Endothelin effects in isolated, perfused lamb lungs: role of cyclooxygenase inhibition and vasomotor tone. *Am J Physiol* 261: H443-H450, 1991.

261. **Tremblay L, Valenza F, Ribeiro SP, Li J and Slutsky AS**. Injurious ventilatory strategies increase cytokines and c-fos m-RNA expression in an isolated rat lung model. *J Clin Invest* 99: 944-952, 1997.

262. **Tremblay LN, Miatto D, Hamid Q, Govindarajan A and Slutsky AS**. Injurious ventilation induces widespread pulmonary epithelial expression of tumor necrosis factor-alpha and interleukin-6 messenger RNA. *Crit Care Med* 30: 1693-1700, 2002.

263. **Tremblay LN and Slutsky AS**. Ventilator-induced injury: from barotrauma to biotrauma. *Proc Assoc Am Physicians* 110: 482-488, 1998.

264. **Trepat X, Grabulosa M, Puig F, Maksym GN, Navajas D and Farre R**. Viscoelasticity of human alveolar epithelial cells subjected to stretch. *Am J Physiol Lung Cell Mol Physiol* 287: L1025-L1034, 2004.

265. **Tschernig T, Neumann D, Pich A, Dorsch M and Pabst R**. Experimental bronchial asthma - the strength of the species rat. *Curr Drug Targets* 9: 466-469, 2008.

266. **Tschumperlin DJ, Dai G, Maly IV, Kikuchi T, Laiho LH, McVittie AK, Haley KJ, Lilly CM, So PT, Lauffenburger DA, Kamm RD and Drazen JM**. Mechanotransduction through growth-factor shedding into the extracellular space. *Nature* 429: 83-86, 2004.

267. **Tschumperlin DJ and Margulies SS**. Alveolar epithelial surface area-volume relationship in isolated rat lungs. *J Appl Physiol* 86: 2026-2033, 1999.

268. **Tschumperlin DJ, Oswari J and Margulies AS**. Deformation-induced injury of alveolar epithelial cells. Effect of frequency, duration, and amplitude. *Am J Respir Crit Care Med* 162: 357-362, 2000.

269. **Uhlig S and Gulbins E**. Sphingolipids in the lungs. *Am J Respir Crit Care Med* 178: 1100-1114, 2008.

270. **Uhlig S and Uhlig U**. Pharmacological interventions in ventilator-induced lung injury. *Trends Pharmacol Sci* 25: 592-600, 2004.

271. **Uhlig U, Fehrenbach H, Lachmann RA, Goldmann T, Lachmann B, Vollmer E and Uhlig S**. Phosphoinositide 3-OH kinase inhibition prevents ventilation-induced lung cell activation. *Am J Respir Crit Care Med* 169: 201-208, 2004.

272. **Uhlig U, Haitsma JJ, Goldmann T, Poelma DL, Lachmann B and Uhlig S**. Ventilation-induced activation of the mitogen-activated protein kinase pathway. *Eur Respir J* 20: 946-956, 2002.

273. **Umachandran M, Howarth J and Ioannides C**. Metabolic and structural viability of precision-cut rat lung slices in culture. *Xenobiotica* 34: 771-780, 2004.

274. **Van d, V and Joos G**. Regionally different influence of contractile agonists on isolated rat airway segments. *Respir Physiol* 112: 185-194, 1998.

275. **van TM, Liu J, Groenman F, Ridsdale R, Han RN, Venkatesh V, Tibboel D and Post M**. Iroquois genes influence proximo-distal morphogenesis during rat lung development. *Am J Physiol Lung Cell Mol Physiol* 290: L777-L789, 2006.

276. **Vande Geest JP, Di Martino ES and Vorp DA**. An analysis of the complete strain field within Flexercell membranes. *J Biomech* 37: 1923-1928, 2004.

277. **Vandebriel RJ, De Jong WH, Spiekstra SW, Van DM, Fluitman A, Garssen J and Van LH**. Assessment of preferential T-helper 1 or T-helper 2 induction by low molecular weight compounds using the local lymph node assay in conjunction with RT-PCR and ELISA for interferon-gamma and interleukin-4. *Toxicol Appl Pharmacol* 162: 77-85, 2000.

278. **Vanoirbeek JA, Tarkowski M, Vanhooren HM, De V, V, Nemery B and Hoet PH**. Validation of a mouse model of chemical-induced asthma using trimellitic anhydride, a respiratory sensitizer, and dinitrochlorobenzene, a dermal sensitizer. *J Allergy Clin Immunol* 117: 1090-1097, 2006.

279. **Vietmeier J, Niedorf F, Baumer W, Martin C, Deegen E, Ohnesorge B and Kietzmann M**. Reactivity of equine airways--a study on precision-cut lung slices. *Vet Res Commun* 31: 611-619, 2007.

280. **Villar J**. Low vs high positive end-expiratory pressure in the ventilatory management of acute lung injury. *Minerva Anestesiol* 72: 357-362, 2006.

281. **Villar J, Ribeiro SP, Mullen JB, Kuliszewski M, Post M and Slutsky AS**. Induction of the heat shock response reduces mortality rate and organ damage in a sepsis-induced acute lung injury model. *Crit Care Med* 22: 914-921, 1994.

282. **Vlahakis NE, Schroeder MA, Limper AH and Hubmayr RD**. Stretch induces cytokine release by alveolar epithelial cells in vitro. *Am J Physiol* 277: L167-L173, 1999.

283. **von Bethmann AN, Brasch F, Nusing R, Vogt K, Volk HD, Muller KM, Wendel A and Uhlig S**. Hyperventilation induces release of cytokines from perfused mouse lung. *Am J Respir Crit Care Med* 157: 263-272, 1998.

284. **Wagenaar GT, ter Horst SA, van Gastelen MA, Leijser LM, Mauad T, Van D, V, de HE, Hiemstra PS, Poorthuis BJ and Walther FJ**. Gene expression profile and histopathology of experimental bronchopulmonary dysplasia induced by prolonged oxidative stress. *Free Radic Biol Med* 36: 782-801, 2004.

285. **Wang HM, Bodenstein M and Markstaller K**. Overview of the pathology of three widely used animal models of acute lung injury. *Eur Surg Res* 40: 305-316, 2008.

286. **Wang SW, Oh CK, Cho SH, Hu G, Martin R, missie-Sanders S, Li K, Moyle M and Yao Z**. Amphiregulin expression in human mast cells and its effect on the primary human lung fibroblasts. *J Allergy Clin Immunol* 115: 287-294, 2005.

287. **Ware LB and Matthay MA**. The acute respiratory distress syndrome. *N Engl J Med* 342: 1334-1349, 2000.

288. **Webb HH and Tierney DF**. Experimental pulmonary edema due to intermittent positive pressure ventilation with high inflation pressures. Protection by positive end-expiratory pressure. *Am Rev Respir Dis* 110: 556-565, 1974.

289. **Weimann J, Ullrich R, Hromi J, Fujino Y, Clark MW, Bloch KD and Zapol WM**. Sildenafil is a pulmonary vasodilator in awake lambs with acute pulmonary hypertension. *Anesthesiology* 92: 1702-1712, 2000.

290. **Wenzel SE, Westcott JY and Larsen GL**. Bronchoalveolar lavage fluid mediator levels 5 minutes after allergen challenge in atopic subjects with asthma: relationship to the development of late asthmatic responses. *J Allergy Clin Immunol* 87: 540-548, 1991.

291. **Wheeler AP, Bernard GR, Thompson BT, Schoenfeld D, Wiedemann HP, deBoisblanc B, Connors AF, Jr., Hite RD and Harabin AL**. Pulmonary-artery versus central venous catheter to guide treatment of acute lung injury. *N Engl J Med* 354: 2213-2224, 2006.

292. **Whitehead TC, Zhang H, Mullen B and Slutsky AS**. Effect of mechanical ventilation on cytokine response to intratracheal lipopolysaccharide. *Anesthesiology* 101: 52-58, 2004.

293. **Wiechert L, Metzke R and Wall WA**. Modeling the mechanical behavior of lung tissue at the micro-level. *J Eng Mech* 2008.

294. **Wiedemann HP, Wheeler AP, Bernard GR, Thompson BT, Hayden D, deBoisblanc B, Connors AF, Jr., Hite RD and Harabin AL**. Comparison of two fluid-management strategies in acute lung injury. *N Engl J Med* 354: 2564-2575, 2006.

295. **Wiener-Kronish JP, Albertine KH and Matthay MA**. Differential responses of the endothelial and epithelial barriers of the lung in sheep to Escherichia coli endotoxin. *J Clin Invest* 88: 864-875, 1991.

296. **Wijeweera JB, Gandolfi AJ, Parrish A and Lantz RC**. Sodium arsenite enhances AP-1 and NFkappaB DNA binding and induces stress protein expression in precision-cut rat lung slices. *Toxicol Sci* 61: 283-294, 2001.

297. **Willmarth NE and Ethier SP**. Amphiregulin as a novel target for breast cancer therapy. *J Mammary Gland Biol Neoplasia* 13: 171-179, 2008.

298. **Wilson MR, Choudhury S, Goddard ME, O'Dea KP, Nicholson AG and Takata M**. High tidal volume upregulates intrapulmonary cytokines in an in vivo mouse model of ventilator-induced lung injury. *J Appl Physiol* 95: 1385-1393, 2003.

299. **Wilson MR, Choudhury S and Takata M**. Pulmonary inflammation induced by high-stretch ventilation is mediated by tumor necrosis factor signaling in mice. *Am J Physiol Lung Cell Mol Physiol* 288: L599-L607, 2005.

300. **Winston FK, Macarak EJ, Gorfien SF and Thibault LE**. A system to reproduce and quantify the biomechanical environment of the cell. *J Appl Physiol* 67: 397-405, 1989.

301. **Wirtz HR and Dobbs LG**. The effects of mechanical forces on lung functions. *Respir Physiol* 119: 1-17, 2000.

302. **Witschi HP and Hakkinen PJ**. The role of toxicological interactions in lung injury. *Environ Health Perspect* 55: 139-148, 1984.

303. **Wohlsen A, Martin C, Vollmer E, Branscheid D, Magnussen H, Becker WM, Lepp U and Uhlig S**. The early allergic response in small airways of human precision-cut lung slices. *Eur Respir J* 21: 1024-1032, 2003.

304. **Wohlsen A, Uhlig S and Martin C**. Immediate allergic response in small airways. *Am J Respir Crit Care Med* 163: 1462-1469, 2001.

305. **Wright JL and Churg A**. Short-term exposure to cigarette smoke induces endothelial dysfunction in small intrapulmonary arteries: analysis using guinea pig precision cut lung slices. *J Appl Physiol* 104: 1462-1469, 2008.

306. **Xu L, Tripathy A, Pasek DA and Meissner G**. Potential for pharmacology of ryanodine receptor/calcium release channels. *Ann N Y Acad Sci* 853: 130-148, 1998.

307. **Yamamoto H, Teramoto H, Uetani K, Igawa K and Shimizu E**. Cyclic stretch upregulates interleukin-8 and transforming growth factor-beta1 production through a protein kinase C-dependent pathway in alveolar epithelial cells. *Respirology* 7: 103-109, 2002.

308. **Yu J**. Airway mechanosensors. *Respir Physiol Neurobiol* 148: 217-243, 2005.

309. **Yu LJ, Matias J, Scudiero DA, Hite KM, Monks A, Sausville EA and Waxman DJ**. P450 enzyme expression patterns in the NCI human tumor cell line panel. *Drug Metab Dispos* 29: 304-312, 2001.

310. **Yuan H, Ingenito EP and Suki B**. Dynamic properties of lung parenchyma: mechanical contributions of fiber network and interstitial cells. *J Appl Physiol* 83: 1420-1431, 1997.

311. **Zachlederova M and Jarolim P**. The dynamics of gene expression in human lung microvascular endothelial cells after stimulation with inflammatory cytokines. *Physiol Res* 55: 39-47, 2006.

312. **Zapol WM, Snider MT, Hill JD, Fallat RJ, Bartlett RH, Edmunds LH, Morris AH, Peirce EC, Thomas AN, Proctor HJ, Drinker PA, Pratt PC, Bagniewski A and Miller RG, Jr.** Extracorporeal membrane oxygenation in severe acute respiratory failure. A randomized prospective study. *JAMA* 242: 2193-2196, 1979.

313. **Zeiss CR, Patterson R, Pruzansky JJ, Miller MM, Rosenberg M and Levitz D**. Trimellitic anhydride-induced airway syndromes: clinical and immunologic studies. *J Allergy Clin Immunol* 60: 96-103, 1977.

314. **Zosky GR, Larcombe AN, White OJ, Burchell JT, Janosi TZ, Hantos Z, Holt PG, Sly PD and Turner DJ**. Ovalbumin-sensitized mice are good models for airway hyperresponsiveness but not acute physiological responses to allergen inhalation. *Clin Exp Allergy* 38: 829-838, 2008.

315. **Zosky GR and Sly PD**. Animal models of asthma. *Clin Exp Allergy* 37: 973-988, 2007.

Danksagung

Weiterhin möchte ich mich bei Dr. Boris Kramer für die Bereitstellung der Schafslungen und die gute Zusammenarbeit bedanken.

Prof. Gerd Müller-Newen danke ich für die Zusammenarbeit bei der Konfokalmikroskopie und Dr. Bernd Denecke für die Kooperation bei dem Genarray.

Für fachliche, technische und moralische Unterstützung danke ich besonders Jürgen Sarau, Hanna Czajkowska, Hiltrud Königs, Dr. Anna Reßmeyer, Anke Kowallik, Sophie Rausch, Dennis Lex und Nadine Ruske.
Weiterhin danke ich in diesem Zusammenhang Dr. Ulrike Uhlig, Martina Barrenschee, Dr. Eike Reppien, Dag Friedrichs, Dr. Tanja Nußbaum, Dr. Thomas Eisele, Birgit Feulner, Theodora Mashiah, Dr. Ralf Hausmann, Christiane Rosefort, Marco Schlepütz, Marion Peters und Vera Lothmann.

Außerdem möchte ich mich bei meiner Familie bedanken und ganz besonders natürlich bei Ansgar Kretschmer.

Lebenslauf

Persönliche Angaben

Name: Dassow

Vorname: Constanze

Geburtstag: 3. Juni 1981

Geburtsort: Bad Oldesloe

Staatsangehörigkeit: Deutsch

Qualifikationen

2000:	Abitur , Integrierte Gesamtschule Bad Oldesloe
2000-2005:	Studium der Humanbiologie, Ernst-Moritz-Arndt-Universität Greifswald
2005:	Abschluss zur Diplom-Humanbiologin
2005-2006:	Beginn der Promotion in der Laborgruppe Lungenpharmakologie des Forschungszentrums Borstel
2006-2010:	Fortführung der Promotion am Institut für Pharmakologie und Toxikologie der RWTH Aachen